WADD TR 61-72
Volume XXXIV

RESEARCH AND DEVELOPMENT ON ADVANCED GRAPHITE MATERIALS

VOLUME XXXIV-OXIDATION-RESISTANCE COATINGS FOR GRAPHITE

TECHNICAL DOCUMENTARY REPORT NO. WADD TR 61-72,
Volume XXXIV

June 1963

Air Force Materials Laboratory
Research and Technology Division
Air Force Systems Command
Wright-Patterson Air Force Base, Ohio

Project No. 7350, Task No. 735002
Project No. 7381, Task No. 738102
Project No. 7-817

(Prepared under Contract No. AF 33(616)-6915
by the
Advanced Materials Laboratory, National Carbon Company
Division of Union Carbide Corporation, Lawrenceburg, Tennessee;
D. A. Schulz, P. H. Higgs and J. D. Cannon, Authors.)

NOTICES

When Government drawings, specifications, or other data are used for any purpose other than in connection with a definitely related Government procurement operation, the United States Government thereby incurs no responsibility nor any obligation whatsoever; and the fact that the Government may have formulated, furnished, or in any way supplied the said drawings, specifications, or other data, is not to be regarded by implication or otherwise as in any manner licensing the holder or any other person or corporation, or conveying any rights or permission to manufacture, use, or sell any patented invention that may in any way be related thereto.

Qualified requesters may obtain copies of this report from the Defense Documentation Center (DDC), (formerly ASTIA), Cameron Station, Bldg. 5, 5010 Duke Street, Alexandria 4, Virginia.

This report has been released to the Office of Technical Services, U. S. Department of Commerce, Washington 25, D. C., in stock quantities for sale to the general public.

Copies of this report should not be returned to the Aeronautical Systems Division unless return is required by security considerations, contractual obligations, or notice on a specific document.

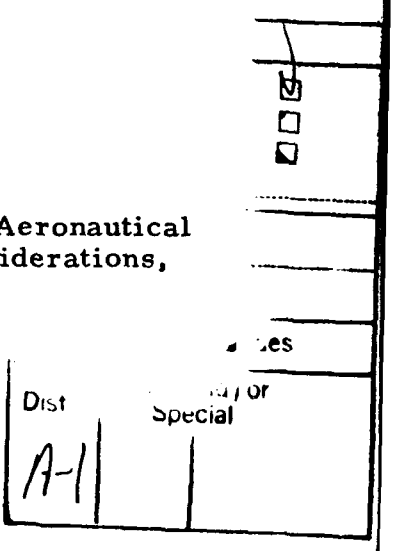

FOREWORD

This volume is the thirty-fourth of the series WADD Technical Report 61-72 describing various phases of research and development on advanced graphite materials conducted by National Carbon Company, a Division of Union Carbide Corporation, under USAF Contract No. AF 33(616)-6915.

The work covered in this report was conducted from December 1961 through March 1963 at the Advanced Materials Laboratory of National Carbon Company, Lawrenceburg, Tennessee, under the management of R. M. Bushong, Director of the Advanced Materials Project, and of R. C. Stroup, Manager of the Advanced Materials Laboratory.

The contract for this R&D program was initiated under Project No. 7350, "Refractory Inorganic Non-Metallic Materials," Task No. 735002, "Refractory Inorganic Non-Metallic Materials:Graphitic;"Project No. 7381, "Materials Application," Task No. 738102, Materials Processes;" and Project No. 7-817, "Process Development for Graphite Materials." The work was administrated by the Air Force Materials Laboratory, Research and Technology Division. Major R. H. Wilson, L. J. Conlon and W. P. Conrardy acted as Project Engineers.

Other volumes in this WADD Technical Report 61-72 series are:

Volume I - Observations by Electron Microscopy of Dislocations in Graphite, by R. Sprague.

Volume II - Applications of Anisotropic Elastic Continuum Theory to Dislocations in Graphite, by G. B. Spence.

Volume III - Decoration of Dislocations and Low Angle Grain Boundaries in Graphite Single Crystals, by R. Bacon and R. Sprague.

Volume IV - Adaptation of Radiographic Principles to the Quality Control of Graphite, by R. W. Wallouch.

Volume V - Analysis of Creep and Recovery Curves for ATJ Graphite, by E. J. Seldin.

Volume VI - Creep of Carbons and Graphites in Flexure at High Temperature, by E. J. Seldin.

Volume VII - High-Density, Recrystallized Graphite by Hot-Forming, by E. A. Neel, A. A. Kellar and K. J. Zeitsch.

Supplement - High-Density, Recrystallized Graphite by Hot-Forming, by G. L. Rowe and M. B. Carter.

Volume VIII - Electron Spin Resonance in Polycrystalline Graphite, by L. Singer and G. Wagoner.

Volume IX - Fabrication and Properties of Carbonized Cloth Composites, by W. C. Beasley and E. L. Piper.

Volume X - Thermal Reactivity of Aromatic Hydrocarbons, by I. C. Lewis and T. Edstrom.

Supplement - Thermal Reactivity of Aromatic Hydrocarbons, by I. C. Lewis and T. Edstrom.

Volume XI - Characterization of Binders Used in Fabrication of Graphite Bodies, by E. deRuiter, A. Halleux, V. Sandor and H. Tschamler.

Supplement - Characterization of Binders Used in Fabrication of Graphite Bodies, by E. deRuiter, J. F. M. Oth, V. Sandor and H. Tschamler.

Volume XII - Development of an Improved Large-Diameter, Fine-Grain Graphite for Aerospace Applications, by C. W. Waters and E. L. Piper.

Supplement - Development of an Improved Large-Diameter, Fine-Grain Graphite for Aerospace Applications, by R. L. Racicot and C. W. Waters.

Volume XIII - Development of a Fine-Grain Isotropic Graphite for Structural and Substrate Applications, by R. A. Howard and E. L. Piper.

Supplement - Development of a Fine-Grain Isotropic Graphite for Structural and Substrate Applications, by R. A. Howard and R. L. Racicot.

Volume XIV - Study of High-Temperature Tensile Properties of ZTA Grade Graphite, by R. M. Hale and W. M. Fassell.

Volume XV - Alumina-Condensed Furfuryl Alcohol Resins, by C. W. Boquist, E. R. Neilsen, H. J. O'Neil and R. E. Putcher.

Volume XVI - An Electron Spin Resonance Study of Thermal Reactions of Organic Compounds, by L. L. Singer and I. C. Lewis.

Volume XVII - Radiography of Carbon and Graphite, by T. C. Furnas, Jr. and M. R. Rosumny.

Volume XVIII - High-Temperature Tensile Creep of Graphite, by E. J. Seldin.

Volume XIX - Thermal Stresses in Anisotropic Hollow Cylinders, by Tu-Lung Weng.

Volume XX - The Electric and Magnetic Properties of Pyrolytic Graphite, by G. Wagoner and B. H. Eckstein.

Volume XXI - Arc Image Furnace Studies of Graphite, by M. R. Null and W. W. Lozier.

Volume XXI - Photomicrographic Techniques for Carbon and Graphite, by G. L. Peters and H. D. Shade.

Volume XXIII - A Method for Determining Young's Modulus of Graphite at Elevated Temperatures, by S. O. Johnson and R. B. Dull.

Volume XXIV - The Thermal Expansion of Graphite in the c-Direction, by C. E. Lowell.

Volume XXV - Lamellar Compounds of Nongraphitized Petroleum Cokes, by H. F. Volk.

Volume XXVI - Physical Properties of Some Newly Developed Graphite Grades, by R. B. Dull.

Volume XXVII - Carbonization Studies of Aromatic Hydrocarbons, by I. C. Lewis and T. Edstrom.

Volume XXVIII - Polarographic Reduction of Polynuclear Aromatics, by I. C. Lewis, H. Leibecki, and S. L. Bushong.

Volume XXIX - Evaluation of Graphite Materials in a Subscale Solid-Propellant Rocket Motor, by D. C. Hiler and R. B. Dull.

Supplement - Evaluation of Graphite Materials in a Subscale Solid-Propellant Rocket Motor, by S. O. Johnson and R. B. Dull.

Volume XXX - Oxidation-Resistant Graphite-Base Composites, by K. J. Zeitsch and J. Criscione.

Volume XXXI - High-Performance Graphite by Liquid Impregnation by C. E. Waylett, M. A. Spring and M. B. Carter.

Volume XXXII - Studies of Binder Systems for Graphite, by T. Edstrom, I. C. Lewis, R. L. Racicot and C. F. Stout.

Volume XXXIII - Investigation of Hot-Worked, Recrystallized Graphites, by J. H. Turner and M. B. Carter.

ABSTRACT

The refractory materials that could be used for high-temperature, oxidation-resistant coatings for graphite are reviewed. A study of these materials shows which are thermodynamically stable when applied directly to graphite and those which are thermodynamically stable when an intermediate coating is applied between an oxidation-resistant outer coating and the graphite. Calculations are made showing that, with properly selected intermediate reaction barriers, many very refractory oxides, such as thoria, can be used as coatings at temperatures up to their melting points.

The application of TiB_2, B_6Si, $MgO \cdot ZrO_2$, $CaZrO_3$ and $SrZrO_3$ coatings by arc-plasma spraying is described and the results of oxidation studies to determine the protection afforded graphite by these coatings are presented. Coating of TiC-TiN and SiC-Si applied to graphite by vapor deposition using the source-target method are discussed. Techniques of applying SiC coatings by pack-diffusion methods are reported and the oxidation protection afforded by the coatings is compared with that of the SiC produced by the source-target method.

This report has been reviewed and is approved.

W. G. RAMKE
Chief, Ceramics and Graphite Branch
Metals and Ceramics Division
AF Materials Laboratory

TABLE OF CONTENTS

TABLE OF CONTENTS (CONT'D)

TABLE OF CONTENTS (CONT'D)

LIST OF ILLUSTRATIONS

LIST OF ILLUSTRATIONS (CONT'D)

LIST OF ILLUSTRATIONS (CONT'D)

LIST OF ILLUSTRATIONS (CONT'D)

LIST OF ILLUSTRATIONS (CONT'D)

LIST OF TABLES

1. THEORETICAL AND PRACTICAL ASPECTS OF COATINGS TO PROTECT GRAPHITE FROM OXIDATION

1.1. Introduction

The numerous advantages of graphite over other refractory materials at elevated temperatures are well known and have been discussed elsewhere.[1] At temperatures where the physical properties of graphite are particularly attractive, its chemical affinity for oxygen often prohibits its use in any but neutral or reducing environments. In addition, the oxidation of graphite results in oxides which are gaseous and which subsequently afford no protection or barrier against further attack. The use of graphite at high temperatures in oxidizing atmospheres must consequently depend upon preventing or drastically retarding its contact with oxygen. Perhaps the most direct approach for doing this is by cladding the graphite article with an adherent, protective coating.

A prime requisite for a permanent protective coating on any material is that it be thermochemically and physically compatible with both its substrate and the hostile atmosphere for which its use is intended. Oxidation-resistant coatings for graphite, then, must be stable with regard to carbon on one side and to oxygen on the other. Physically, they should be continuous and nonporous, should be similar to their substrates in thermal expansion and should be sufficiently tough to resist erosion by impinging gases. The coatings themselves should, of course, be refractory and nonvolatile throughout the desired temperature range. Some additional requirements for special applications would include such characteristics as good thermal-shock resistance, a self-healing mechanism, chemical inertness to other gases such as water vapor, and selective heat-transfer properties.

The list of materials fulfilling the requirements for oxidation-resistant coatings is not an imposing one, even when one considers only relatively low temperatures of application, and at higher temperatures the list diminishes drastically. At very high temperatures, only the oxides are thermodynamically stable in oxidizing atmospheres, and only one of these, beryllia, is stable with respect to graphite above 2000°C.[2] It appears unlikely that any single material exists which would be satisfactory above this point. Multilayer coatings, however, do offer possibilities and will be discussed later.

Manuscript released by the authors June 1963 for publication as an ASD Technical Documentary Report.

Recent advances in graphite technology have made it possible in many cases to fabricate a graphite to approximate the thermal-expansion characteristics of a potential coating.[3] This procedure allows a greater choice of coating materials from a list which is already quite short due to thermodynamic considerations. Slight mismatches in thermal expansion can usually be tolerated if relatively thin coatings are used. Thus, except in the case where the coating material undergoes an abrupt change in CTE (coefficient of thermal expansion) selection of the proper graphite could render the thermal expansion problem of little consequence. This matching is, of course, limited to the materials whose CTE's are equal to or less than that of the "C direction CTE of single-crystal graphite.

In general, thermodynamic calculations show that a particular reaction is favorable or unfavorable but do not predict positively that it will or will not take place. For example, the oxidation of graphite to form the gaseous oxides is thermodynamically favorable even at room temperature and below, but this reaction proceeds at a negligible rate until temperatures in excess of about 500°C are attained.[1] Conversely the formation of water vapor from liquid water is unfavorable below 100°C, and yet it is well known that water evaporates readily at room temperature. Both cases indicate apparent contradictions to the thermodynamics of their respective systems. However, in the former example, kinetic factors – unpredictable by thermodynamics – are dominant and in the latter the lack of an equilibrium vapor phase is responsible.

The possibility exists, therefore, that satisfactory protective coatings for graphite may be obtained which are not in thermodynamic harmony with their surroundings. Such coatings, if effective, are certainly no less desirable than those which are thermodynamically sound, but their discovery must be more or less accidental. A program of applied research directed toward the finding of protective coatings should be founded on a more fundamental basis. The results of extensive high-temperature-materials research in recent years have made available much of the basic information necessary to begin such a program. In the following considerations, the effective protection of graphite by various coating systems at high temperatures has been predicted on the basis of coating refractoriness, volatility, and chemical stability. On the other hand, diffusion effects, which could modify the conclusions considerably, were not considered due to the lack of pertinent data.

1.2. Single-Layer Coatings

1.2.1. Criteria for Selecting Coating Materials

In general, the simpler coatings for the oxidation protection of graphite are preferred over those which are more complex. The problems of application, bonding and compatibility, which increase drastically with the number of layers, are reduced to a minimum when single-layer coatings are considered. In each case the material in contact with the oxidizing atmosphere must be thermodynamically stable with respect to

oxygen. As previously stated, only the refractory oxides fulfill this requirement at high temperatures. This means, of course, that a single-layer protective coating must consist merely of an oxide layer on the graphite article it is to protect.

The selection of promising coating materials, which are thereby limited to the list of refractory oxides, is governed by two main factors: the volatility of the material and its thermodynamic behavior with graphite. For most applications, liquid coatings are objectionable and must be eliminated from consideration even though their volatility may be acceptably low. For this reason, a high melting point also becomes a necessary coating characteristic.

Silicon dioxide has been used successfully as an oxidation-resistant coating and has provided protection for graphite up to about 1723°C, or the melting point of the SiO_2.[4] The search for protection at higher temperatures, therefore, should begin by considering only oxides with higher melting points. In Table 1 are listed some of the simple oxides and their melting points which fall into this category.[5] Missing from this table are the oxides of scandium, actinium, and the rare earths, which are thought to be refractory, but for which the melting-point data are lacking or uncertain.

Table 1. Melting Points of Pure, Simple, Refractory Oxides*

Alphabetical			By Melting Point		
Material	Formula	M. P., °C	Material	Formula	M. P., °C
Aluminum Oxide	Al_2O_3	2045	Thorium Oxide	ThO_2	3000
Barium Oxide	BaO	1917	Magnesium Oxide	MgO	2800
Beryllium Oxide	BeO	2550	Hafnium Oxide	HfO_2	2777
Calcium Oxide	CaO	2600	Cerium Oxide	CeO_2	2730
Cerium Oxide	CeO_2	2730	Zirconium Oxide	ZrO_2	2687
Chromic Oxide	Cr_2O_3	2265	Calcium Oxide	CaO	2600
Cobalt Oxide	CoO	1805	Beryllium Oxide	BeO	2550
Gallium Oxide	Ga_2O_3	1740	Strontium Oxide	SrO	2415
Hafnium Oxide	HfO_2	2777	Yttrium Oxide	Y_2O_3	2410
Lanthanum Oxide	La_2O_3	2305	Lanthanum Oxide	La_2O_3	2305
Magnesium Oxide	MgO	2800	Uranium Oxide	UO_2	2280
Manganese Oxide	MnO	1780	Chromic Oxide	Cr_2O_3	2265
Nickel Oxide	NiO	1950	Aluminum Oxide	Al_2O_3	2045
Niobium Oxide	Nb_2O_5	1772	Vanadium Oxide	V_2O_3	1977
Silicon Oxide	SiO_2	1723	Zinc Oxide	ZnO	1975
Strontium Oxide	SrO	2415	Nickel Oxide	NiO	1950
Tantalum Oxide	Ta_2O_5	1890	Barium Oxide	BaO	1917
Thorium Oxide	ThO_2	3000	Tantalum Oxide	Ta_2O_5	1990
Titanium Oxide	TiO_2	1853	Titanium Oxide	TiO_2	1853
Uranium Oxide	UO_2	2280	Cobalt Oxide	CoO	1805
Vanadium Oxide	V_2O_3	1977	Manganese Oxide	MnO	1780
Yttrium Oxide	Y_2O_3	2410	Niobium Oxide	Nb_2O_5	1772
Zinc Oxide	ZnO	1975	Gallium Oxide	Ga_2O_3	1740
Zirconium Oxide	ZrO_2	2687	Silicon Oxide	SiO_2	1723

Note: Scandium, actinium, and certain rare-earth oxides have been omitted because of missing or uncertain melting-point data.

* Taken mainly from Reference (5). More recent melting-point data have been substituted when available.

There are several compound oxides which also have high melting points and some of the more promising ones are given in Table 2.[6]

Table 2. Melting Points of Pure, Compound, Refractory Oxides

Alphabetical Listing			By Melting Point		
Material	Formula	M.P., °C	Material	Formula	M.P., °C
Aluminum Silicate	$3Al_2O_3 \cdot 2SiO_2$	1830*	Thorium Zirconate	$ThO_2 \cdot ZrO_2$	2800
Aluminum Titanate	$Al_2O_3 \cdot TiO_2$	1855	Strontium Zirconate	$SrO \cdot ZrO_2$	2700
Aluminum Titanate	$Al_2O_3 \cdot 2TiO_2$	1895	Barium Zirconate	$BaO \cdot ZrO_2$	2700
Barium Aluminate	$BaO \cdot Al_2O_3$	2000	Beryllium Zirconate	$3BeO \cdot 2ZrO_2$	2535
Barium Aluminate	$BaO \cdot 6Al_2O_3$	1860	Zirconium Silicate	$ZrO_2 \cdot SiO_2$	2420*
Barium Silicate	$2BaO \cdot SiO_2$	1755	Calcium Zirconate	$CaO \cdot ZrO_2$	2345
Barium Zirconate	$BaO \cdot ZrO_2$	2700	Calcium Chromite	$CaO \cdot Cr_2O_3$	2170
Beryllium Aluminate	$BeO \cdot Al_2O_3$	1870	Calcium Chromate	$CaO \cdot CrO_3$	2160
Beryllium Silicate	$BeO \cdot SiO_2$	1755	Calcium Titanate	$3CaO \cdot TiO_2$	2135
Beryllium Silicate	$2BeO \cdot SiO_2$	1750*	Magnesium Aluminate	$MgO \cdot Al_2O_3$	2135
Beryllium Titanate	$3BeO \cdot TiO_2$	1800	Calcium Silicate	$2CaO \cdot SiO_2$	2120
Beryllium Zirconate	$3BeO \cdot 2ZrO_2$	2535	Magnesium Zirconate	$MgO \cdot ZrO_2$	2120
Calcium Chromate	$CaO \cdot CrO_3$	2160	Zinc Zirconium Silicate	$ZnO \cdot ZrO_2 \cdot SiO_2$	2078
Calcium Chromite	$CaO \cdot Cr_2O_3$	2170	Magnesium Lanthanate	$MgO \cdot La_2O_3$	2030
Calcium Phosphate	$3CaO \cdot P_2O_5$	1730	Nickel Aluminate	$NiO \cdot Al_2O_3$	2015
Calcium Silicate	$3CaO \cdot SiO_2$	1900*	Strontium Aluminate	$SrO \cdot Al_2O_3$	2010
Calcium Silicate	$2CaO \cdot SiO_2$	2120	Barium Aluminate	$BaO \cdot Al_2O_3$	2000
Calcium Silicon Phosphate	$5CaO \cdot SiO_2 \cdot P_2O_5$	1760	Magnesium Chromite	$MgO \cdot Cr_2O_3$	2000
Calcium Titanate	$CaO \cdot TiO_2$	1975	Calcium Titanate	$CaO \cdot TiO_2$	1975
Calcium Titanate	$2CaO \cdot TiO_2$	1800	Cobalt Aluminate	$CoO \cdot Al_2O_3$	1955
Calcium Titanate	$3CaO \cdot TiO_2$	2135	Zinc Aluminate	$ZnO \cdot Al_2O_3$	1950
Calcium Zirconate	$CaO \cdot ZrO_2$	2345	Calcium Silicate	$3CaO \cdot SiO_2$	1900*
Cobalt Aluminate	$CoO \cdot Al_2O_3$	1955	Aluminum Titanate	$Al_2O_3 \cdot 2TiO_2$	1895
Magnesium Aluminate	$MgO \cdot Al_2O_3$	2135	Magnesium Silicate	$2MgO \cdot SiO_2$	1885
Magnesium Chromite	$MgO \cdot Cr_2O_3$	2000	Beryllium Aluminate	$BeO \cdot Al_2O_3$	1870
Magnesium Ferrite	$MgO \cdot Fe_2O_3$	1760	Barium Aluminate	$BaO \cdot 6Al_2O_3$	1860
Magnesium Lanthanate	$MgO \cdot La_2O_3$	2030	Aluminum Titanate	$Al_2O_3 \cdot TiO_2$	1855
Magnesium Silicate	$2MgO \cdot SiO_2$	1885	Magnesium Titanate	$2MgO \cdot TiO_2$	1835
Magnesium Titanate	$2MgO \cdot TiO_2$	1835	Aluminum Silicate	$3Al_2O_3 \cdot 2SiO_2$	1830*
Magnesium Zirconate	$MgO \cdot ZrO_2$	2120	Beryllium Titanate	$3BeO \cdot TiO_2$	1800
Magnesium Zirconium Silicate	$MgO \cdot Zr_2O_3 \cdot SiO_2$	1793	Calcium Titanate	$2CaO \cdot TiO_2$	1800
Nickel Aluminate	$NiO \cdot Al_2O_3$	2015	Potassium Aluminum Silicate	$K_2O \cdot Al_2O_3 \cdot 2SiO_2$	1800
Potassium Aluminum Silicate	$K_2O \cdot Al_2O_3 \cdot 2SiO_2$	1800	Magnesium Zirconium Silicate	$MgO \cdot ZrO_2 \cdot SiO_2$	1793
Strontium Aluminate	$SrO \cdot Al_2O_3$	2010	Strontium Phosphate	$3SrO \cdot P_2O_5$	1767
Strontium Phosphate	$3SrO \cdot P_2O_5$	1767	Calcium Silicon Phosphate	$5CaO \cdot SiO_2 \cdot P_2O_5$	1760
Strontium Zirconate	$SrO \cdot ZrO_2$	2700	Magnesium Ferrite	$MgO \cdot Fe_2O_3$	1760
Thorium Zirconate	$ThO_2 \cdot ZrO_2$	2800	Barium Silicate	$2BaO \cdot SiO_2$	1755
Zinc Aluminate	$ZnO \cdot Al_2O_3$	1950	Beryllium Silicate	$BeO \cdot SiO_2$	1755
Zinc Zirconium Silicate	$ZnO \cdot ZrO_2 \cdot SiO_2$	2078	Beryllium Silicate	$2BeO \cdot SiO_2$	1750*
Zirconium Silicate	$ZrO_2 \cdot SiO_2$	2420*	Calcium Phosphate	$3CaO \cdot P_2O_5$	1730

*Incongruent Melting

If any of these oxides are to react with graphite, the process may be described by one or a combination of the following general reactions:

Simple reduction of the oxide to its metallic constituent with the evolution of carbon monoxide,

$$\left(\frac{1}{y}\right) M_xO_y + C \rightarrow \left(\frac{x}{y}\right) M + CO; \qquad (1)$$

Formation of an oxide in which the metallic constituent has been reduced to a lower valence state, again with the evolution of carbon monoxide,

$$\left(\frac{z}{yz - wx}\right) M_xO_y + C \rightarrow \left(\frac{x}{yz - wx}\right) M_zO_w + CO; \qquad (2)$$

Formation of a stable carbide and the evolution of carbon monoxide,

$$\left(\frac{1}{y}\right) M_xO_y + \left(\frac{vx + yz}{yz}\right) C \rightarrow \left(\frac{x}{yz}\right) M_zC_v + CO. \qquad (3)$$

It is quite possible in certain instances for the condensed phase-reaction products, especially in equations (2) and (3), to form boundary layers and prevent further reaction between oxide and graphite (e.g., a C-SiC-SiO_2 sequence). It is more likely, however, that an oxide coating initially in contact with graphite would rupture due to buildup of CO pressure between layers before substantial reaction interference by the intermediate phase could be effected. Rupture and subsequent failure of the coating should become important when the partial pressure of carbon monoxide exceeds the environmental ambient pressure. If all reaction components except CO are condensed phases, and if the ambient pressure is considered to be one atmosphere, then the point of rupture is theoretically approached at the temperatures which render the Gibbs free energies of the above equations zero.

Figure 1 presents the free energy-versus-temperature curves for the reactions between some of the more promising oxides and graphite.[7, 8, 9] It can readily be seen that in most cases the maximum temperature at which these oxides can be used appears drastically reduced when they must be in contact with graphite. Unfortunately, thermodynamic data are not available for all the oxide-graphite reactions of interest, and in many cases the existing information is not reliable. For example, yttrium oxide with its melting point of 2410°C is an attractive coating material, but the thermodynamic properties of its carbide, YC_2,

were not recorded in the literature consulted. As a further example, it has been reported that beryllium oxide is stable in contact with carbon to 2300°C.[2] Some recent thermodynamic information appears to substantiate this finding,[7] yet in other recent work this oxide is said to react with carbon below 2000°C.[10] According to these latter authors, there is no oxide which will not react with carbon above 2000°C. Of course, the most conclusive way to resolve this discrepancy is by actually applying and testing the oxide coating; however, it is time consuming and expensive.

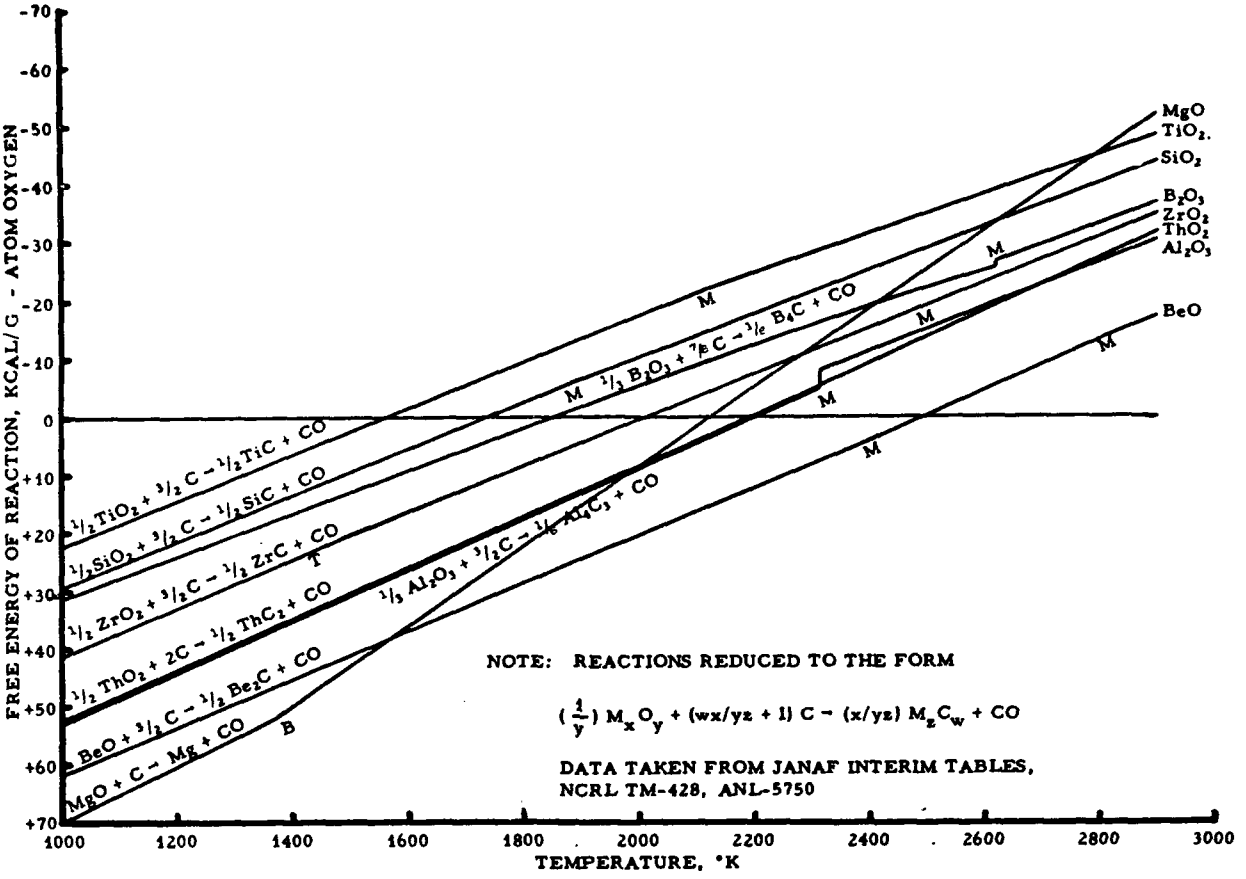

L-387

Figure 1. Free Energy of Reaction Between Graphite and Various Refractory Oxides

1.2.2. Simple Oxides as Coatings

Simple oxides, that is, those oxides which contain only one cation, generally are more refractory than compound oxides. Although there are no stable refractory oxides of the elements in Groups I-a, I-b, V-a, VI-a, VII-a and 0,[8] other groups of the periodic table do contain elements which

have refractory oxides of interest as coating materials. These groups will be considered separately in the following sections.

1.2.2.1. Group II-a Oxides

In Group II-a, only BeO and MgO do not react with water vapor at room temperature. CaO, SrO, BaO and perhaps RaO are all refractory, but if bodies of these oxides are stored for more than a few days even in low-humidity atmospheres, they will hydrate and disintegrate.[11] MgO also shows this tendency, but to a somewhat lesser degree. However, it has been found that a process known as "dead-burning"[11] will produce a fairly stable form of MgO. This does not hold true for the heavier Group II-a oxides. Beryllium oxide (melting point 2550°C) is the oxide most stable with respect to graphite, although, as mentioned earlier, the maximum temperature at which it may be used in contact with graphite is subject to some disagreement. Recent kinetic studies[12] have indicated that a temperature of 1707°C is required for 0.1 per cent of the oxide to be reduced in 15 minutes. The free energy of reaction (see Figure 1) becomes favorable at 2220°C. Magnesium oxide has a melting point of about 2800°C. There are no stable carbides of magnesium,[13] but the oxide can be reduced to elemental Mg and CO at temperatures in excess of about 1850°C. Thus, both MgO and BeO are good possibilities for single-layer coating material. BeO is known to be quite toxic,[14] however, and the manner in which it is applied and handled must be supervised closely.

1.2.2.2. Group III-b Oxides

Very little high-temperature work has been done on the compounds of the Group III-b elements, scandium and yttrium. They are both known to form sesquioxides which are quite stable and refractory.[15,16] They are also known to form the carbides ScC and YC_2,[17] but apparently no thermodynamic data have been reported for these compounds. Until information to the contrary is obtained, these oxides should be regarded as possibilities for coating materials.

1.2.2.3. Group IV-b Oxides

Titanium, zirconium and hafnium, from Group IV-b form both refractory oxides and carbides. The fact that titanium can have many different oxide compositions makes it the least desirable of the three. As for the dioxide of titanium, it is very difficult to obtain a dense, strong shape without at least partial reduction to a lower form of oxide.[18] A lower oxide, Ti_2O_3, has a higher melting point (1900°C) than the dioxide (1850°C), but an intermediate oxide composition, $2Ti_2O_3 \cdot 3TiO_2$, has a

melting point of only 1640°C. Using TiO_2 as a coating on graphite will almost assuredly result in its reduction to $2Ti_2O_3 \cdot 3TiO_2$. With this behavior, titania certainly is not as good a coating material as silica and, therefore, it will be discarded as a high-temperature coating possibility. Zirconia, especially zirconia stabilized to prevent radical phase changes,[19] is an excellent refractory with a high melting point, low affinity for water vapor, and only one oxide composition - ZrO_2. As shown in Figure 1, ZrO_2 is stable with respect to carbon to about 1730°C which would put its temperature limit as a single-layer coating in the same range as the successful $SiC-SiO_2$ double-layer coating. The maximum temperature of serviceability of zirconium should be increased a great deal when applied on graphite as a carbide-oxide double-layer coating. Hafnium oxide, which is very similar to zirconia, yet is more refractory, forms a stable carbide, and its oxide should not react with carbon below about 1750°C, making HfO_2 an even more promising coating material than zirconia. Here the thermodynamics of the carbon reaction had to be estimated in part,[20] and this threshold temperature might be considered unreliable and overly optimistic. However, recent experimental evidence has been presented which indicates a threshold temperature of 1732°C.[21] The thermodynamic estimations are thereby confirmed and HfO_2 has to be considered a very promising coating material.

1.2.2.4. Group V-b Oxides

In Group V-b, vanadium and niobium sesquioxides have rather high melting points, 1977°C and 1772°C, respectively, but they also have the rather rare and disappointing characteristic of being unstable in oxidizing atmospheres.[11] These two oxides react with oxygen to form V_2O_5 and Nb_2O_5 with low melting points (670°C and 1460°C) which make these materials unacceptable as high-temperature coatings. The third member of the group, tantalum, forms only the pentoxide, Ta_2O_5, with a melting point of 1890°C. It forms two stable carbides, Ta_2C and TaC, the latter having the very high melting point of 3877°C;[22] however, limited thermodynamic data indicate that the oxide should react with graphite above 1100°C. For the reasons given above, none of the oxides in this group should provide adequate high-temperature oxidation protection for graphite.

1.2.2.5. Group VI-b Oxides

The oxides of molybdenum and tungsten in Group VI-b are both volatile at the temperatures of interest.[8] MoO_3 and WO_3 reach one atmosphere pressure at about 1100°C and 1800°C, respectively. Chromic oxide, while not nearly so volatile as MoO_3 and WO_3, should react with graphite at temperatures even below 1200°C. The other oxides of chromium are not refractory and tend to decompose readily at only moderate

temperatures; i.e., less than 1000°C.

1.2.2.6. Group VII-b Oxides

The Group VII-b oxides also do not appear to be satisfactory. MnO, with a melting point only about 50°C higher than silica, would offer very little improvement over present coatings even if it could be prevented from oxidizing to one of its less refractory oxides. Technetium is a synthetic element and as such is extremely expensive. Technetium dioxide is said to have a melting point of around 2100°C, but it, too, should be subject to oxidation to lower-melting-point oxides. None of the oxides of rhenium have high enough melting points to make them worth considering as high-temperature, oxidation-protection coatings for graphite.

1.2.2.7. Group VIII Oxides

In Group VIII, the oxides of iron have melting points lower than SiO_2. NiO with a melting point of 1950°C is refractory enough to be considered as a coating material, but it is reduced by graphite at very low temperatures. CoO is both easily oxidized to Co_3O_4 with a low melting point and reduced by carbon to elemental Co. The oxides of the platinum group metals, also in Group VIII, are all gaseous or unstable with respect to disproportionation at high temperatures. However, the elements themselves could offer oxidation protection. Platinum and paladium have melting points of only 1770°C and 1555°C, respectively, and are not refractory enough to offer substantial improvement over present coatings. Eutectics with carbon make the liquidus temperatures for these elements even lower. At moderate temperatures (600-1000°C) iridium oxidizes visibly in air.[23] At higher temperatures it remains bright, but loses weight rapidly, more so than would be expected from its equilibrium vapor pressure. Presumably this is due to some catalytic action by oxygen. Iridium has one of the highest metal-carbon eutectics (2296°C) and is very interesting because of this property. Iridium recently has been deposited onto refractory metals by an electron bombardment technique and apparently protects these metals from oxidation.[24] It appears that graphite should be coated as easily with iridium by this method, and that the oxidation protection should be comparable to that afforded the refractory metals. Although the reported high-vaporization rate in air is unpromising, iridium-coated graphite should certainly warrant actual laboratory investigation. Rhodium is known to oxidize slowly in air at 600°C, the rate reaching a maximum at 800°C.[23] The oxidation rate decreases between 800 and 1000°C and the oxide disappears altogether above 1000°C. However, oxygen may increase the rate of volatilization at high temperatures. Rhodium has a minimum metal-carbon eutectic below

that of platinum[13] and does not offer much potential as a high-temperature coating. Osmium oxidizes very readily, yielding the poisonous and volatile tetroxide[23] which, of course, eliminates this element from consideration as an outside coating. The possible use of osmium as an intermediate layer in a multilayer coating is suggested by the fact that it has a minimum metal-carbon eutectic of 2732°C, higher than that of any other element except tantalum (2902°C).[13] Ruthenium resembles iridium with respect to its high-temperature behavior in air[23] since it oxidizes slowly above 450°C, forming the dioxide which is only slightly volatile below 1100°C. At higher temperatures, where the oxide is unstable, ruthenium is a bit more volatile than iridium. The minimum ruthenium-carbon eutectic occurs at about 1950°C,[13] making it refractory enough to be acceptable. Although the volatility data are suspect, it appears that both iridium and ruthenium could be possible coating materials.

1.2.2.8. Group II-b Oxides

Zinc has the only refractory oxide in Group II-b. However, ZnO volatilizes readily at 1700°C and decomposes under atmospheric pressure at 1950°C,[25] never reaching its melting point (1975°C) under these conditions.

1.2.2.9. Group III-a Oxides

Group III-a contains two elements whose oxides have relatively high melting points, aluminum and gallium. Gallium oxide, Ga_2O_3, is not very interesting as a high-temperature coating material because it has a melting point of only 1740°C and it is easily reduced to a lower, volatile oxide (Ga_2O) by carbon at very low temperatures.[26] Aluminum oxide, Al_2O_3, has a higher melting point (2045°C) and is thermodynamically stable with respect to graphite up to about 1900°C (see Figure 1). These temperatures offer some improvement over silica and place Al_2O_3 in the category of possible coating materials.

1.2.2.10. Group IV-a Oxides

There are only two elements in Group IV-a, silicon and tin, which form refractory oxides. Tin has an oxide with a reported melting point of over 1900°C, but it is known to sublime at about 1510°C.[26] It is also easily reduced below this temperature and as a consequence need not be considered further. Silica, as has already been mentioned, has proved to be the most successful protective coating material for graphite, but there must be an intermediate layer between the silica and the graphite substrate for the protection to be achieved. As shown in Figure 1, silica should react with graphite at temperatures above about 1475°C. In practice the silica

coating is generally achieved by subjecting a silicon carbide-coated article to oxidation. This produces a graphite-silicon carbide-silicon dioxide sequence, with the intermediate layer of SiC preventing contact between the inner and outer (potentially reactive) layers. Formation of the intermediate SiC layer by reaction of an SiO_2 coating on graphite would not achieve the same result. The evolution of CO gas at the reaction interface would, in all probability, tend to rupture the protective SiO_2 coating. Therefore, silica cannot be considered as a possibility for a single-layer protective coating.

1.2.2.11. Lanthanide Series Oxides

Very few definite conclusions can be drawn as to the usefulness of the oxides of the rare-earth lanthanide series. The thermodynamic properties of many of these compounds have never been ascertained. Others have been only estimated, or assigned tentative values based on qualitative or incomplete investigations. The lanthanide series oxides in general appear to have quite high melting points. Those known with some degree of certainty are La_2O_3 (2305°C), CeO_2 (2600°C), Nd_2O_3 (2270°C), Sm_2O_3 (2300°C), Eu_2O_3 (2050°C), Gd_2O_3 (2300°C), and Dy_2O_3 (2340°C).[27] Very favorable free energies of formation at high temperature (about -100 kilocalories at 2000°K)[8] indicate that these lanthanide oxides are among the most stable oxides. Carbides of this series are also known to exist, but data on the stability of these compounds have not been reported. It is known that they have dicarbide stoichiometry and that they are decomposed by water vapor.[28]

Most of the rare-earth oxides should undergo only limited reaction with graphite up to temperatures of about 1900-2000°C if it is assumed that rare-earth carbide formation is not as favorable as that of zirconium or titanium which are two of the most stable carbides. Cerium dioxide is, however, easily reduced to the lower melting (1690°C) sesquioxide by carbon at much lower temperatures.[29] Praseodymium and terbium are other rare earths known to have more than one oxide composition,[30] but these should be unstable at high temperatures and thus should have little effect on the oxide-carbon equilibrium. With the exceptions of: (a) lanthanum oxide, which hydrates readily and is unstable in air;[26] (b) the oxide of promethium, which is a radioactive, synthetic element; and (c) cerium oxide, the rare-earth oxides appear, in the light of the limited data, to be interesting possibilities for protective coatings. Perhaps the major objection to the use of these materials is their relatively high cost, but with the exception of europium and lutetium, the rare earths are no more costly than hafnium, previously considered to be a promising coating material.

1.2.2.12. Antinide Series Oxides

All elements in the actinide series, except actinium, thorium, protactinium and uranium, are synthetic. Uranium and protactinium dioxides have high melting points (2280°C and 2290°C, respectively), but both are unstable with respect to higher oxides in oxidizing atmospheres. Actinium sesquioxide is also refractory, having a melting point of approximately 1980°C, and its free energy of formation at elevated temperatures is more negative than that reported for any other oxide.[8] Furthermore, no oxide compositions other than Ac_2O_3 are known to exist in the Ac-O system. This means that Ac_2O_3 is one of the most stable oxides known. There are apparently no thermodynamic data available on the carbide of this element but, assuming its free energy of formation is not greatly different from those of the carbides of thorium and uranium, there should be no reaction between graphite and actinium oxide at temperatures below the oxide melting point (1980°C). This would place Ac_2O_3 near BeO in the list of oxides most stable in contact with graphite. Beryllia is now accepted as the best oxide in this category. Although the melting point (estimated) of actinium oxide is lower than that of beryllia (2550°C), structural shapes of the latter oxide exhibit a tendency to disintegrate at temperatures in the vicinity of 2000°C[31] and therefore may not provide the necessary continuous protection required of coatings. There are no stable isotopes of the elements in the actinide series. It is unfortunate that the most abundant isotope of actinium, whose oxide appears so promising, has one of the shorter half-lives of the naturally occurring elements in this series. With a half-life of only 22 years, and a rapid decay through its daughter elements to lead 207 and 208, actinium in oxide form will contain a substantial amount of low-melting lead oxide in a matter of only a few years. Therefore, if refractoriness is required in a coating, it would be necessary for actinium oxide coatings to be used within a reasonable time after their application – say, two or three years.

Thorium oxide has the highest melting point (3000°C) of all the oxides; higher by 200° than the melting points of MgO and HfO_2, the next most refractory oxides. The vapor pressure of ThO_2 is also low at high temperatures[32] and, as shown in Figure 1, it should be thermodynamically stable in contact with graphite to about 1925°C. In confirmation of the latter, experimental evidence indicates that no surface-to-surface contact reaction occurs below 2000°C.[2] The most disappointing characteristic of ThO_2 is its poor thermal-shock resistance,[33] primarily due to the fact that it has the undesirable combination of low thermal conductivity and high thermal expansion. Hopefully, the application of rather thin coatings of ThO_2 to a graphite having the proper thermal expansion characteristics would overcome this thermal-shock handicap. Though radioactive, the most abundant isotope of thorium has a very long half-life (1.4×10^{10} years),

and thus the time problem associated with actinium is not present to any significant extent with thorium.

1.2.2.13 Summary of Simple Materials for Single-Layer Coatings

Based on thermodynamic considerations, the simple oxides that appear to offer the best possibilities for single-layer oxidation protection of graphite (superior to that afforded by SiC-SiO_2 coatings) are small in number and have severe limitations on their use. With but one exception, Ac_2O_3, none of the oxides considered as promising can be used at temperatures near their melting points, due to the onset of their respective reactions with graphite. In some extreme cases, the maximum-use temperature is lowered by over 1000°C from their melting points.

The few oxides that successfully meet the thermodynamic requirements for single-layer, oxidation protection coatings for graphite are given in Table 3.

Table 3. Thermodynamically Promising Single-Layer Simple Oxide Coating Materials for High-Temperature Oxidation Protection of Graphite

Material	M.P., °C	Temperature of Onset Reaction with Graphite °C	Remarks
Ac_2O_3	1980	2000	Radioactive, short half-life
Al_2O_3	2045	1925	No apparent limitations
BeO	2550	2220	Toxic; possibly decrepitates at 2000°C
HfO_2	2777	1750	Undergoes phase inversion at 1600-1700°C
MgO	2800	1850	Must be dead-burned to prevent hydration
ThO_2	3000	1925	Radioactive; low thermal-shock resistance
ZrO_2	2687	1730	Undergoes severe phase inversion at approx. 1200°C
R.E.O.*	> 2000	-	Data lacking; La, Ce and Pm oxides excluded

*Many of the thermodynamic data on the rare-earth oxide(R.E.O.)-carbon systems are unavailable and consequently the stabilities of these oxides are not calculable. Scandium and yttrium oxides also fall into this category.

Iridium and ruthenium coatings should also offer oxidation protection for graphite, Although they are not oxides, they should be included with this group of coating materials.

1.2.3. Compound Oxides as Coatings

The compound oxides, especially the zirconates which are very refractory, provide additional possibilities for single-layer coatings. There are many of these compound oxides for which melting points are known (see Table 2), and probably many more have acceptably high melting points. Except for two or three rare instances, the thermodynamic properties of the compound oxides are either incompletely known or are missing entirely. This is readily understandable, considering the fact that these data are also lacking for a good many simple oxides.

Generally speaking, the melting point of a compound oxide will be lower than that of its highest-melting constituent oxide. (Strontium zirconate is apparently one exception.) The use of a compound oxide as a coating material must usually come, therefore, at the expense of some sacrifice of refractoriness; and only when it shows some marked improvement over its most refractory constituent oxide in other properties is this sacrifice justified. This improvement may take the form of a reduced tendency to hydrate, as when calcium and heavier Group II-a oxides are combined with other oxides. Unusable in simple oxide form because of this hydrating characteristic, these oxides may provide excellent protection for graphite when they are used in the compound form.

Undesirable phase changes in simple oxides may vanish when they are incorporated into compound oxides. Phase changes that produce an abrupt volumetric expansion or contraction are particularly troublesome and coating materials undergoing these changes may rupture or fail to provide the protection desired for the substrate beneath. This expansion-contraction problem is alleviated in a great many instances, when a simple oxide is combined with another. The disastrous monoclinic-tetragonal phase change in zirconium oxide occurring near 1200°C may, for example, be eliminated by the formation of various zirconates. In the case of calcium zirconate, undesirable properties of both constituent oxides are obviated. The hydration tendency of CaO and the abrupt phase change of ZrO_2 are both missing in $CaO \cdot ZrO_2$. This is brought about, however, with a sacrifice in refractoriness since zirconium oxide melts at a temperature about 350°C higher than calcium zirconate. In zirconium silicate (which also may be considered a zirconate), not only is the zirconia phase change eliminated, but also a great reduction in thermal expansion over both single oxides is effected. Low coefficients of thermal expansion are especially desirable where the materials are subject to thermal shock or thermal cycling as is the case with oxidation-resistant refractory coatings. Since $ZrO_2 \cdot SiO_2$ melts at 2420°C, a 270°C reduction from the ZrO_2 melting point must be tolerated.

No general statement can be made as to whether compound oxides will be more, or less, thermodynamically stable with respect to graphite than the most stable constituent oxide. Because the free energy of formation of compound oxides from the single oxides is usually quite small, the tendency is for the compound oxide to be less stable. However, in cases where this quantity is substantial, and where the single oxides are of nearly the same stability, it is possible for the reaction-threshold temperature to be increased by the use of the compound oxide.

The system $MgO\text{-}SiO_2$ can be used to illustrate the more common case in which the compound oxide is less stable than its most stable constituent oxide. Figure 1 shows that MgO will react with graphite above about 1852°C, and SiO_2 above 1465°C. In the temperature range of interest, the free energies of these reactions are given by the following equations:

$$MgO_{(s)} + C_{(gr)} \rightarrow Mg_{(s)} + CO_{(g)};\ \Delta F_T = -0.0688T + 146.3 \text{ kcal} \quad (4)$$

$$\tfrac{1}{2}\ SiO_{2\,(s)} + \tfrac{3}{2}\, C_{(gr)} \rightarrow \tfrac{1}{2}\ SiC_{(s)} + CO_{(g)};\ \Delta F_T = -0.0388T + 67.6 \text{ kcal.} \quad (5)$$

The free energy of combination of these oxides is given by

$$MgO_{(s)} + \tfrac{1}{2}\ SiO_{2\,(s)} \rightarrow \tfrac{1}{2}\ Mg_2SiO_{4\,(s)};\ \Delta F_T = -7.6 \text{ kcal.} \quad (6)$$

The free energy of the graphite reaction with the compound oxide can then be represented by

$$\tfrac{1}{2}\, Mg_2SiO_{4\,(s)} + \tfrac{5}{2}\, C_{(gr)} \rightarrow Mg_{(s)} + \tfrac{1}{2}\, SiC_{(s)} + 2CO_{(g)};\ \Delta F_7 = \Delta F_4 + \Delta F_5 - \Delta F_6$$

$$\text{or}\quad \Delta F_7 = -0.1076T + 221.5 \text{ kcal.} \quad (7)$$

The threshold temperature for this reaction is that temperature for which the free energy becomes zero (1786°C). Therefore, $2MgO \cdot SiO_2$ is less stable with respect to graphite than is MgO alone. The compound oxide system has a melting point about 900°C lower than the melting point of MgO.

The magnesium silicate example is a rare case in which the reactions can be thermodynamically characterized. None of the more refractory compounds have been investigated completely enough to allow drawing conclusions as to stability. It is to be expected, however, that

little improvement with regard to graphite reaction temperature will be realized by these oxides. Justification as to their use as single-layer coatings will have to come from improvements in other properties. Coatings for higher temperatures must probably be relegated to those of the multiple-layer variety.

1.3. Multiple-Layer Coatings

The conception of coatings of more than one layer is a natural consequence of the thermodynamic inadequacies of single-layer coatings. Most refractory oxides should provide serviceable coatings up to temperatures close to their melting points, yet, because of the strong reducing tendencies of graphite, few oxides can remain unreacted at these temperatures. In some cases, such as chromic oxide and thorium oxide, the temperature of serviceability is reduced more than 1000°C by reactions of the oxides with graphite. It is only logical, therefore, that some material be sought which, when interposed between the oxide coating and graphite, would prevent or hamper the reduction process.

The simplest of such reaction barriers are the refractory metals. They can be applied as coatings with relative ease by several methods, and the thermochemistry of the resulting layered coatings is not exceedingly complex. The temperature at which a liquid phase occurs is of prime importance in selecting a coating material. Seven refractory metals have minimum metal-carbon (eutectic) solidus temperatures above 2200°C,[10] and these are listed in Table 4.

Table 4. Refractory Metal-Carbon Eutectics with Solidus Temperatures Above 2200°C

Metal	Melting Point, °C	Min. M-C Eutectic, °C
Tantalum	3000	2902
Osmium	2700	2732
Tungsten	3380	2732
Rhenium	3180	2486
Niobium	2500	2328
Iridium	2450	2296
Molybdenum	2620	2210

Tantalum, tungsten, niobium and molybdenum are carbide formers and, as such, cannot remain unreacted in thermodynamic equilibrium with

carbon. If totally reacted, the corresponding carbide-carbon eutectics for these metals will be higher than the values given in Table 4. Depending upon the method of application of these metals, they could be unreacted, partially reacted to the point at which a carbon-carbide-metal sequence exists, or totally reacted. In many cases it is desirable to have at least partial reaction because a stronger chemical bond can be acquired between the graphite and the coating. However, unreacted, diffusion-type bonds have shown excellent strength in other instances.[34]

The refractory metals, osmium, rhenium and iridium, which do not form carbides, are much more expensive than the others in this group. Osmium, for example, is over 300 times as expensive as molybdenum (per unit volume). The cheapest nonreactive metal, rhenium, is about 30 times as costly as the most expensive carbide former, tantalum.[10] Rhenium has, however, recently been applied as a coating on graphite by aqueous electrodeposition with excellent results[35] and may warrant the rather high cost should other lower-cost coatings prove to be less satisfactory.

Once the refractory metal coating has been successfully applied, the problem changes from the oxidation protection of graphite to that of the metal. It would appear at first glance that the problem is relatively unchanged, and perhaps no less difficult than the original task. But an important thermochemical distinction exists. In the first case, the relatively amphoteric nature of graphite provides thermodynamic impetus to the failure of an oxide coating by allowing both chemical components of the oxide to enter into reaction. In other words, the energy released by an oxide-graphite reaction is enhanced because graphite not only can react to form its oxide, but also can release more energy by reacting with the oxide cation to form the carbide. This dual-reaction drive is not shared by the refractory metals. The energy released by an oxide-metal reaction can come only from the reduction of the oxide cation and its displacement by the refractory metal.

Another important difference exists between graphite and the refractory metals. The free energy of formation of carbon monoxide becomes more negative with increasing temperatures,[8] and free energies of formation of the refractory oxides become more positive with increasing temperatures. An increase in temperature will always render an oxide-graphite reaction more favorable, but an oxide-metal reaction will become more favorable only if the free energy of formation of the refractory metal oxide becomes more positive at a rate slower than that of the coating oxide. When this latter condition is not met, it is conceivable that such systems may become even more stable with increasing temperature.

The above considerations, theoretically at least, indicate that the protection of a refractory metal from oxidation should be a much simpler affair than providing the same protection for graphite.

The refractory carbides form another group of materials that should prove to be favorable as the intermediate layer in multilayered coatings. These materials have some of the highest melting points known and their minimum eutectic temperatures with graphite are also very high. Some of the higher-temperature eutectics which have been measured or estimated are given in Table 5.

Table 5. Carbide-Graphite Eutectics

Carbide	Melting Point,[9] °C	Min. MC-C Eutectic, °C
HfC	3887	3250[36]
TaC	3875	3310[36]
ZrC	3530	2920[36]
NbC	3500	3150[36]
Ta_2C	3400	*
TiC	3250	3080[36]
VC	2830	-
Al_4C_3	2800	-
W_2C	2730	*
MoC	2692	2400[37]
Mo_2C	2687	*
ThC_2	2655	2500[38]
WC	2630	2525[39]
ThC	2625	*
SiC	2540	2540[40]
B_4C	2470	2390[40]
UC_2	2450	2390[41]
UC	2350	*

* See the eutectic temperature for the more carbon-rich phase.

As can be seen from this table, carbides of the Group IV-b and V-b elements are the most refractory and have the highest minimum carbide-graphite eutectics. Due to the natural limitations of the oxides with regard to refractoriness, multiple-layer coating sequences should be designed so that failure of the coatings will not occur before the limi-

tations of the outer or oxide layers are exceeded. In other words, the oxide layer should be the weakest link in the chain. Failure of the coating because of the formation of a liquid phase below the outer layer can and should be avoided. For this reason, carbide-graphite eutectic temperatures should be as high as practicable.

An oxide in contact with a carbide is subject to the same chemical reaction as is an oxide in contact with graphite; viz, the possibility of the formation of carbon monoxide. As mentioned previously, CO increases in stability at higher temperatures, while the refractory oxides decrease. Thus an increased driving force against a decreased resistance tends to promote oxide reactions with both graphite and the carbides at high temperatures. In the case of the carbides, however, this tendency is not nearly so great. The fact that the free energy of formation of the carbide enters into the thermodynamic calculations as a reactant rather than a reaction product is often enough to shift the minimum reaction temperature several hundred degrees higher. The zirconium-oxygen-carbon system can serve as an example of this temperature shift. For a zirconium oxide coating on graphite, the following reactions must be considered:

$$Zr_{(s)} + C_{(gr)} \rightarrow ZrC_{(s)};\ \Delta F^\circ_T = (0.00195)T - 39.71\ \text{kcal};\qquad (8)$$

$$Zr_{(s)} + O_{2(g)} \rightarrow ZrO_{2(s)};\ \Delta F^\circ_T = (0.04246)T - 257.69\ \text{kcal};\qquad (9)$$

$$Zr_{(l)} \rightarrow Zr_{(s)};\ \Delta F^\circ_T = (0.00175)T - 3.73\ \text{kcal};\qquad (10)$$

$$C_{(gr)} + {}^1/_2\ O_{2(g)} \rightarrow CO_{(g)};\ \Delta F^\circ_T = (-0.02005)T - 27.81\ \text{kcal}.\qquad (11)$$

Equations (8), (9), and (11) may be combined to describe the desired reaction:

$$3C_{(gr)} + ZrO_{2(s)} \rightarrow ZrC_{(s)} + 2CO_{(g)};\ \Delta F^\circ_T = \Delta F^\circ_8 + 2\Delta F^\circ_{11} - \Delta F^\circ_9$$

$$\Delta F^\circ_T = (-0.08061)T + 162.36\ \text{kcal}.\qquad (12)$$

The equilibrium temperature for this reaction occurs when ΔF°_{12} reaches zero at 1741°C.

For a zirconium oxide coating on zirconium carbide, equations (8) through (11) may be combined in a different manner to yield the following:

$$2ZrC_{(s)} + ZrO_{2(s)} \rightarrow 3Zr_{(l)} + 2CO_{(g)};$$

$$\Delta F^\circ_T = 2\,\Delta F^\circ_{11} - 2\,\Delta F^\circ_8 - \Delta F^\circ_9 - 3\,\Delta F^\circ_{10},$$

or

$$\Delta F^\circ_T = (-0.09171)T + 292.68 \text{ kcal}. \qquad (13)$$

The free energy of this equation becomes zero when the temperature reaches 2918°C. Above this temperature, zirconium oxide-zirconium carbide coatings will fail because of the reduction of the oxide outer layer. Coincidentally, the minimum graphite-zirconium carbide eutectic occurs at 2920°C[42] which is, for all intents and purposes, the same temperature as that of the oxide reduction. Thus, chemical failure for both layers of this coating sequence occurs above 2900°C. However, zirconium oxide melts at 2687°C (see Table 1) causing the coating to fail mechanically before chemical failure occurs. Chemical failure prevents the use of single-layer zirconia coatings above 1741°C, far below the zirconia melting point and the use of this coating is an undesirable waste of refractoriness.

By using a zirconium carbide intermediate layer to prevent graphite-zirconium oxide contact, the serviceable temperature of ZrO_2 protective coatings can theoretically be increased to about 2687°C. In the case of other oxides the improvement in protection temperature by the use of an intermediate layer is not quite as spectacular. The melting point of an oxide is the highest temperature at which it reasonably can be expected to perform. For zirconia, a carbide reaction barrier would appear to make it possible to use the coating up to the melting point of the oxide. For other materials this may not be true since oxides such as ceria and titania are reduced by many carbides to lower oxides at temperatures far below their melting points. These are instances in which it is not necessary for the entire free energy of formation of the oxide to be expended by the reduction process in order that a reaction occur. The step-wise reduction to a lower oxide can be driven to completion with less energy than is required for reduction to a metallic element.

The most interesting oxide from a high-temperature standpoint is thoria. It has the highest melting point of all the oxides (3000°C) and should theoretically provide oxidation protection for graphite to higher temperatures than any other material. As shown in Table 3, ThO_2 will react with graphite above 1925°C but this reaction temperature can be increased considerably with an intermediate layer as a reaction barrier. Zirconium carbide serves as an example of the improvement such a barrier can provide. The calculation requires the use of equations (8), (10) and (11), as well as the following:

$$Th_{(l)} + O_{2(g)} \rightarrow ThO_{2(s)};\ F^\circ_T = (0.0492)T - 301.0 \text{ kcal}. \qquad (14)$$

These equations may be combined to yield the reaction:

$$2ZrC_{(s)} + ThO_{2(s)} \rightarrow 2\,Zr_{(l)} + Th_{(l)} + 2\,CO_{(g)};$$

$$\Delta F^\circ_T = 2\,\Delta F^\circ_{11} - 2\,\Delta F^\circ_8 - 2\Delta F^\circ_{10} - \Delta F^\circ_{14} =$$

$$(-0.0967)T + 332.3\ \text{kcal}. \qquad (15)$$

The equilibrium temperature for this reaction is calculated to be 3163°C, well above the melting point of thoria. However, thorium has a lower oxide (ThO), the existence of which is almost certain to lower the minimum reaction temperature of the coatings under consideration. The calculation of the new reaction temperature requires the following information:

$$Th_{(l)} + {}^1/_2\ O_{2(g)} \rightarrow ThO_{(l)};\ \Delta F^\circ_T = (0.0188)T - 138.9\ \text{kcal}. \qquad (16)$$

Combining equations (8), (10), (11), (14) and (16) yields:

$$ZrC_{(s)} + ThO_{2(s)} \rightarrow Zr_{(l)} + ThO_{(l)} + CO_{(g)};$$

$$\Delta F^\circ_T = \Delta F^\circ_{11} + \Delta F^\circ_{16} - \Delta F^\circ_8 - \Delta F^\circ_{10} - \Delta F^\circ_{14} =$$

$$(-0.0542)T + 177.7\ \text{kcal}. \qquad (17)$$

The equilibrium temperature for the reaction is calculated to be 3010°C. The lower oxide reduces the theoretical carbon-oxide reaction temperature by over 150°C. However, unlike the ceria and titania examples previously discussed, this reduction does not bring the theoretical reaction temperature below the oxide melting point.

Despite the fact that the chemical inertness of ThO_2 is tempered somewhat by the existence of ThO, it still will remain unreacted with ZrC at temperatures near its melting point. Table 5 gives the melting point of the ZrC-C eutectic as 2920°C. Since this is lower than the ZrC-ThO_2 reaction temperature, the coating should fail by formation of an interior liquid phase before any substantial oxide reaction or oxide melting occurs. The eutectic temperatures given in Table 5 indicate that HfC, TaC, NbC and TiC could possibly offer some improvement over ZrC as the intermediate layer. However, any improvement in temperature will be so slight that a choice is rather arbitrary. Experimental errors in both the eutectic and thermodynamic data are large enough at the present to mask

any obvious advantages of selecting one particular carbide out of the group. One major disadvantage of ThO_2 as a coating is its poor resistance to thermal shock.

Magnesium and hafnium oxides also have high melting points, and while not as refractory, they have much better thermal-shock resistance than thoria. Magnesia may not be of much value above 2400°C because of its volatility. Hafnia, however, is not nearly as volatile even up to its melting point (2777°C). Other single oxides are less refractory and are not nearly as interesting for oxidation-resistant coating of graphite. As mentioned in the previous section, the high-melting compound oxides may provide desirable coating properties not found in single oxides. These compound oxides, however, usually have lower melting points than their more refractory constituent oxides, and their use is accompanied by a sacrifice in refractoriness.

Other refractory materials to be considered as intermediate layers are mainly the nitrides, borides, silicides and sulfides. The sulfides and silicides do not appear to be as promising as the refractory metals and carbides. In general, the sulfides have rather low melting points. Cerium monosulfide, with a melting point of 2450°C is the most refractory sulfide reported.[43] The silicides are of about the same refractoriness as the sulfides; the highest melting silicides are two phases of tantalum silicide, both of which melt at approximately 2200°C.[44] All of the nitrides are rather volatile above 2300°C,[45] although B, Sc, Ti, Zr, Hf, Ta and U nitrides have high melting points. The nitrides, sulfides and silicides, therefore, are not very desirable as materials for reaction barriers. Interior layers of these materials would cause the failure of a coating sequence below the melting points of most of the more refractory oxides considered for use as outer layers. Since the oxide layer should be the limiting factor in multilayer coatings, the nitrides, silicides and sulfides should not be considered further for the intermediate layer.

There are several borides that could prove to be excellent reaction barriers. The borides of titanium, zirconium, hafnium, and perhaps cerium are the most stable and refractory.[46] Zirconium and hafnium borides have melting points of about 3000°C; the melting point of TiB_2 is less but still quite high. Cerium boride is known to melt "above 2100°C". It has been reported that cerium boride can be used in vacuo above 2500°C, which indicates both a high melting point and a reasonably low vapor pressure.

There have been very few thermodynamic data reported on these borides[47] so that stability calculations with regard to either graphite or

oxide reactions cannot be made. Since the free energy of formation of B_2O_3 is not especially large in comparison with those of the oxides that are likely to be used as outer layers, and since the unknown free energies of formation of the borides must also be added to those of the outer-layer oxides, the driving force behind boride-oxide reactions should not be large enough to carry them to completion. Moreover, titanium boride and graphite mixtures have been compressed and fired to 3000°C for substantial time periods with no apparent reaction (carbide formation).[48] This would indicate that titanium boride, at least, should be thermodynamically stable with regard to graphite. There is no reason to suppose that zirconium and hafnium borides will behave differently. The literature contains no indications as to cerium boride-graphite stability.

The foregoing discussion indicates that the carbides, borides, and refractory metals are the most promising materials for use as reaction barriers between graphite and the oxidation-protection coatings. Boron nitride, cerium sulfide and tantalum silicide are isolated examples of materials which show limited promise from other groups of refractory compounds. It has been shown thermodynamically that single-layer oxide coatings are insufficient protection against the oxidation of graphite at temperatures above 2000°C. If graphite is to be used for any length of time above this temperature in oxidizing atmospheres, multiple-layer coatings consisting of an oxide outer layer with an intermediate layer of the above-mentioned reaction-barrier materials must be employed.

1.4. Methods of Application

The manner in which a protective coating is applied to graphite is equally as important as the selection of the coating material itself. Such vastly significant properties as coverage, porosity, thickness, texture, adhesion, inter-particle bond strength, crystallographic orientation and others are, for the most part, a result of the technique and method for depositing the coating on the substrate. Although coatings may be applied in many ways, it is usually more convenient, efficient or economical to resort to only one or two methods for any particular coating. The choice of a coating method is not always obvious, but after consideration of the coating material to be used, the size of the substrate and the quantity of coated articles desired, the more likely methods should be indicated.

Some of the older ceramic methods for depositing protective coatings, such as room-temperature dipping, dusting, spraying, and painting, have been used with moderate success for graphite substrates.[49]

These coatings must be cured or baked to eliminate suspension media and/or to promote bonding both between the coating particles and between the coating and substrate. The coating of a graphite article by immersing it into a bath of molten coating material has the advantage that no other liquid vehicle is necessary and hence no additional firing treatment is required to cure the coating. Coatings obtained in this manner should be free of large particles or grains which tend to lower bond strength and increase porosity. With this dipping method, it is necessary that the molten coating material wet the graphite surface and many promising materials, which do not have this characteristic, are thereby eliminated. A rather simple type of coating process that has been used recently in connection with certain re-entry applications is the cladding of a graphite article with a large number of small, refractory, oxidation-resistant tiles.[50] The main advantages of these ceramic-coating methods lie in their simplicity and low cost; however, they do not produce the high-quality coatings of which other, more complex methods have been shown to be capable.

The more complex coating methods include electrodeposition, vapor deposition, plasma spraying and incorporation. The last of these, incorporation, involves the blending of the protective coating material with a basic graphite mix before forming. Upon oxidation of the formed article, the graphite at the surface is initially volatilized as CO and CO_2. The coating material associated with this surface graphite is concentrated until it forms a continuous layer and protects the article against further oxidation. Although incorporation produces a protective coating in the strictest sense, it should be remembered that the coating is on a composite-graphitic material, not on a pure-graphite base. The advantages and disadvantages of this method are discussed fully elsewhere.[48]

Electrodeposition in broad terminology includes the deposition, by electrical potential, of ions, charged particles (electrophoresis) and uncharged particles driven onto the substrate by ion collision (cermet deposit). This method may be carried out in either aqueous or fused-salt media. Electrodeposited metallic coatings (with the exception of the platinum metals) are themselves subject to oxidation. After the initial oxidation, however, the coating should be continuous and nonporous so as to protect the graphite beneath. In the case of multiple-layer coatings, electrodeposited metallic coatings can be used as intermediate diffusion-barrier layers to prevent contact between the oxide layer and the graphite substrate.

Ceramic compounds recently have been electrodeposited on graphite[51] by suspending ceramic particles in a conventional chromic-

acid plating solution. A high electric current density is applied to the suspension and causes the metal ions to drive the ceramic particles toward the graphite cathode. The result is a cermet coating consisting of a uniform dispersion of ceramic particles in a metal matrix.

Electrodeposition techniques for applying coatings are among the most efficient methods known. After the initial bath concentration is established, the amount of material expended during a coating cycle equals precisely the amount of material deposited on the substrate. Coating by electrodeposition is especially efficient for operations involving a large number of pieces to be coated in separate steps. In this way, the expense involved in attaining the initial bath concentration becomes a small percentage of the total coating-material cost. Electrodeposition also performs admirably in cases where intricate shapes, such as the throat area of rocket nozzles, need be coated. The chief disadvantage of this method is the limited number of coating materials that can be handled in this way.

In recent years, a great deal of attention has been directed toward coating by vapor deposition. The term "vapor deposition" has been applied to many distinct processes, all of which involve, in some manner, the transporting of the coating material to the substrate through the vapor phase. Actually, it is little more descriptive of the various techniques than would be the term "solid deposition" or "liquid deposition" for methods concerned with these states of matter.

Basically, the types of vapor deposition processes may be divided into two main groups: (a) those which involve the deposition of a coating by the pyrolytic cracking of gaseous molecules on a hot substrate; and (b) those which do not. In the latter group, the substrate may be either "hot" or "cold" as required by the process involved. Each of these groups may be further divided into subgroups according to whether the substrate undergoes a chemical reaction with the vapor. There are thus four fundamental processes.

Experimental setups to carry out these processes fall into two categories: (a) those in which the article to be coated is surrounded by a matrix containing the coating material (pack diffusion apparatuses); and (b) those which utilize a source-target arrangement in which there is a physical separation between the object to be coated and the source of coating material. The manner in which the vapor flow is achieved is much the same for both. Solid coating materials can be either heated to where their vapor pressures become significant (often necessitating

liquification), or they may be reacted with other materials, such as halogens, to form volatile compounds. Liquid coating materials may be vaporized in the same manner as solids, but they also may be transported by carrier gases saturated with vapor from the liquid. It should be noted that the pack-diffusion setup invariably requires that the vapor react with the substrate. Both vapor and substrate, because of their intimate contact, are necessarily at approximately the same temperature and the possibility of simple condensation of the vapor on the substrate is eliminated.

An outline of the major vapor-deposition processes is presented in Table 6. Included are typical examples of the application of these processes to the coating of graphite articles. Most of the examples given represent actual experiments performed under this contract, the details of which are covered in other sections of this report.

The variety of protective coatings that may be applied by vapor-deposition methods is extremely large. Practically any type of refractory coatings can be applied to any type of refractory substrate.[34] Method II-B-2 has been used successfully to deposit carbides (example given), nitrides, borides, silicides and even oxides on refractory metal substrates. The other methods, while not as universal in their scope, have been used to great advantage in cases where the thermodynamics of a particular substrate-coating system is compatible with the relative simplicity of these techniques. For example, using graphite as the substrate, silicon carbide coatings may be applied by nearly all of the methods. The relatively complicated vapor equilibrium inherent in the method presented in II-B-2 can thus be obviated. For substrates other than graphite this is not true.

The all-around quality, and especially purity, of vapor-deposited coatings is as high as, or higher than, that of coatings deposited by other techniques. Many materials have been prepared in their highest state of purity by bulk vapor deposition.[52] Smoothness, low porosity, good adherence and high strength can all be achieved if vapor-deposited coatings are applied discreetly. In cases where the substrate enters into chemical reaction with the coating vapor, coverage of the substrate can be complete and uniform, even for rather complex shapes. The inside walls of long, narrow tubes have been evenly coated by the injection of a reactive vapor at one end.[52] Nonreactive, condensible-type vapors would, of course, tend to pile up at the entrance of such a tube. Pack-diffusion processes also use the reactive-vapor principle and afford similarly good coverage of substrates. In general, however, the coverage for intricately shaped substrates by vapor deposition falls short of that produced by conforming-anode electrodeposition.

Table 6. Outline of Vapor-Deposition Methods

I. No decomposition of vapor on substrate

A. Reaction of vapor with substrate to form a compound

1. Pack-diffusion method

Ex.: $C\ (\text{graphite substrate, 2000°C}) + Si\ (\text{vapor, 2000°C}) \xrightarrow[\text{pack}]{TiC} SiC\ (\text{coating on graphite, 2000°C})$

2. Source-target method

Ex.: $C\ (\text{graphite substrate, 1600°C}) + Ti\ (\text{vapor, 1600°C}) \xrightarrow{\text{vac.}} TiC\ (\text{coating on graphite, 1600°C})$

B. Condensation of vapor on substrate (no mass reaction with substrate, source-target method only)

1. Single-vapor condensation

Ex.: $C\ (\text{graphite substrate, 1200°C}) + Si\ (\text{vapor, 1600°C}) \xrightarrow{\text{vac.}} Si\ (\text{metal coating on graphite, 1200°C})$

2. Multiple-vapor condensation (simultaneous or intermittent)

Ex.: $C\ (\text{graphite substrate, 1500°C}) + Ti\ (\text{vapor, 1700°C}) + {}^1/_2 N_2\ (\text{gas, R.T.}) \xrightarrow[N_2\ \text{flush}]{\text{vac.}} TiN\ (\text{coating on graphite, 1500°C})$

II. *Decomposition of vapor on substrate (pyrolytic cracking)*

A. Reaction of cracking product with substrate to form a compound

1. Pack-diffusion method

With the exception of one rather complex case of questionable significance, no practical examples of this type of process have been reported.

2. Source-target method

Ex.: $C\ (\text{graphite substrate, 2000°C}) + TiCl_4\ (\text{vapor, R.T.}) + 2H_2\ (\text{gas, R.T.}) \xrightarrow[\text{flush}]{\text{gas}} TiC\ (\text{coating on graphite, 2000°C}) + 4HCl\ (\text{gas})$

B. Condensation of cracking product(s) on substrate (no mass reaction with substrate, source-target method only)

1. Single cracking-product condensation

Ex.: $C\ (\text{graphite substrate, 2000°C}) + CH_4\ (\text{vapor, R.T.}) \xrightarrow[\text{flush}]{\text{gas}} C\ (\text{pyrolytic carbon coating on graphite, 2000°C}) + 2H_2\ (\text{gas})$

2. Multiple cracking-product condensation (with or without reaction between cracking products)

Ex.: $C\ (\text{graphite substrate, 2000°C}) + SiCl_4\ (\text{vapor, R.T.}) + CH_4\ (\text{gas, R.T.}) \xrightarrow[\text{flush}]{\text{gas}} SiC\ (\text{coating on graphite, 2000°C}) + 4HCl\ (\text{gas})$

Deposition of coatings by plasma spraying also has been the subject of a great deal of interest recently. In this method, molten particles of coating material are sprayed onto a substrate by means of a carrier gas which has been heated and accelerated while passing through an electric arc. The three main types of plasma apparatuses are differentiated by the manner in which the coating material is introduced into the carrier-gas stream. In the first of these, the carrier gas passes into the arc and is heated rapidly to a very high temperature which causes great expansion of the gas. This expansion accelerates the gas through a nozzle where a consumable rod of coating material protrudes into the gas system. The rod is ablated by the hot, on-rushing gas, and the molten particles are carried to and deposited on the substrate. The second method involves the use of the coating material as a consumable electrode to form the arc and supply the coating particles. The carrier gas passes through the arc and carries with it the particles produced by the destruction of the electrode. Particles and gas then pass out through the nozzle and impinge onto the substrate. This method requires that the coating material (since it is used as one of the electrodes) be a conductor of electricity. Although ceramic materials are considered as electrical nonconductors, they can become conductive if heated initially to a high enough temperature and can be used as electrodes. The third method consists in transporting fine powders of the coating material by the carrier gas through the arc, out the nozzle and onto the substrate. Because the coating material is in powder form and thus does not have to be formed into rods or electrode shapes, the method is adaptable to a greater variety of coating systems than are the other two.

The methods of plasma spraying differ, therefore, as to whether the coating material is introduced into the carrier gas before, during, or after it passes through the arc. Other aspects are much the same for all three methods.

The main advantage offered by plasma spraying is that it can be used to apply a wide variety of coating materials. Virtually all refractory materials can be applied as coatings by this method. In addition, the time required for coating by plasma spraying is usually much shorter than the application of the same coating by other techniques. On the other hand, plasma-sprayed coatings frequently lack the adherence and low porosity that coatings applied by other methods exhibit.

Included in this report are the results of coating experiments performed by use of plasma spraying, source-target, and pack-diffusion vapor-deposition techniques. In this study, coatings were applied by the various methods, to samples of different sizes and configurations. It was necessary, therefore, to devise oxidation tests which could be used

for evaluation of the coatings on each type of sample. As a result, three methods were used for measuring the oxidation protection afforded by the various coatings. The oxidation-test method used depended upon the type coating and size and shape of the sample involved in each specific instance. If the specimen was coated on all surfaces, oxidation was measured on an apparatus which continuously recorded the weight change of the specimen as it was heated in a regulated, oxidizing gas stream. The specimen used for some trials consisted of a hollow cylinder, only the outside of which was coated. In this case, the oxidation resistance provided by the coating was evaluated by a direct-flame-impingement method described in Section 2.3.2 of this report. A third method for measuring oxidation, called the resistance-oxidation test, is described in Section 2.3.4. This method was used for evaluation of coatings applied to the center section of a $^1/_4$-inch diameter graphite rod.

2. PLASMA-SPRAYED COATINGS TO PROTECT GRAPHITE FROM OXIDATION

2.1. Introduction

The existence of the arc-stabilized plasma has been known for a long time, and the first plasma torch was designed about 1910. However, little research had been done on this subject until about 1956. Since that time, there has been an increasing interest in the plasma torch both for material application and material testing. The advent of ballistic and space vehicles requiring materials to withstand high temperatures has led to the investigation of the plasma torch as a means for depositing protective coatings on other substances which, by themselves, will not withstand the environmental conditions.

In the past few years, the plasma torch has been utilized extensively for the deposition of protective coatings on metal surfaces. In many applications, graphite, because of its relatively low density and excellent thermal properties, would offer advantages over metal components if an adequate oxidation- or erosion-resistant coating could be placed on the graphite.

This report will cover the work that has been done under this effort to develop a high-temperature oxidation- and erosion-resistant coating for graphite by use of plasma spraying.

2.2. Literature Survey

A survey of current literature pertaining to the use of the plasma arc has resulted in the following references. These references are broken down into three groups for easy identification of particular applications. Group I contains information concerning the application of plasma jets for deposition of coatings on various materials. Group II contains information pertaining to the use of the plasma jet as a materials evaluation vehicle. Group III contains information on the theoretical and measured properties of the plasma jet itself, along with uses not covered in Groups I and II.

2.2.1. Group I - Plasma-Sprayed Coatings

Kramer, B. E., The Effect of Arc-Plasma Deposition on the Stability of Non-Metallic Materials, General Electric Co., Bi-Monthly Report No. 6, ASTIA Document No. AD 255945.

Kramer, B.E., Development of Arc-Spraying Processes and Materials for Solid-Rocket Nozzles, General Electric Co., BuWeps Contract NOrd 18119, Task 2, RGIFPD156, March 1, 1961.

Laszlo, T.S., Mechanical Adherence of Flame-Sprayed Coatings, Ceramic Bulletin, Vol. 40, No. 12, 1961, pp 751-775.

Levinstein, M.A., Properties of Plasma-Sprayed Materials, General Electric Co., WADD TR 60-654.

Levinstein, M.A., Properties of Plasma-Sprayed Materials, General Electric Co., Tech. Documentary Report No. ASD TDR 62-201.

Mark, S.D., Jr., Editor, High-Intensity Arc Symposium, Central Research Laboratory, Carborundum Co., May 1958.

Reed, T.B., Growth of Refractory Crystals Using the Induction Plasma Torch, Journal of Applied Physics, Vol. 32, No. 12, Dec. 1961, pp 2534-2535.

Singleton, R.H., Fabrication of Tungsten Shapes Using the Arc-Plasma-Spray Forming Technique, Allison Div., G.M.C., presented at Fourth Meeting of the Refractory Composites Working Group, Nov. 16, 1960, Evendale, Ohio.

Thorpe, M.L., Plasma Jet - Progress Report No. 2, Research/Development, June 1961, pp 77-89.

Unger, R., Rosenberry, J. W., Wurst, J. C., Arc-Sprayed Graduated Coatings, presented at National Meeting, Society of Aerospace Material and Process Engineers, Nov. 1961, Dayton, Ohio.

Westerholm, R.J., Flame-Sprayed Coatings, Machine Design, Aug. 31, 1961, pp 82-92.

2.2.2. Group II - Materials Evaluation

Steinberg, P., S., The Study of Chemical Surface Reactions In a High-Temperature Flow System with Arc-Heated Gases, AVCO Corp., R&D Division, From Work on Air Force Contract AF 04(647)-258, Ballistic Missile Division, Inglewood, California.

Christensen, D., Buhler, R.D., Arc-Jet Measurements Related to Ablation Test Validity, ASTM Special Publication 279, 1959.

Eschenbach, R.C., Arc Air Heaters for Hypersonic Wind Tunnels, Linde Co., Submitted to ARS Journal for publication.

Molella, D.J., Evaluation of Oxidation-Resistant Coatings in a Water-Stabilized Electric Arc at Temperatures to 2325°C (4215°F), Technical Memorandum No. ME-1-62, Ammunition Group, Picatinny Arsenal, Dover, New Jersey.

Peters, R.W., Rasnick, T.A., Investigation of Oxidation-Resistant Coatings on Graphite and Molybdenum in Two Arc-Powered Facilities, Langley Research Center, NASA TN D-838.

Rosenbery, J. W., Smith, H.E., Wurst, J. C., Progress Report on Arc-Plasma Material Evaluation Studies, U. of Dayton Research Institute, reports for April, July, September 1961. Contract No. AF 33(616)-7838, Project No. 7381, Task No. 73812.

2.2.3. Group III - Plasma Properties, Miscellaneous Uses

Boldman, D.R., Shepard, C.E., Fakan, J.C., Electrode Configurations for a Wind-Tunnel Heater Incorporating the Magnetically Spun Electric Arc, Lewis Research Center, NASA TND-1222, April 1962.

John, R., Bade, W.L., Recent Advances in Electric Arc-Plasma Generation Technology, ARS Journal, January 1961, pp 4-17.

Leutner, H.W., The Production of Cyanogen From the Elements Using a Plasma Jet, Research Institute of Temple University.

Stine, H.A., Watson, V.R., The Theoretical Enthalpy Distribution of Air in Steady Flow Along the Axis of a Direct-Current Electric Arc, Ames Research Center, NASA TN 0-1331, August 1962.

Stokes, C.S., Knipe, W.W., The Plasma Jet in Chemical Synthesis, I & E Chem., Vol. 52, No. 4, April 1960, pp 287-290.

Thiene, P.G., Basic Study of Energy Exchange Process Between an Electric Arc and a Gas Flow, Plasmadyne Corp., ASTIA Document No. AD 263203.

Thorpe, M.L., The Plasma Jet and its Uses, Research/Development, Jan. 1960, pp 5-15.

2.3. Investigation and Results of Various Coating Materials Applied to Graphite by Plasma-Spraying Technique

2.3.1. General

The plasma torch used for a spray-coating work described in this report was capable of a continuous 120-kw output and utilized an M-4 arc-plasma generator. The M-4 generator, shown in Figure 2, is a gas-vortex and geometry-stabilized arc device. The electrodes generally used were a 2-per cent thoriated tungsten rear cathode emitter and a front copper anode. The arc was wholly contained within the front electrode. This type of plasma-spray gun is used only with a powdered feed material.

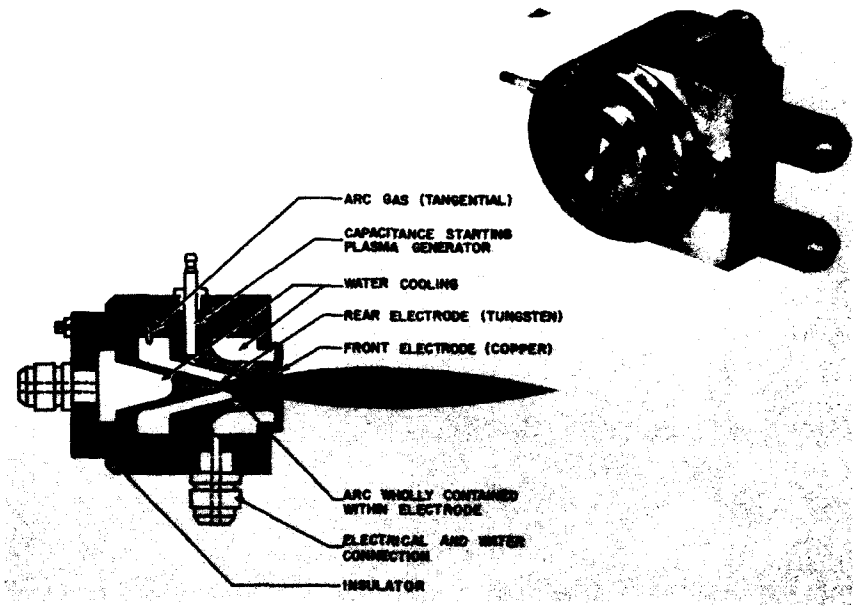

Figure 2. The M-4 Arc-Plasma Generator

To insure uniform deposition of the sprayed materials on the sample, the M-4 generator was mounted on a track to permit lateral movement at rates from 0.2 to 60 feet per minute, and the sample was mounted in a lathe where it could be rotated at variable speeds between 1 and 200 revolutions per minute. The distance between the torch and sample could be adjusted between 2 and 12 inches and the whole assembly was enclosed in a chamber where atmosphere control could be provided. This equipment is shown in Figure 3.

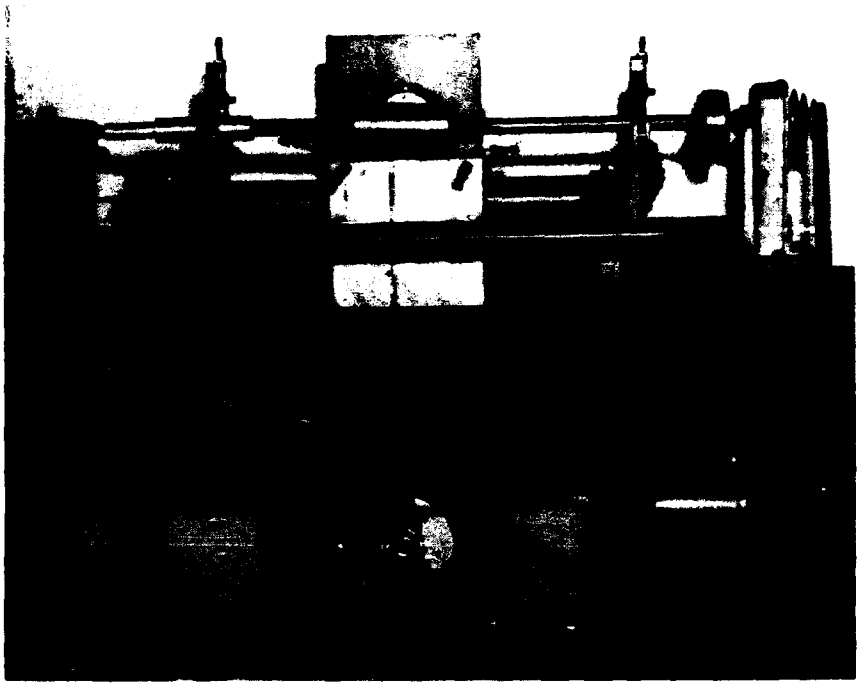

Figure 3. Plasma-Spraying Chamber with Graphite Sample Mounted in Place

Several factors which influence the quality of the coating applied by plasma spraying are as follows:

1) Power input,
2) Powder particle size,
3) Type and flow rate of the arc-perpetuating gas,
4) Type and flow rate of the powder feed gas,
5) Distance between the torch and the sample.

The power input to the torch must be adjusted so that the particles are heated to a molten state. The operating limits for the power input are quite narrow for a specific material of specific size passing through the arc at specified gas-flow rates. The temperature of the particles is a major factor in the adherence of the coating to the substrate. The particle size of the powder fed into the torch must also be carefully controlled to eliminate excessive amounts of fine or coarse particles from entering the torch. If the particle size is not controlled, the fines will be heated excessively which causes agglomeration and plugging of the front electrode port and the coarser particles will not be heated sufficiently to adhere to the substrate upon impact. The arc-gas flow must be regulated so that the flame is long enough to maintain the

particles at the correct temperature when they impinge on the sample. When adjusting this gas flow, it must be remembered that the flow has to be sufficient to stabilize the arc while being kept below the point where it will disrupt the arc path. The powder-gas flow adjustment is quite critical since it controls two factors: (a) The powder-gas flow determines the velocity at which the particles enter the torch and this, combined with the additional volume of gas which must expand on heating, determines the residence time of the particles within the arc; (b) the powder-gas flow rate determines the amount of powder that is fed into the torch because the powder is fed through a simple carburetor-type feed hopper. The optimum distance between the torch and the sample must be determined so that the sample is not subject to oxidation by overheating, and the sample temperature is such that the rate of quenching the molten particles will insure adherence of the coating to the substrate.

All of the afore-mentioned parameters are interdependent. The particular combination of operating characteristics to produce the best coating must be determined for each coating material being considered. Slight changes in any one of these parameters often produce significant changes in the resulting coating.

The speed with which the torch travels laterally and with which the sample rotates also influences the adhesion of the particles to the sample. Too fast a rotational or translational speed results in angular impingement and increases the amount of particle rebound. Too slow rotational or translational speeds result in overheating the substrate and/or eroding the sample surface.

2.3.2. Titanium Diboride

The first material to be investigated as an oxidation-resistant coating for graphite was titanium diboride. It was theorized that the mechanism by which this material would offer protection would be a slow conversion to TiO_2 similar to the behavior of titanium nitride. A literature search did not reveal any previous work on this subject, so the actual behavior of the material at elevated temperatures in an oxidizing atmosphere was not known.

The samples used in all of the following experiments were cylinders, cut from grade ATJ graphite, with an outside diameter of 3 inches, an inside diameter of 2.5 inches and a length of 6 inches. The titanium diboride used was of technical grade. Coatings of various thicknesses, between 0.003 and 0.020 inch, were deposited for test evaluations.

The first samples were plasma-spray coated under the following conditions:

Power input	-	40 kw at 33 volts,
Arc-gas flow rate, argon	-	2.16 std ft^3/min,
Powder-gas flow rate, argon	-	2.13 std ft^3/min,
Particle size, TiB_2	-	95 per cent through 250- and on 325-mesh screen,
Torch-to-sample distance	-	4.0 in
Torch lateral speed	-	2.7 ft/min,
Sample rotational speed	-	20 rpm,
Deposition time	-	10 min.

The control chamber of the plasma assembly was flushed with argon prior to coating the samples. During the coating process, argon at 40 std ft^3/min was used to sweep the chamber and the chamber was maintained at a slightly reduced pressure (0.8 inch of H_2O). The coating produced at the above conditions had a weight of 17.3 grams and was 0.023 inch thick. The bulk density of the coating was 2.54 g/cc which is only 56 per cent of the theoretical density of TiB_2. This density is reflected in the quality of the coating which was very soft, had no apparent bonding between particles, and was easily removed from the substrate. Figure 4 is a photomicrograph of the coating structure at a point of deliberate fracture of the substrate. The particles of the coating were loose because of the poor bonding and were ground into the substrate and surrounding mounting material during polishing. These results show that the particles were much too cold when they struck the sample and, consequently, did not bond either to the substrate or to each other.

In successive trials, all operating conditions were held the same except the power input which increased by 5-kw increments. When a power input of 80 kw at 38 volts was reached, a thin, hard coating was formed which was well bonded within itself, but the bond between the coating and substrate was weak. This coating, shown in Figure 5, had a bulk density of 3.93 g/cc which is about 87 per cent of theoretical density. It was apparent that a hard, integral coating of TiB_2 could be plasma sprayed onto graphite, and the next step was to achieve maximum bonding between the coating and the substrate while retaining the integrity of the coating.

The powder-gas flow rate was increased to 2.54 std ft^3/min for the next several tests and the power input was varied from 40 to 70 kw. Following are the operating conditions for these tests:

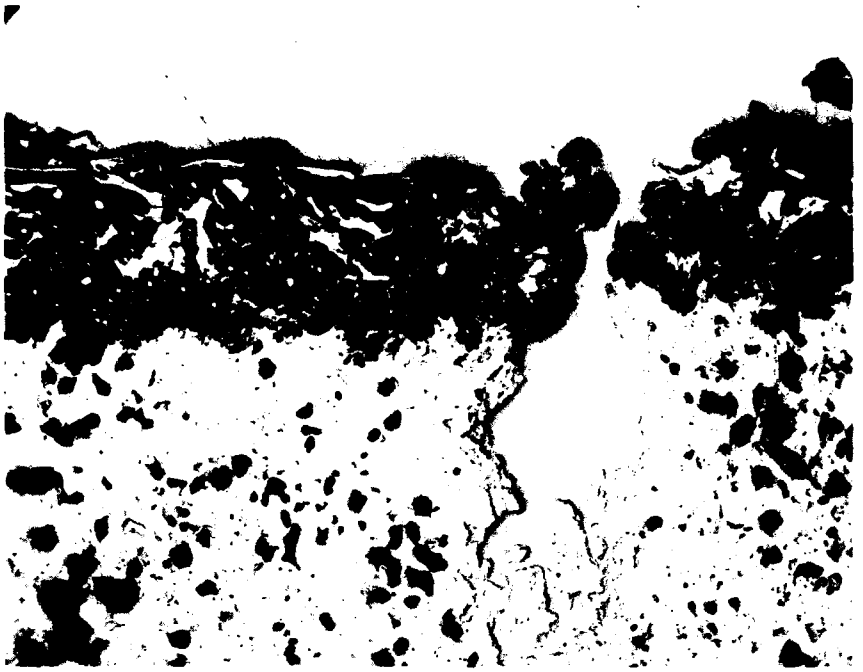

Figure 4. Low-Density Coating of TiB_2 on Graphite, 100X

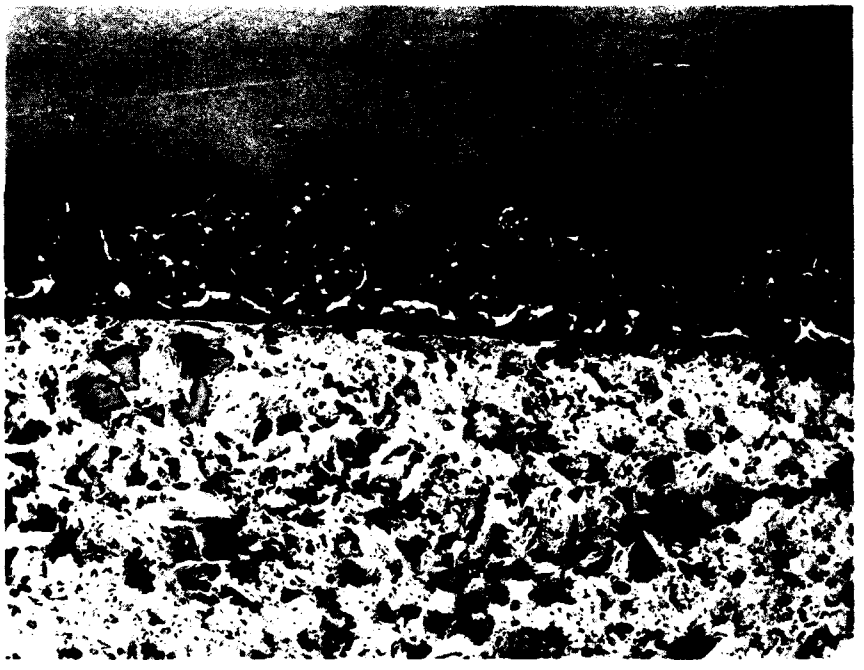

Figure 5. High-Density Coating of TiB_2 on Graphite, 100X

Power input	-	40-70 kw,
Arc-gas flow rate, argon	-	2.16 std ft^3/min,
Powder-gas flow rate, argon	-	2.54 std ft^3/min,
Particle size, TiB_2	-	95 per cent through 250- and on 325-mesh screen,
Torch-to-sample distance	-	4.0 in,
Torch lateral speed	-	2.7 ft/min,
Sample rotational speed	-	20 rpm,
Deposition time	-	10 min.

The following conditions were noted with the higher powder flow rate. At the low end of the power series, the coating was large grained with a pebbled surface, was quite soft and easily damaged, and the substrate-to-coating bond was not noticeably improved. As the power was increased by 5-kw increments, the coating became more fine grained and much harder but there still was no improvement in the coating-to-substrate bond.

The graphite samples in all the foregoing tests had polished surfaces. Succeeding tests, using a machined but not polished sample surface, produced only slightly better coating-to-substrate bonds. Grit blasting the sample resulted in surface contamination and again only slightly improved the bonding.

A good coating-to-graphite bond finally was achieved by the following means: The samples were machined smooth but were not polished and the torch-to-sample distance was decreased from 4.0 inches to 2.75 inches. The operating conditions were varied until a good coating was obtained at this distance under the following conditions:

Power input	-	70 kw at 36 volts,
Arc-gas flow rate, argon	-	2.16 std ft^3/min,
Powder-gas flow rate, argon	-	increased at 2-min intervals, 2.05, 2.10 and 2.13 std ft^3/min,
Particle size, TiB_2	-	95 per cent through 250- and on 325-mesh screen,
Torch-to-sample distance	-	2.75 in,
Torch lateral speed	-	2.0 ft/min,
Sample rotational Speed	-	52 rpm.

Figure 6 shows the structure of a coating produced under these conditions.

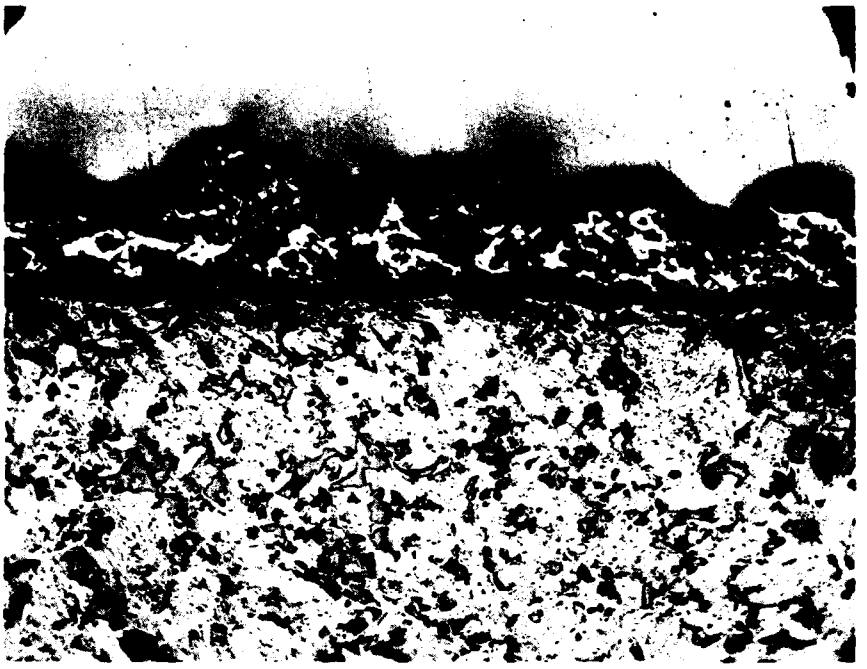

Figure 6. Good Coating of TiB_2 on Graphite, 100X

The rotational speed of the sample was necessarily increased to control the substrate temperature when the torch-to-sample distance was decreased from 4.0 inches to 2.75 inches. The traverse speed was decreased to give adequate coverage, since particle rebound was slightly greater at the higher rotational speeds. During the course of this investigation, it was found that if the substrate temperature exceeded 400°C, a small amount of surface oxidation and erosion of the graphite occurred which drastically reduced the coating-to-substrate bond. Although the actual spraying of these samples was done in essentially an argon atmosphere, complete atmosphere control was not provided. There was not enough oxygen present to react with the TiB_2 as it passed out of the torch, but there was enough oxygen present to react with the graphite at temperatures over 400°C.

A test program was initiated to evaluate the TiB_2 coating once the proper method of application had been established. Since there is no oxidation or ablation test reported in the literature that is used universally to evaluate such coatings, an arbitrary flame-oxidation test was devised. The test consisted of impinging an oxyacetylene flame on the surface of the sample. The flow rates of the oxygen and acetylene were adjusted to give the maximum temperature and the most highly oxidizing

flame that could be produced. Temperature of the sample was controlled by adjusting the distance between the torch and the sample. The torch was securely mounted and a sample holder was placed at a specified distance from the torch (see Figure 7). The sample was held on a mounting device as shown in Figure 8. This mounting device consisted of a steel

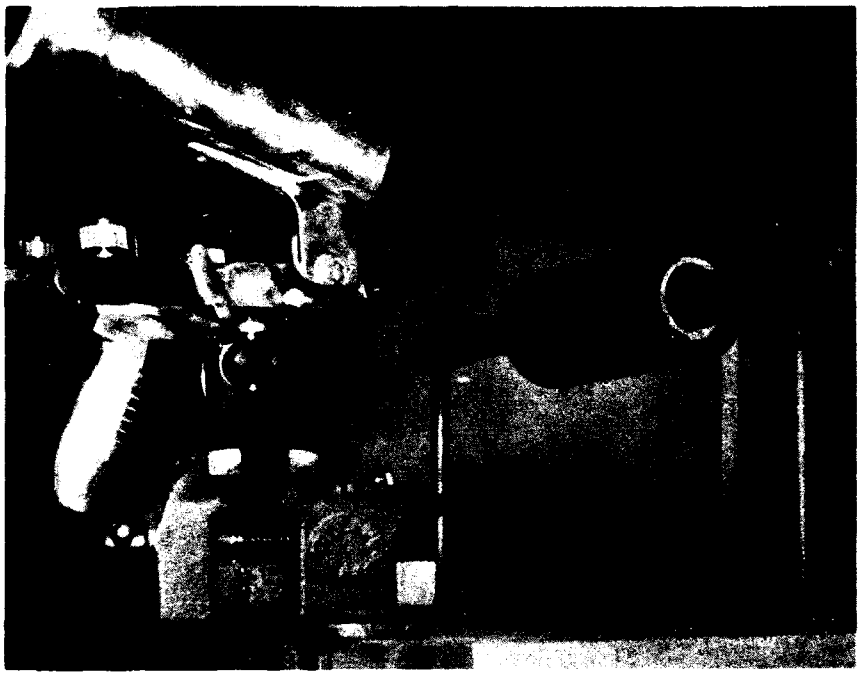

Figure 7. Oxyacetylene Flame Spray Gun as Mounted for Oxidation Tests of Coated Graphite

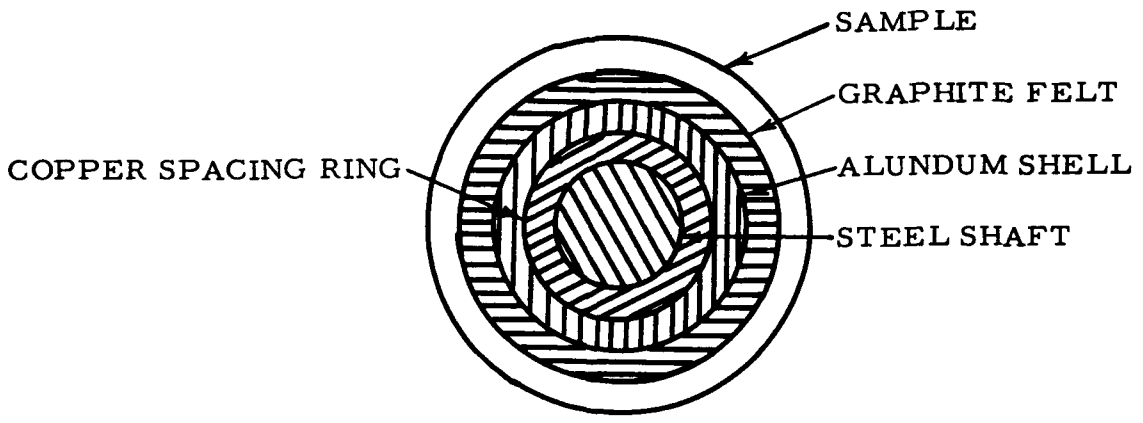

Figure 8. Mounting Device to Hold Coated Graphite Sample for Oxidation Test

shaft upon which a copper spacing ring and a $^1/_4$-inch alundum shell had been placed. A $^1/_4$-inch layer of graphite felt was placed between the sample and the alundum shell. Mounting the sample in this manner allowed a constant substrate temperature to be maintained.

Uncoated graphite samples were tested by the flame-oxidation method described above in order that a standard of comparison could be established. Samples coated with TiB_2 were tested in an identical manner. Figure 9 shows a plot of the weight loss by oxidation of the uncoated samples versus the number of 5-minute cycles at 1420°C. The curves are average figures for 6 samples of the uncoated graphite and 12 samples of the TiB_2-coated graphite. The test procedure was as follows.

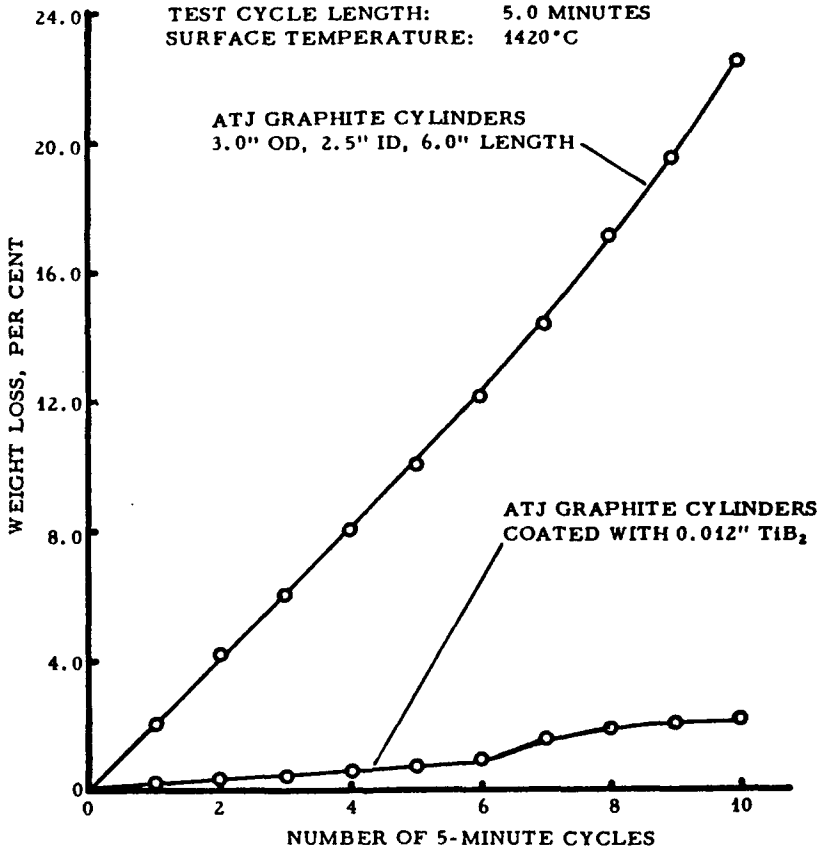

L-388

Figure 9. Oxidation Weight Loss of TiB_2-Coated and Uncoated Graphite Samples versus Number of Cycles, 1420°C

The samples on the mounting device were placed in the path of the flame at a distance of 4.75 inches. The flame produced a maximum surface temperature of 1420°C at that distance. Each sample was held

in the flame path for 5 minutes, was removed and weighed, and again placed in the flame path for another 5-minute period. This procedure was repeated until a total of 10 cycles had been made.

Failure of the coating usually came within the 7th cycle or between 30 and 35 minutes. Failure occurred by conversion of the TiB_2 to TiO_2, and the resultant volume change cracked the coating. Even though the coating had cracked at some points, these areas of graphite still covered by the coating showed no sign of oxidation at the end of 10 cycles. The ability of the coating to continue to offer oxidation protection, even though spot penetration had occurred, explains the continued low weight loss after penetration. None of the coatings failed by thermal shock.

Other coated specimens were tested at temperatures up to 2000°C. Conversion of the TiB_2 to TiO_2 takes place very rapidly after 1640°C and causes failure of the coating. Figure 10 is a photomicrograph which shows the complete conversion of the diboride to the oxide as a result of testing at 1650°C. This conversion was complete and

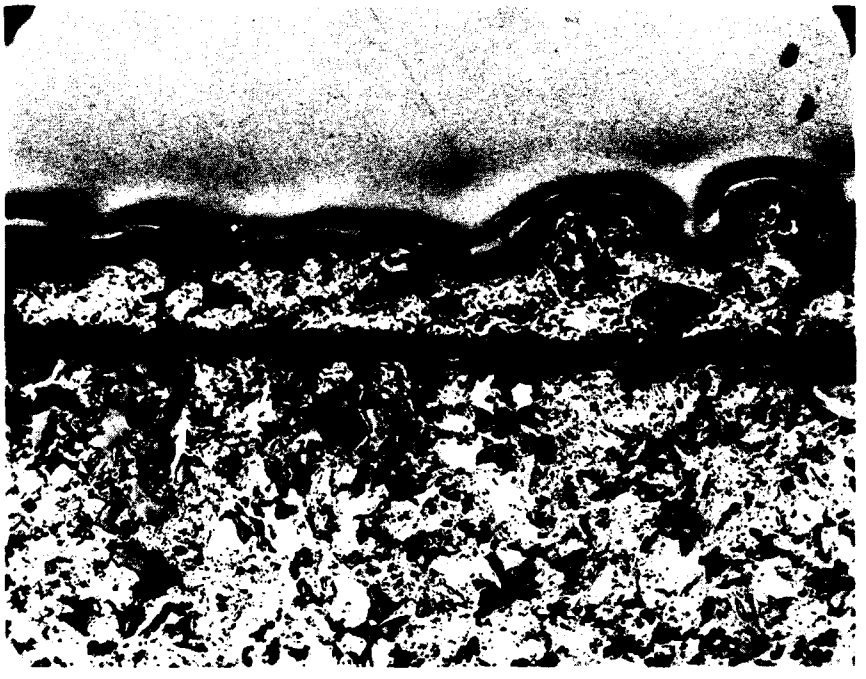

Figure 10. TiB_2 Coating After Oxidation Test, Illustrating Complete Conversion of the Titanium Diboride to the Oxide, 100 X

penetration occurred in 15 minutes. At 2000°C, failure occurred in approximately 7 minutes. In Figure 11, the test area of a typical TiB_2-

coated sample is shown. Penetration in this sample occurred after 7 minutes at 2000°C.

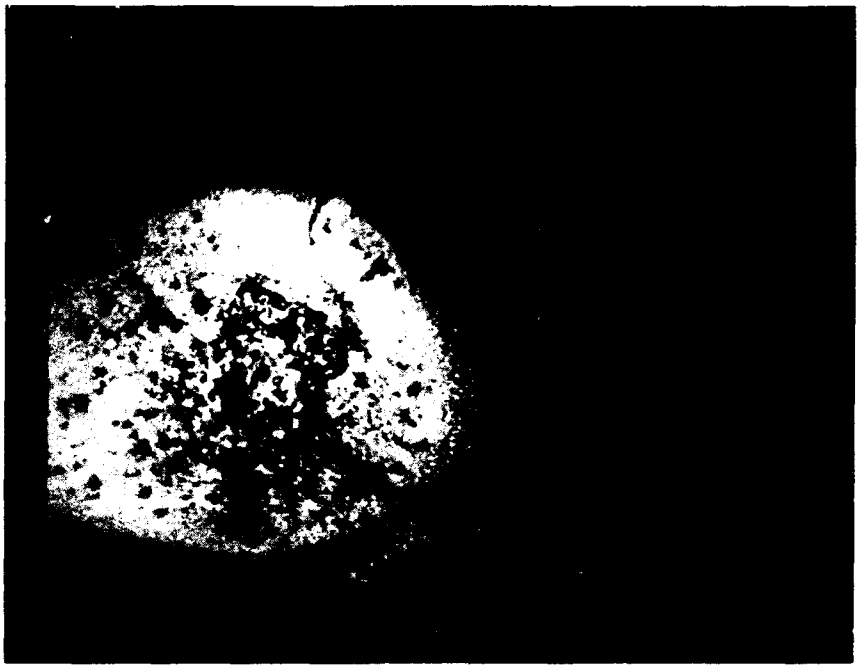

Figure 11. Surface Erosion of TiB_2-Coated Graphite as a Result of Oxidation Test, 7 Minutes at 2000°C

Titanium diboride was expected to protect the graphite by conversion to titanium oxide but this reaction evidently takes place at a much more rapid rate than was expected. Reaction kinetics at elevated temperatures were unknown but proved to be significantly accelerated above 1600 °C. Below 1500°C, a 0.012-inch-thick coating will provide adequate protection for about 30 minutes. Above 1650°C, the protection decreases about 20 per cent for each 100°C temperature rise.

2.3.3. Hexaboron Silicide

The use of silicon carbide as an oxidation barrier for graphite has been well established. Therefore, it was thought that combining the excellent oxidation resistance of silicon at temperatures up to 1650°C with a high-melting-point boride would result in a high-temperature oxidation-resistant coating.

A quantity of B_6Si of two purity levels was obtained. Grade AA contained approximately 98 per cent B_6Si and 2 per cent free silicon, while grade B contained 80 to 85 per cent B_6Si and 15 to 20 per cent free

silicon. Initial tests immediately eliminated grade B because of the formation of SiO_2 and subsequent pinholes in the coating.

The higher-purity B_6Si plasma sprayed quite easily and formed a hard, tightly adhering coating when sprayed under the following conditions:

Power input	-	30 kw at 39 volts,
Arc-gas flow rate, 90 per cent argon, 10 per cent hydrogen	-	1.2 std ft^3/min,
Powder-gas flow rate, argon	-	2.54 std ft^3/min,
Particle size, B_6Si	-	100 per cent through 325-mesh screen,
Torch-to-sample distance	-	2.75 in,
Torch lateral speed	-	1.50 ft/min,
Torch rotational speed	-	20.5 rpm.

A mixture of 90 per cent argon and 10 per cent hydrogen was used as the arc-gas in order to obtain a higher enthalpy flame than produced by pure argon. The use of this mixture keeps the particles at a high enough temperature to bond well, both to the substrate and to each other.

The typical structure of B_6Si coating applied at the conditions listed above is shown in Figure 12. Evidently some slight compositional change occurred as the material passed through the arc because the coating was a complex of B_6Si which as yet has not been identified.

The B_6Si coating was quite porous, did not readily form a glassy phase upon oxidation and offered very little oxidation protection above 1400°C. Investigation of the good oxidation results reported by Allis Chalmers in their technical bulletin 48S9967B revealed that a heat-treatment was necessary after spraying the coating on the sample. Since this heat-treating step was proprietary and the process had not been patented, graphite samples were sent to Allis Chalmers to be coated and heat-treated. A total of eight samples were coated with B_6Si and four of these were heat-treated. Upon return of the samples, both heat-treated and non-heat-treated coatings were subjected to an X-ray diffraction analysis. The coating which had not been heat-treated had the same structure as those discussed above; i.e., a complex form of boron-silicon which could not be identified. However, the coating which had been heat-treated consisted of a mixture of B_4C and the β form of SiC. The structure of the non-heat-treated coating prepared by Allis Chalmers is

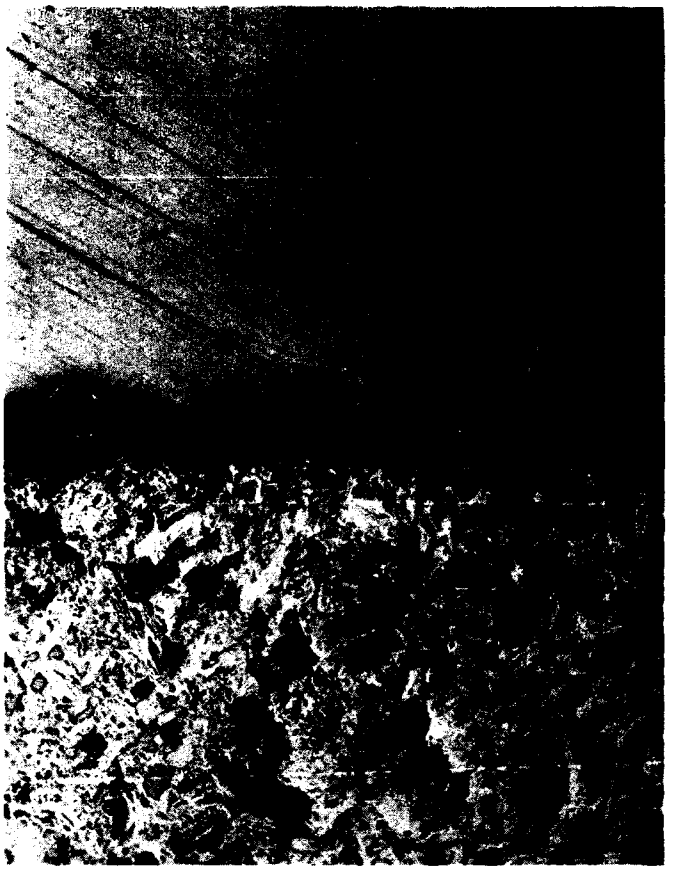

Figure 12. B_6Si Plasma-Sprayed Coating on Graphite by National Carbon Company, 100 X

shown in Figure 13 and the structure of the heat-treated coating is shown in Figure 14.

These samples gave predictable results when tested for oxidation resistance. The coatings which had not been heat-treated offered no protection above 1400°C and penetration of the coating occurred in less than one minute. The heat-treated coatings were tested at a temperature of 1750°C and penetration of the coating occurred in 3 minutes. At the end of 10 minutes, a significant portion of the sample had been destroyed. Figure 15 shows the surface of the sample after being subjected to the flame test for periods of 5 and 10 minutes. For comparison, a sample of the same dimensions was coated with SiC by the pack-diffusion process (see Section 4) and subjected to the same oxidation test. At 1750 °C penetration occurred in 5 minutes, but the overall damage at the end of 10 minutes was much less than that for the B_6Si-coated sample. The surface of the sample is shown in Figure 16 after test periods of 5 and 10 minutes.

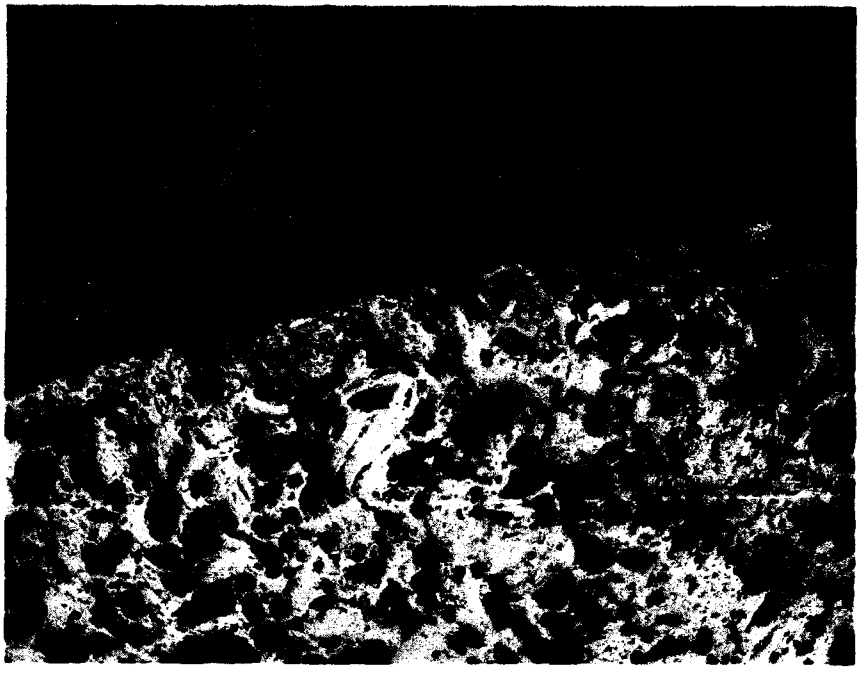

Figure 13. B_6Si Plasma-Sprayed Coating on Graphite by Allis Chalmers, 100 X

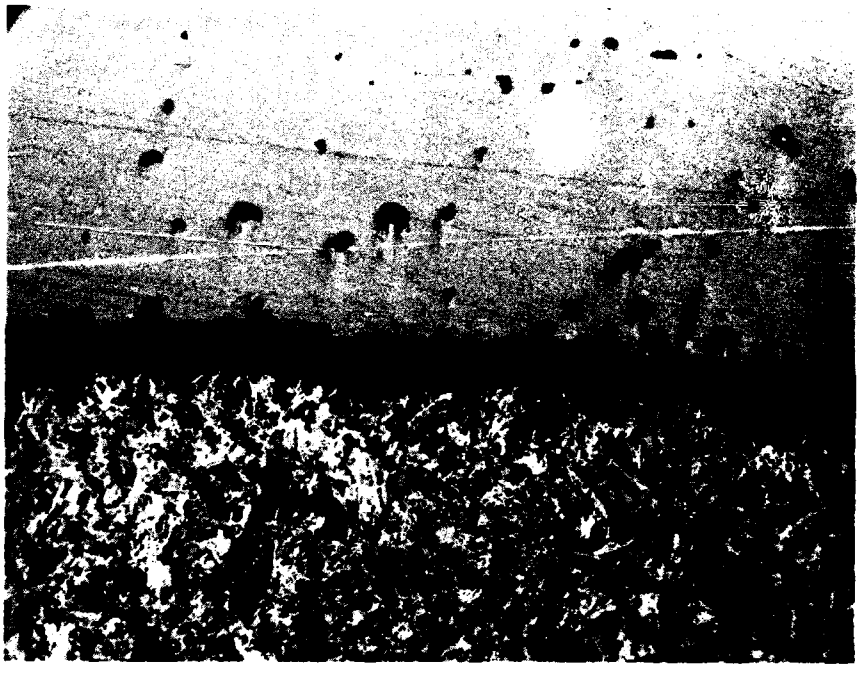

Figure 14. B_6Si Coating Plasma Sprayed on Graphite and Heat-Treated by Allis Chalmers, 100 X

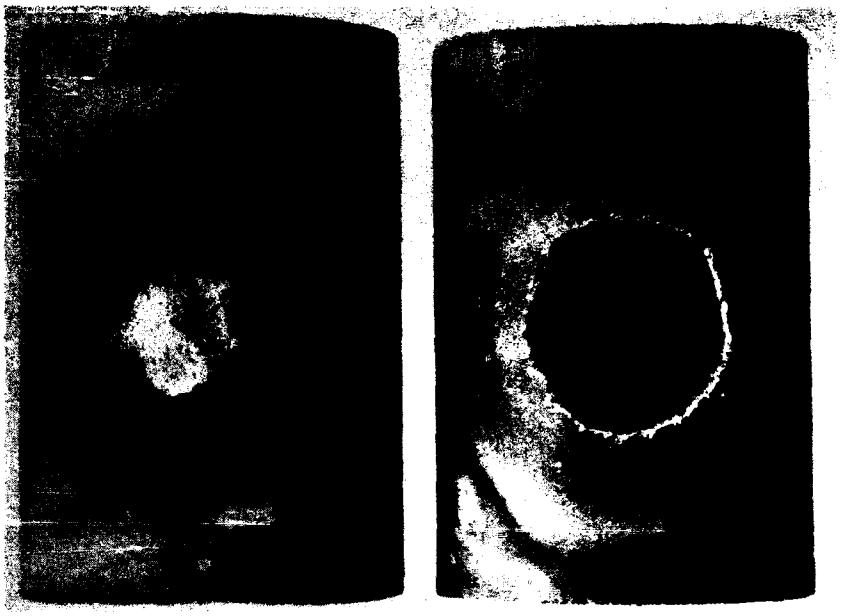

5 Minutes 10 Minutes

Figure 15. Heat-Treated B_6Si Coating on Graphite, Tested in Oxidizing Flame for 5 and 10 Minutes

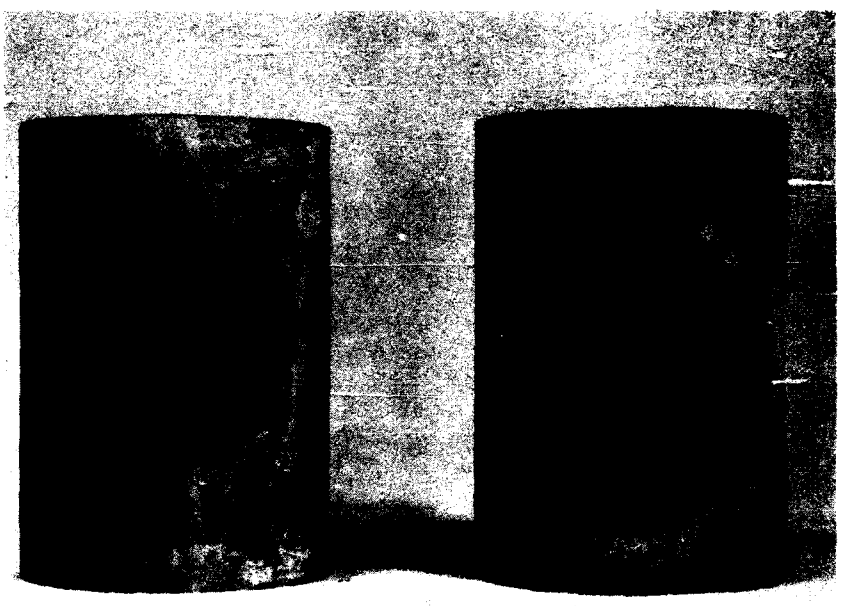

5 Minutes 10 Minutes

Figure 16. SiC Coating Applied on Graphite by Pack-Diffusion Process, Tested in Oxidizing Flame for 5 and 10 Minutes

A second sample coated with B_6Si was subjected, after heat-treating, to a dynamic oxidation test. In this test, the sample was suspended from a recording balance in the hot zone of an induction furnace. An argon atmosphere was provided until the temperature reached 800°C. At this temperature, the flow of argon was stopped and dry air was fed across the sample at a controlled rate. The temperature was increased at a rate of 10°C per minute until the furnace limit of 1685°C was reached. The sample lost no weight up to this temperature, but bubble formation on the sample surface showed that 1700°C would be approximately the maximum temperature to which continuous protection could be provided.

The oxidation protection claimed by Allis Chalmers, therefore, can be obtained only after heat-treating the B_6Si under controlled conditions to convert it to B_4C and SiC. Even with heat-treating, the oxidation protection obtained by use of a B_6Si coating does not exceed that of SiC coatings.

2.3.4. Zirconates

A thermodynamic study of materials with melting points over 2000°C, shows that the oxides, as a group, possess the most favorable characteristics for high-temperature use in oxidizing atmospheres. Although some oxides meet the temperature requirements, they are limited as oxidation barriers by other characteristics such as the tendency to undergo hydrolysis or the susceptibility to thermal shock.

Zirconium oxide, which has been used in oxidizing atmospheres at high temperatures for quite some time, passes through a crystalline transformation from monoclinic to tetragonal at about 1200°C and the volume increase is accompanied by a considerable change in thermal expansion. This volumetric and thermal-expansion change results in poor thermal-shock resistance. The thermal-shock resistance can be improved by stabilizing the ZrO_2 with the addition of various amounts of other materials such as magnesium oxide, calcium oxide or cerium oxide. The zirconates of the alkali earth metals (periodic table Group II-a) are inherently stable at high temperatures and these compounds were investigated as oxidation barriers for graphite.

The first of the Group II-a zirconates studied as an oxidation reaction barrier was magnesium zirconate. The name magnesium zirconate is actually a misnomer because it is a solid solution of MgO and ZrO_2 rather than an actual compound. However, this name is commercially applied to the solid solution which is prepared on a mole-to-mole basis. Physical properties of the solid solution are given in Table 7.

Table 7. Physical Properties of Solid Solution of Magnesium Oxide and Zirconium Oxide

Melting Point, °C	2066
Specific Gravity	4.5
Solubility in H_2O	Insoluble
CTE, Ave. 20-1250°C, 10^{-6}/°C	11.35

The $MgO \cdot ZrO_2$ material can be sprayed quite successfully under the following operating conditions:

Arc-gas flow rate, argon	-	2.17 std ft^3/min,
Powder-gas flow rate, 10 per cent H_2, 90 per cent argon	-	0.42 std ft^3/min,
Amperage	-	600 amps,
Voltage	-	46 volts,
Sample rotational speed	-	20.5 rpm,
Torch lateral travel speed	-	2.5 ft/min,
Torch-to-sample distance	-	3.25 in,
Zirconate particle size	-	100 per cent through 100- and on 140-mesh screen.

Grade ATJ graphite rods 0.25 of an inch in diameter by 3.0 inches in length, were used as the samples for all zirconate coating experiments. This size sample reduced the preparation time, decreased the quantity of graphite and coating material required, and simplified the oxidation testing. The sample shown in Figure 17 was typical for graphite coated with magnesium zirconate. The rough texture of the coating was the direct result of the particle size of the powder. In later experiments, the powder size was reduced to a through 200- and on 325-mesh screen size and this gave a coating of very smooth texture. In Figure 18, a cross-sectional view of a coated sample is shown. The small cracks visible in the edge of the coating were a result of the mounting procedure and were not inherent in the coating. This sectional view illustrates the uniformity of the coating thickness.

A more detailed study of the coating is possible with the photomicrograph of Figure 19. In this picture, both the bonding of the coating to the substrate and the amorphous structure of the coating is illustrated. Figure 20 at 400 X, shows the actual grain boundaries within

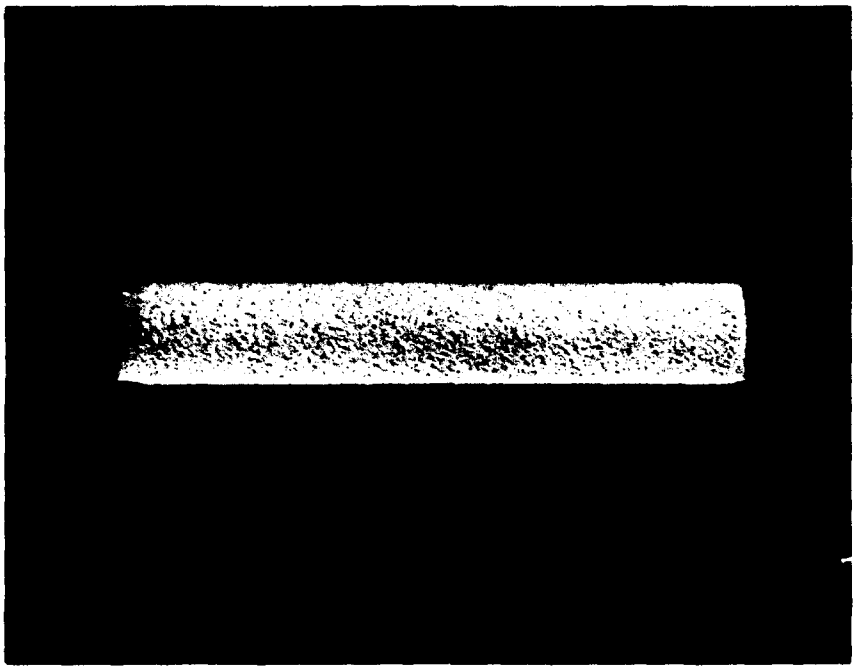

Figure 17. Magnesium Zirconate Coating on Graphite Rod

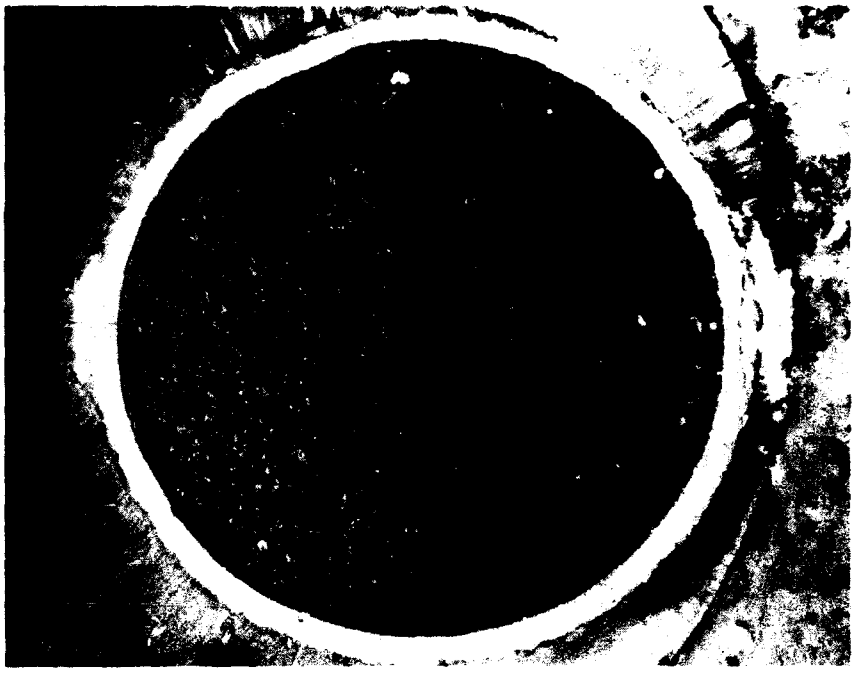

Figure 18. Cross-Sectional View of Magnesium Zirconate Coating on Graphite Rod, 13X

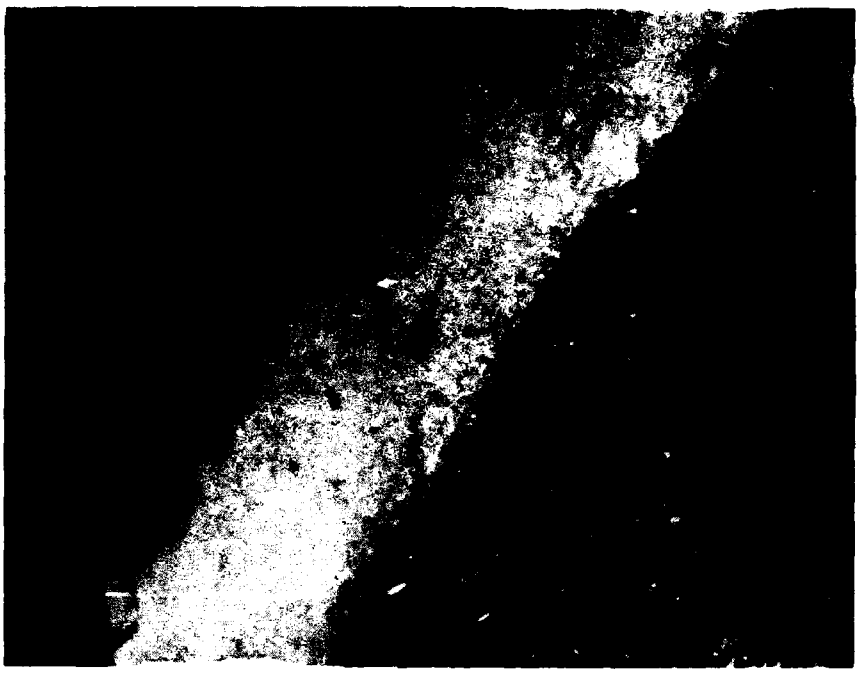

Figure 19. Magnesium Zirconate Coating on Graphite Rod, 100 X

Figure 20. Magnesium Zirconate Coating, Etched, 400 X

the coating. For this photomicrograph, the sample was etched in phosphoric acid to sharpen the grain boundary lines. Definite boundaries existed between the particles; however, mechanical interlocking of particles was evident thus showing that the molten particles molded themselves readily to conform to the surface of the graphite substrate. Although these coatings were not completely impervious, they materially reduced the amount of oxygen that reached the graphite.

The magnesium zirconate coatings, however, would not stand up at temperatures in excess of 1800°C for more than a few minutes and, even at 1400°C, protection of the graphite was maintained for no more than 30 minutes. Coating failure was due to two factors:

1) The difference in CTE of zirconate versus the ATJ (11.35 and 4.0, 10^{-6}/°C, respectively;

2) The reaction of the oxide coating with the graphite.

Since the CTE of the magnesium zirconate is difficult to change to any great degree, another method was used to decrease the effect of the CTE differential. The method used was the spraying of multilayer coatings. First a coating of 0.003-inch thickness of tungsten was applied to the graphite and the zirconate was sprayed on the tungsten. The use of the tungsten greatly reduced the amount of reaction between the oxide and the graphite. Although the tungsten will eventually react with the oxide and the graphite to form WO_2 and WC, respectively, the rate of reaction is not great enough to materially affect the life of the coating. Also, since the CTE of the tungsten (4.87, 10^{-6}/°C, average at 20-1250°C) is intermediate to that of graphite and that of zirconate, the tungsten absorbs part of the thermal stress created by the CTE differential between graphite and the zirconate. The bond between the zirconate and the tungsten appeared to be slightly stronger than the bond between the graphite and the zirconate and this increase in bond strength tended to hold the coatings on the samples at temperatures higher than when the zirconate was applied directly to the graphite.

Tungsten can be successfully plasma sprayed on graphite under the following conditions:

Power input	-	24 kw,
Voltage	-	40 volts,
Amperage	-	600 amps,
Arc-gas flow rate, argon	-	2.17 std ft^3/min,

Powder-gas flow rate, 20 per cent argon, 10 per cent H_2	-	0.23 std ft^3/min,
Powder particle size, W	-	100 per cent through 200- and on 325-mesh screen,
Sample rotational speed	-	20.5 rpm,
Torch lateral travel speed	-	2.5 ft/min,
Torch-to-sample distance	-	2.75 in.

When spraying tungsten in an oxidizing atmosphere, the spraying time was limited to two minutes or less to prevent the formation of tungsten oxide. A 2-minute spraying period resulted in a coating approximately 0.004 of an inch thick. If a thicker coating is desired, the sample must be allowed to cool before spraying again or an external cooling source must be provided to prevent substrate overheating.

A simple oxidation apparatus was constructed in order to evaluate the effectiveness of these coatings. The sample was clamped, by each end, between a pair of copper electrodes and heating was achieved by passing a current through the sample. This equipment, called the resistance-oxidation apparatus, is illustrated in Figure 21.

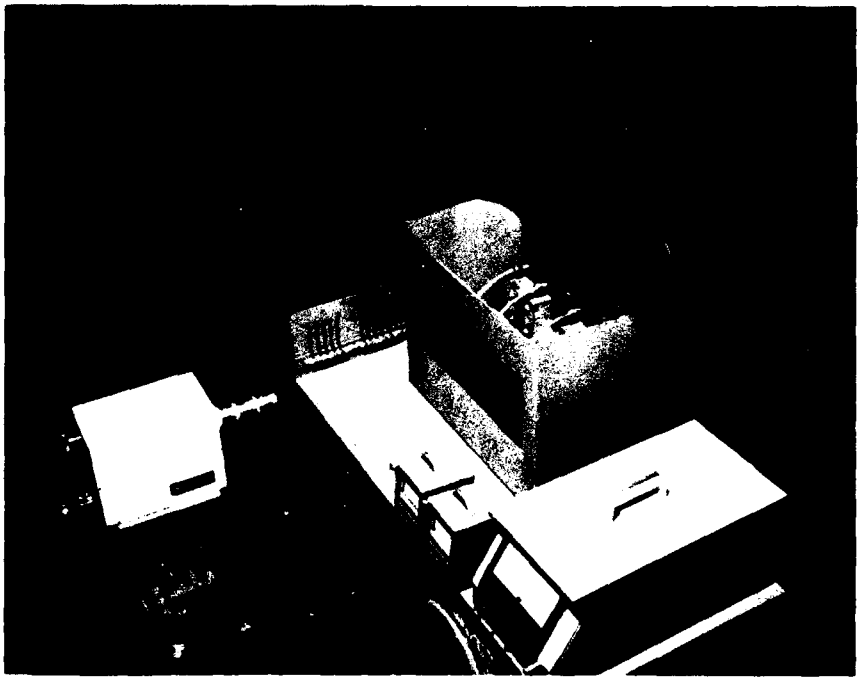

Figure 21. Electrical-Resistance Apparatus for Testing Oxidation-Protection Coatings on Graphite

Temperature was measured on the surface of the coating by means of a two-color pyrometer. The two-color pyrometer was used to correct for any emissivity changes due to a non-black-body radiating surface. The retaining shields and lampblack insulation, shown in Figure 22, were added to each electrode to insure that only coated surfaces of the sample were exposed to an oxidizing atmosphere during the resistance-oxidation test. The section of the substrate not covered by the coating was packed in lampblack, creating a barrier which prohibited oxygen attack of the unprotected graphite. This prevented channeling under the ends of the coating, which would lead to the eventual destruction of the sample and/or the coating. The lampblack provides protection for test periods of at least 5 hours.

This resistance-oxidation test was very severe in that it created some conditions not likely to be found in actual use of the materials. However, it did allow testing up to 3000°C in an air atmosphere which is difficult to achieve by any standard furnacing method.

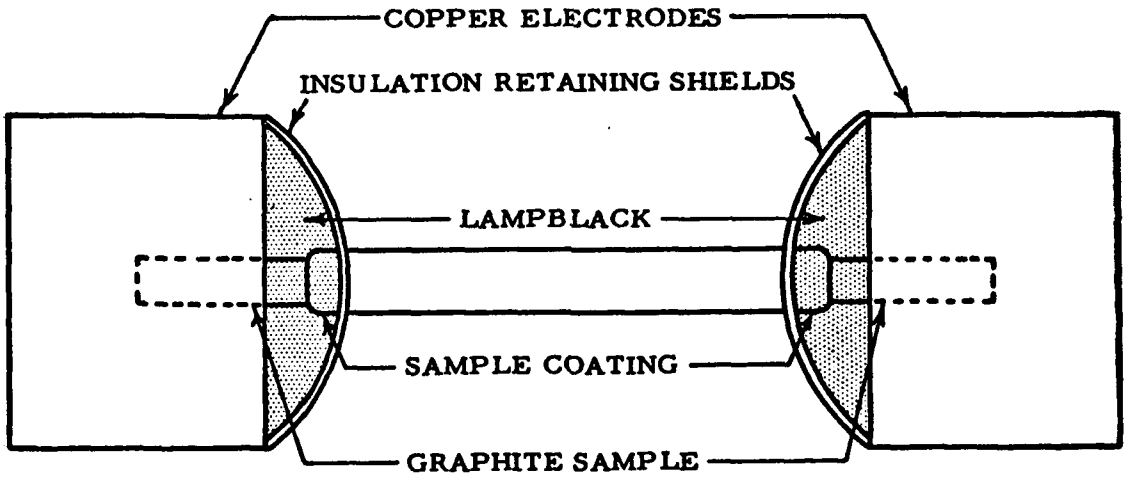

TOP VIEW

L-389

Figure 22. Sketch of Electrical-Resistance-Oxidation Apparatus showing Method of Protecting Uncoated Portion of Sample

The parameters involved in this resistance-oxidation are illustrated by the following facts. The temperature distribution which exists in resistance-heated graphite rods can be computed by the following equation:

$$\gamma = C - \frac{\zeta G^2}{4\lambda} r^2 \qquad (18)$$

where

γ = coordinate temperature,

C = Temperature at the center of the rod,

ζ = Resistivity of the material,

λ = Thermal conductivity,

r = Radius coordinate,

G = Current density.

The current density, G, is determined by the following equation:

$$G = \sqrt{\frac{2}{\zeta \cdot r_o} \left[\alpha + \xi_I C_B \frac{\frac{T_I^4}{100} - \frac{T_{II}^4}{100}}{T_I - T_{II}}\right] (\gamma_o - \gamma_R)} \qquad (19)$$

where

r_o = Outside radius of sample,

α = Heat transfer coefficient,

ξ_I = Integrated emissivity, 0.82,

C_B = Radiation coefficient of the black body,

T_I = Surface temperature, °K,

T_{II} = Room temperature, °K,

γ_o = Surface temperature,

γ_R = Room temperature.

Figure 23 shows the temperature distribution in a 0.250-inch diameter rod of ATJ, cut across the grain, which was calculated by use of the above equations (18) and (19). Even larger temperature gradients

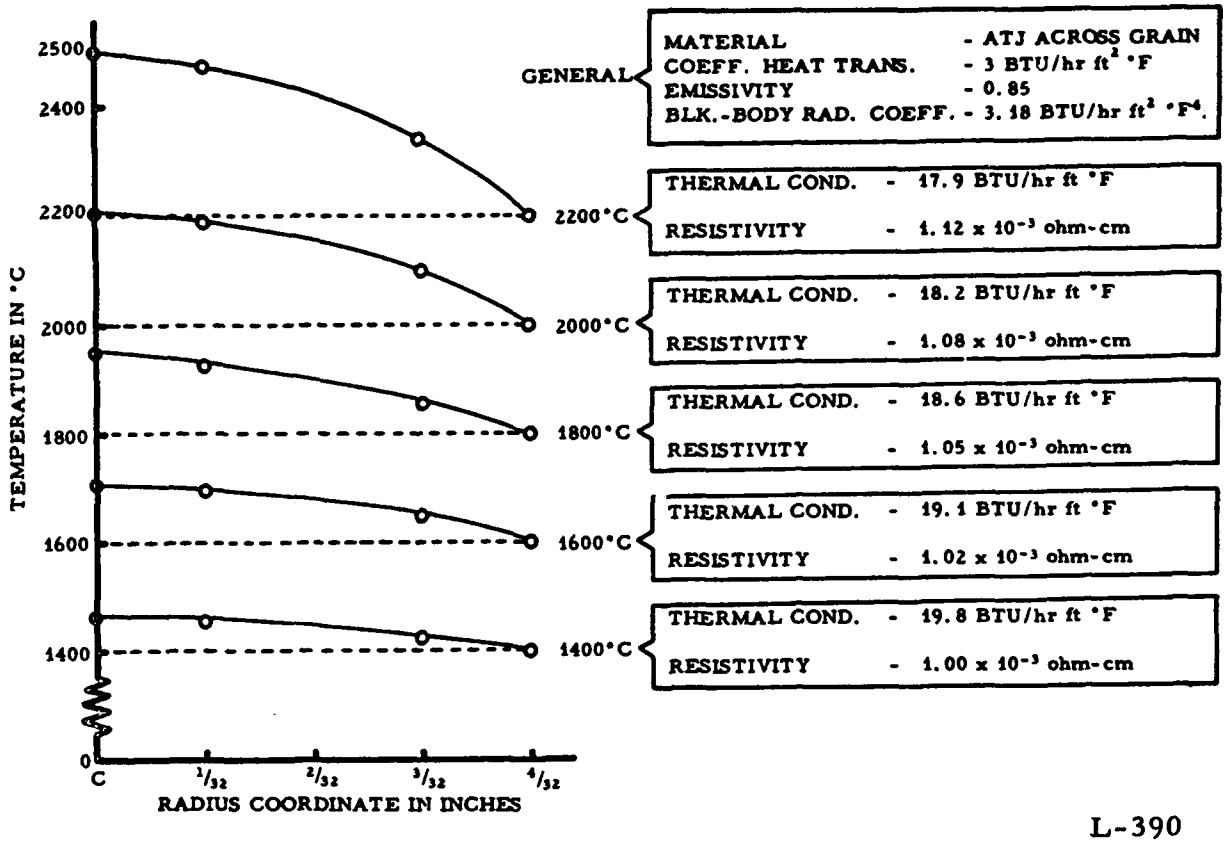

L-390

Figure 23. Temperature Distribution in 0.250-Inch Diameter High-Temperature Oxidation Test Sample, Heating by Resistance

exist in a graphite sample after it has been coated because of the thermal conductivity of the coating and because an interface exists between the coating and the substrate. A typical temperature gradient for magnesium zirconate sprayed directly on graphite is shown in Figure 24. These temperature differentials indicate that for a coated sample heated by resistance, a surface temperature of 2000°C means that the center of the graphite could easily be above 2600°C.

This resistance-oxidation test imposes conditions which would not be encountered normally and it was felt that, if a material could withstand this test, the material would be quite reliable in most applications for which it was chosen.

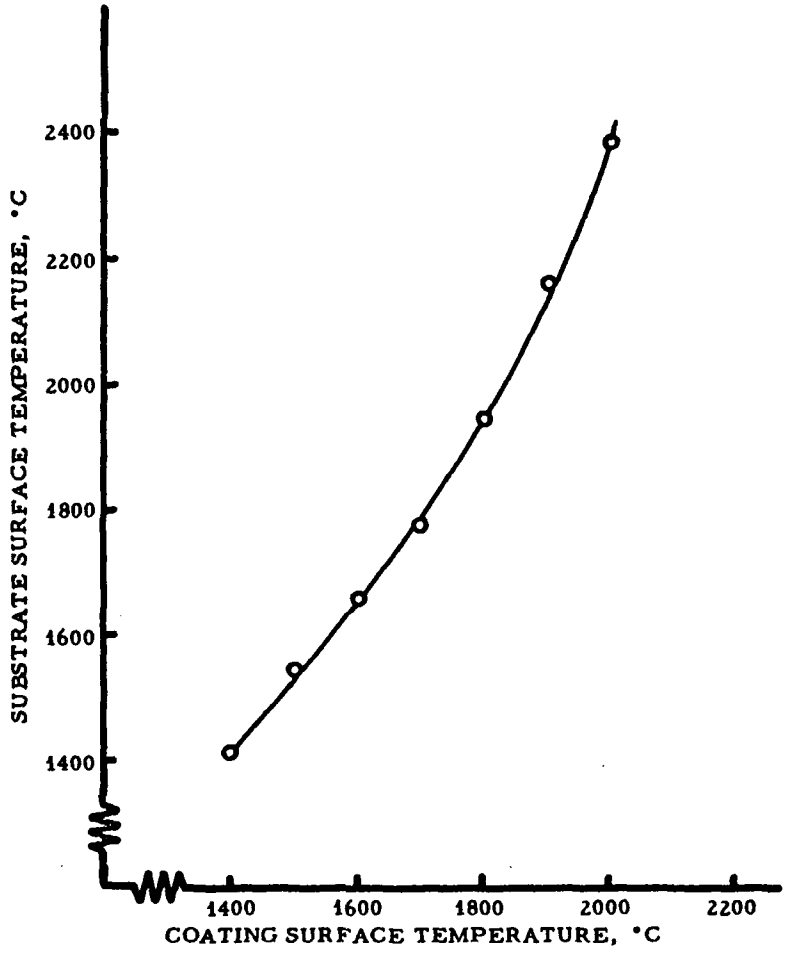

L-391

Figure 24. Temperature Gradient Across a Magnesium Zirconate Coating Deposited on Graphite, Sample Heated Resistively

Calcium zirconate ($CaZrO_3$) which, unlike magnesium zirconate, is actually a compound, was applied as a protective coating over tungsten-coated graphite. Figures 25 through 28 give the comparative weight-loss characteristics at various temperatures for magnesium zirconate-tungsten coatings on ATJ graphite, calcium zirconate-tungsten coatings on ATJ graphite, and uncoated ATJ graphite. Since these values were based on the original weight of the sample, it must be emphasized that they are comparative and not absolute values. In all the samples tested, the tungsten undercoat was 0.003 inch thick while the zirconate coating was 0.010 inch thick. The substrate material, in each case, was ATJ rods 0.25 inch in diameter and 3.0 inches in length. The hot zone or air span between electrodes was 1.125 inches.

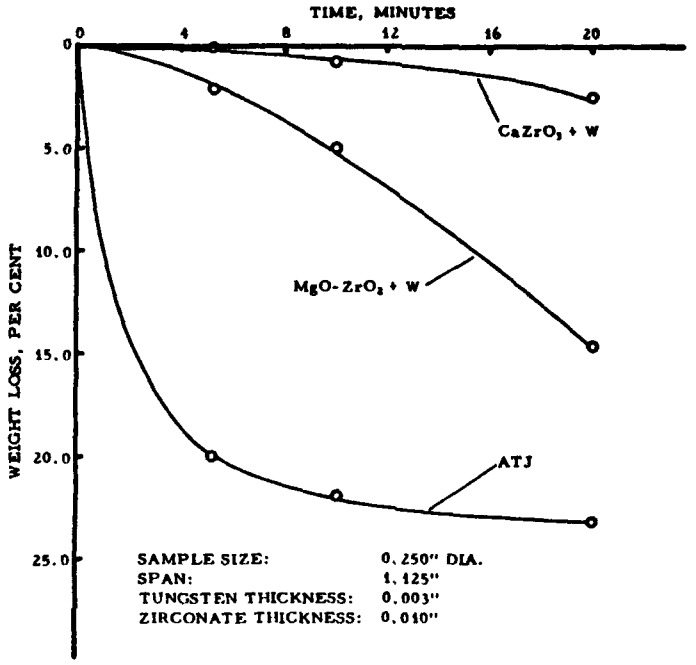

L-392

Figure 25. Oxidation Weight-Loss Characteristics of Zirconate Coatings on Graphite, 1400°C

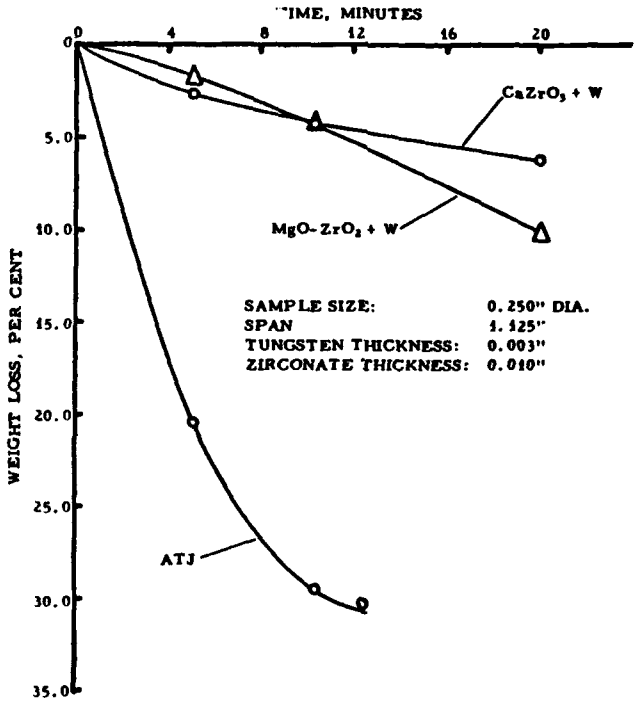

L-393

Figure 26. Oxida[illegible]eight-Loss Characteristics of Zircona[illegible]Coatings on Graphite, 1600°C

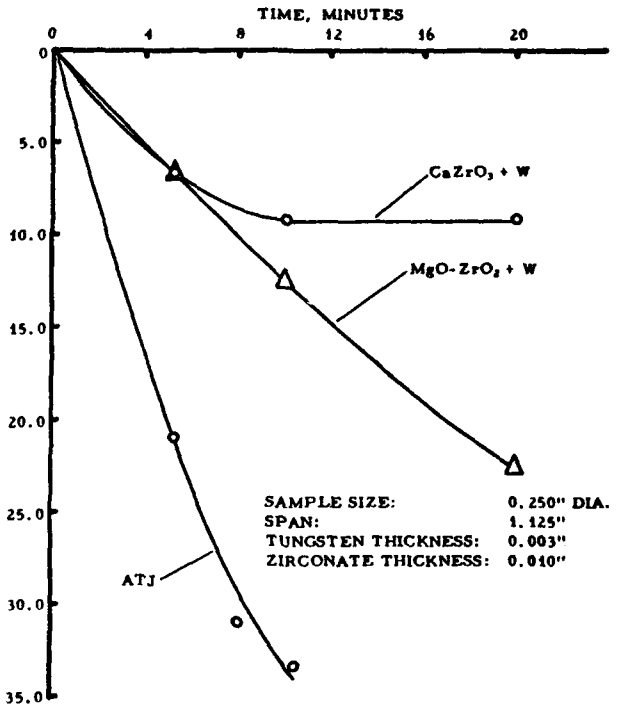

L-394

Figure 27. Oxidation Weight-Loss Characteristics of Zirconate Coatings on Graphite, 1800°C

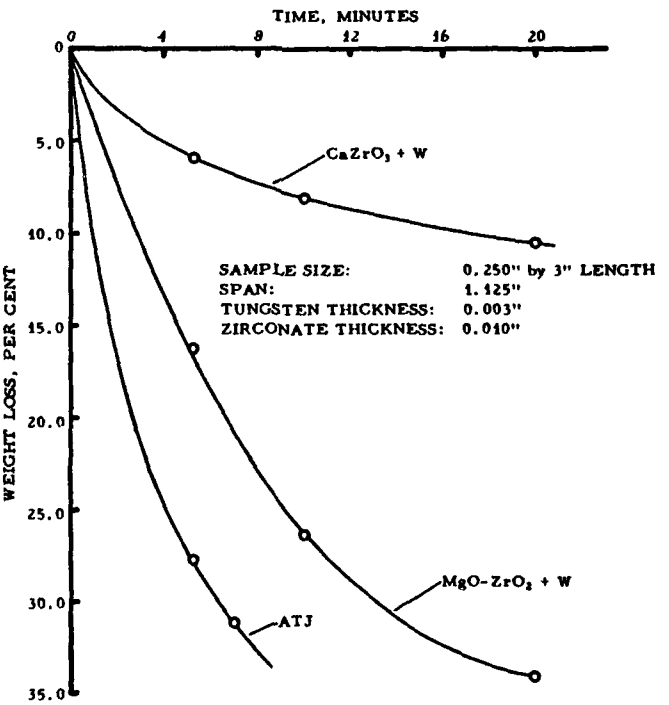

L-395

Figure 28. Oxidation Weight-Loss Characteristics of Zirconate Coatings on Graphite, 2000°C

All samples were heated to the desired temperature in a period of 120 seconds and, during this heating period, there was no damage to the coating even though the CTE of the coating was more than twice that of the graphite. This phenomenon was explained when the test conditions of the samples were examined. Since the graphite was at a higher temperature than the coating at any given time (as illustrated in Figures 23 and 24) the rates of expansion of the graphite and the coating were more nearly equal. Also, and perhaps of more importance, during the heating cycle and even at the desired temperature, the coating was under ring compression which tended to make it resistant to thermal damage. The above conditions were reversed upon cooling the coated sample. The coating, being exposed to air, tended to cool faster than the graphite and the large CTE differential was very noticeable. During cooling, the coating was under tension and, because the tensile strength of these refractory oxides is very poor, fractures quickly developed in the coating. Fractures in the coating were evident in every case where the test temperature exceeded 1500°C and in some cases at temperatures as low as 1200°C. It must be emphasized, however, that since this destruction took place on the cooling cycle, the relative life of the sample was not affected.

A series of samples was tested at various temperatures for periods of time ranging from 10 to 120 minutes in an effort to provide more effective means of evaluation of the zirconate coatings. Pictures were then made of the samples after testing and these pictures, combined with the accompanying tables, indicated the time at which sample failure began and the resulting condition of the sample.

Table 8 and Figures 29, 30 and 31 represent the protection provided by magnesium zirconate coatings applied directly to graphite.

Table 8. Results of Resistance-Oxidation Test of Magnesium Zirconate Coatings on Graphite

Temperature	Time*
1400°C	18 minutes
1500°C	15 minutes
1600°C	14 minutes
1700°C	7 minutes
1800°C	4 minutes
1900°C	2 minutes

* Average time when first pinhole or crack appeared in the coating, does not represent ultimate failure of the coating.

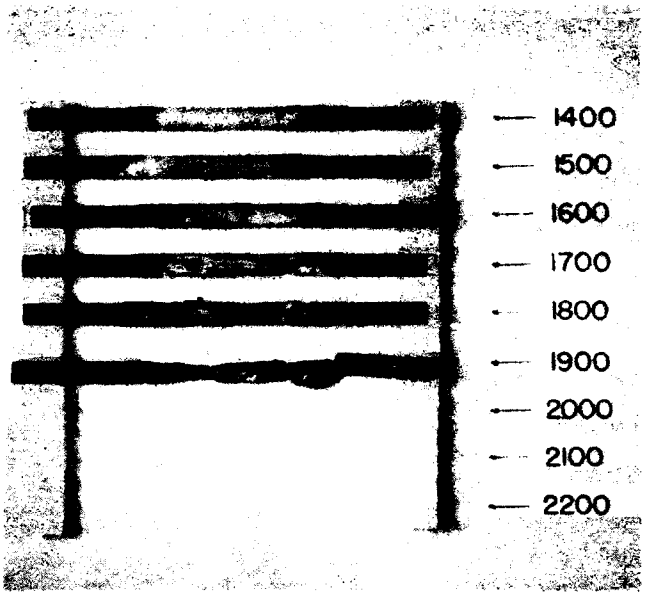

Figure 29. Resistance-Oxidation Test of Magnesium Zirconate, Plasma Sprayed Directly on Graphite, 10 Minutes, 1400 to 1900°C

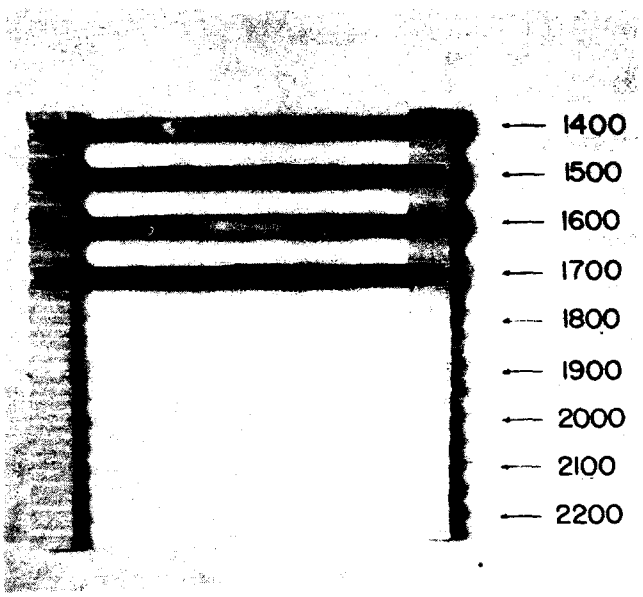

Figure 30. Resistance-Oxidation Test of Magnesium Zirconate, Plasma Sprayed Directly on Graphite, 20 Minutes, 1400 to 1700°C

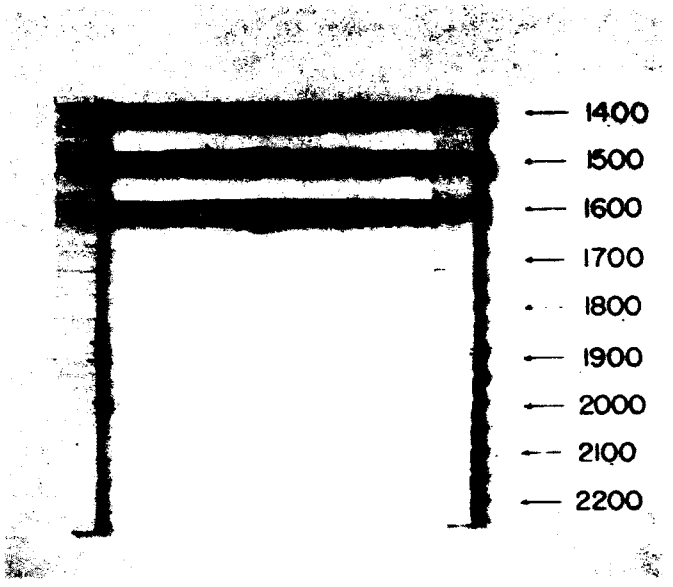

Figure 31. Resistance-Oxidation Test of Magnesium Zirconate, Plasma Sprayed Directly on Graphite, 30 Minutes, 1400 to 1600°C

Table 9 and Figures 32, 33 and 34 illustrate the increase in protection that is provided when an intermediate layer of tungsten is used between the magnesium zirconate and the graphite.

Table 9. Results of Resistance-Oxidation Test of Magnesium Zirconate-Tungsten Coatings on Graphite

Temperature	Time*
1400°C	45 minutes
1500°C	30 minutes
1600°C	25 minutes
1700°C	9 minutes
1800°C	6 minutes

* Average time when first pinhole or crack appeared in coating, does not represent ultimate failure of coating.

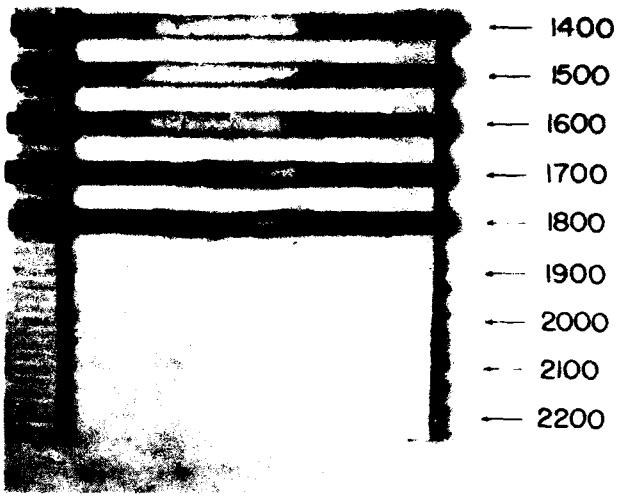

Figure 32. Resistance-Oxidation Test of Magnesium Zirconate-Tungsten System, Plasma Sprayed on Graphite, 10 Minutes, 1400 to 1800°C

Figure 33. Resistance-Oxidation Test of Magnesium Zirconate-Tungsten System, Plasma Sprayed on Graphite, 30 Minutes, 1400 to 1600°C

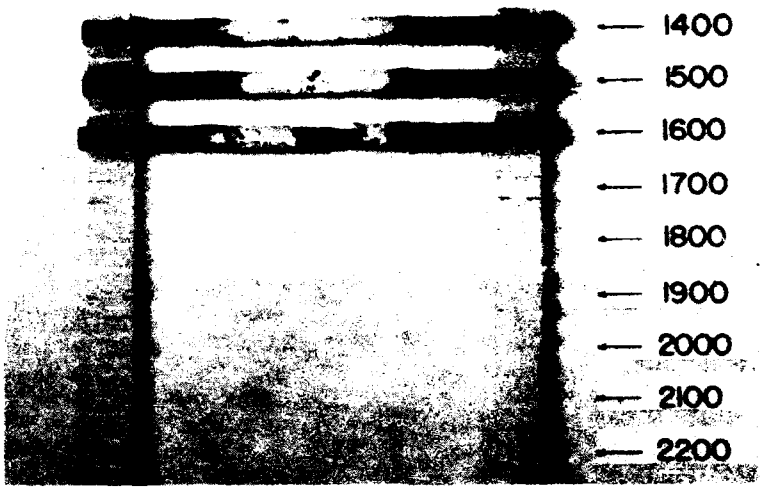

Figure 34. Resistance-Oxidation Test of Magnesium Zirconate-Tungsten System, Plasma Sprayed on Graphite, 30 Minutes, 1400 to 1600°C

The calcium zirconate coatings applied directly to the graphite were studied in the same manner. These coatings, after being exposed to an oxidizing atmosphere at elevated temperatures for periods of 10, 20 and 30 minutes, are illustrated in Figures 35, 36 and 37, respectively. Table 10 lists the average time at which the coatings began to show signs of failure. In several instances, initial cracks healed themselves and the life of the coating was actually much longer than would have been expected.

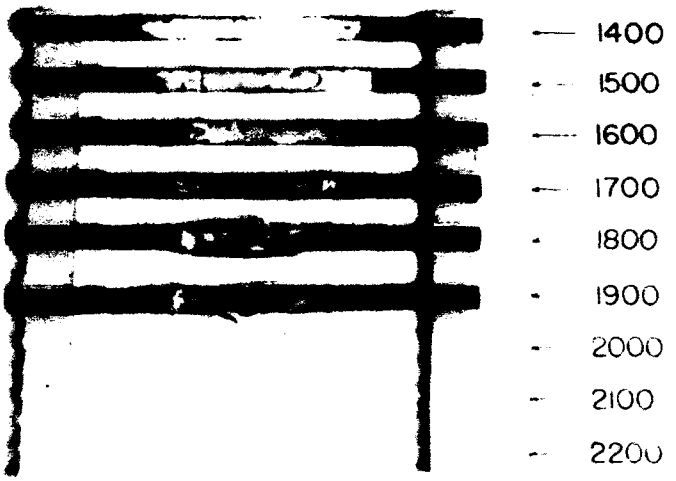

Figure 35. Resistance-Oxidation Test of Calcium Zirconate Plasma Sprayed Directly on Graphite, 10 Minutes 1400 to 1900°C

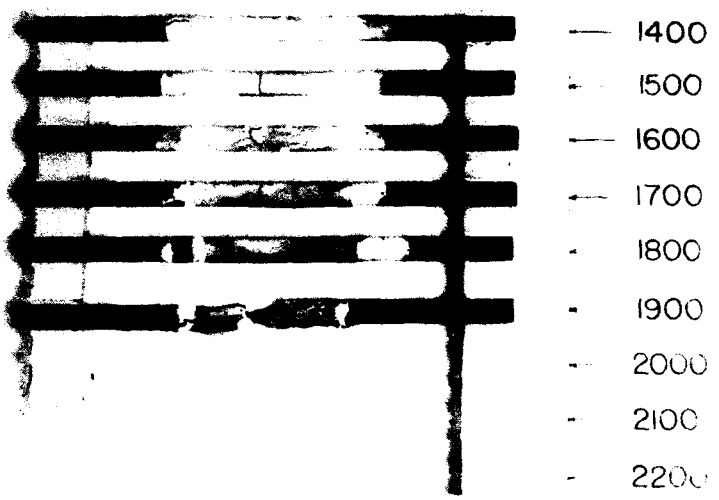

Figure 36. Resistance-Oxidation Test of Calcium Zirconate Plasma Sprayed Directly on Graphite, 20 Minutes 1400 to 1900°C

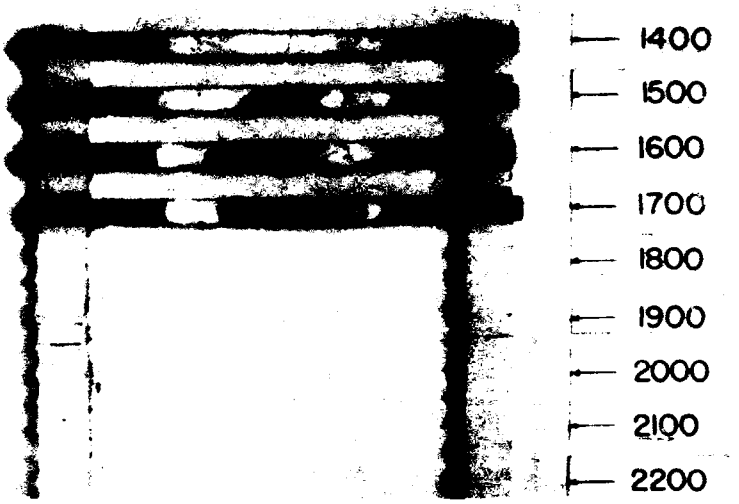

Figure 37. Resistance-Oxidation Test of Calcium Zirconate Plasma Sprayed Directly on Graphite, 30 Minutes 1400 to 1700°C

Table 10. Results of Resistance-Oxidation Test of Calcium Zirconate Coatings on Graphite

Temperature	Time*
1400°C	70 minutes
1500°C	60 minutes
1600°C	30 minutes
1700°C	20-25 minutes
1800°C	15 minutes
1900°C	7 minutes
2000°C	2 minutes

* Average time when first pinhole or crack appeard in coating, does not represent ultimate failure of coating.

The samples shown in Figures 38 through 42 were coated with calcium zirconate after a tungsten undercoat of 0.003 of an inch thick had been placed on the graphite. The test periods were extended to 120 minutes because of the marked increase in protection afforded by this system of coatings. Table 11 gives the times for initial failure of the calcium zirconate-tungsten-coated samples.

From these data, it is evident that the zirconates of magnesium and calcium are useful for the oxidation protection of graphite at elevated temperatures for single-exposure, short-time applications.

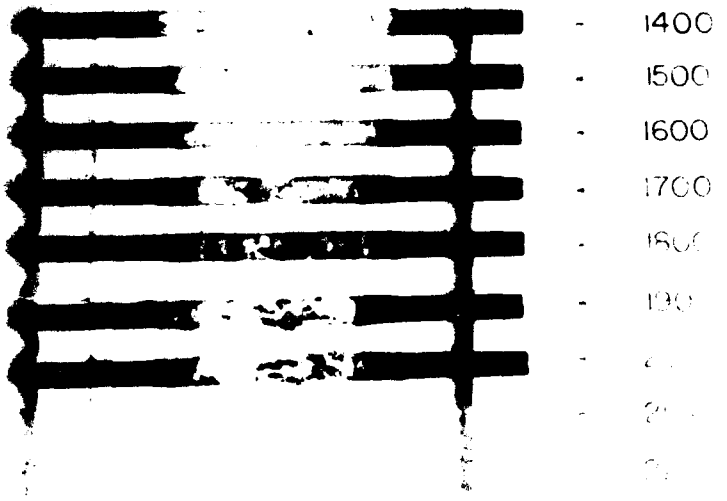

Figure 38. Resistance-Oxidation Test of Calcium Zirconate-Tungsten System Plasma Sprayed on Graphite, 10 Minutes, 1400 to 2000°C

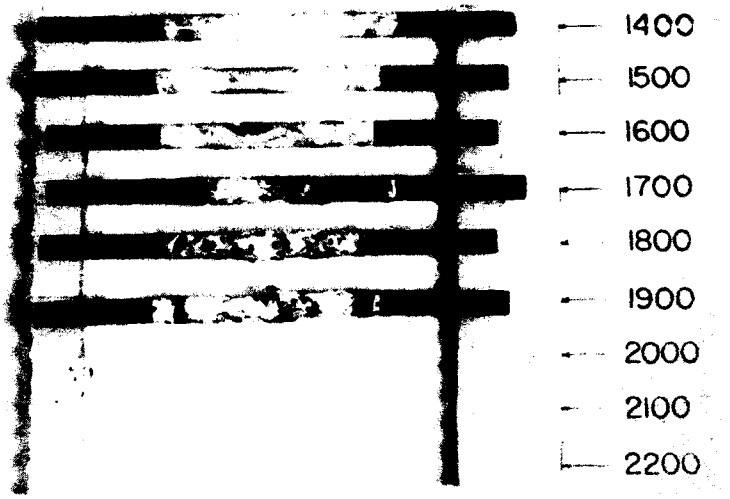

Figure 39. Resistance-Oxidation Test of Calcium Zirconate-Tungsten System Plasma Sprayed on Graphite, 20 Minutes, 1400 to 1900°C

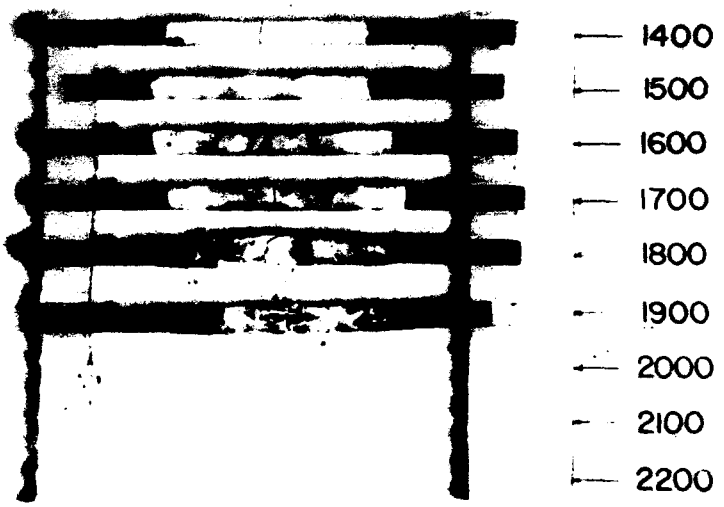

Figure 40. Resistance-Oxidation Test of Calcium Zirconate-Tungsten System Plasma Sprayed on Graphite, 30 Minutes, 1400 to 1900°C

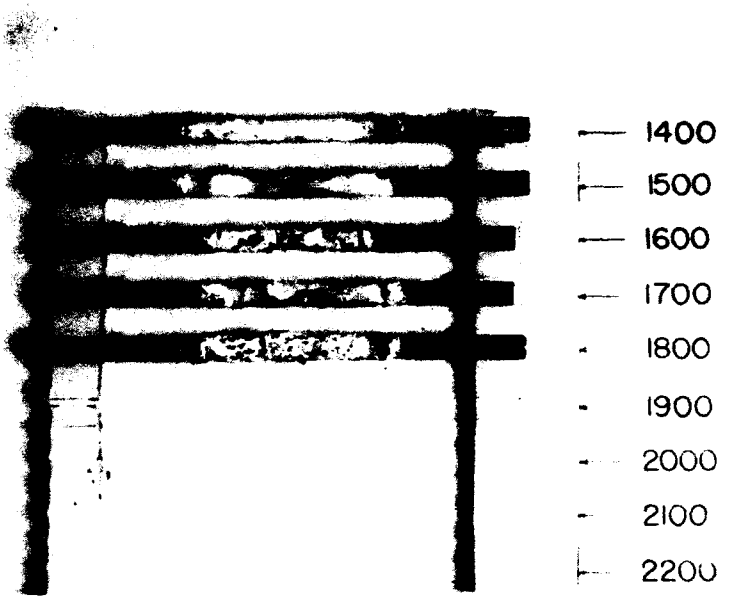

Figure 41. Resistance-Oxidation Test of Calcium Zirconate-Tungsten System Plasma Sprayed on Graphite, 60 Minutes, 1400 to 1800°C

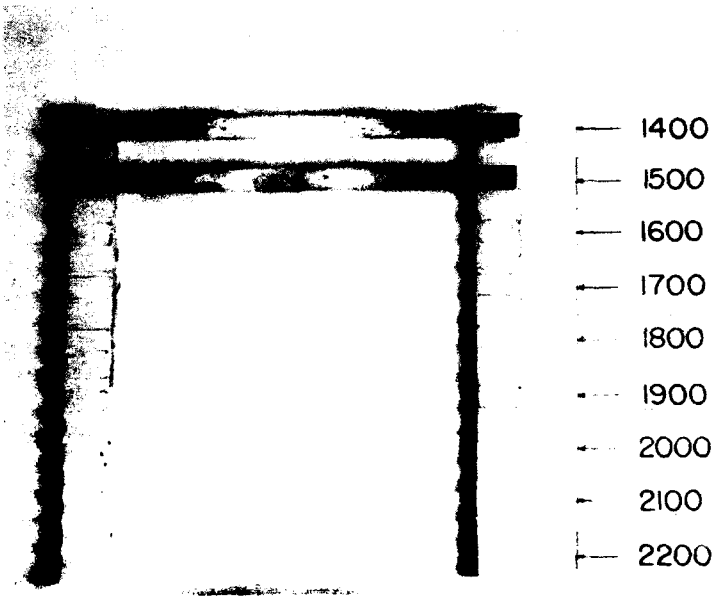

Figure 42. Resistance-Oxidation Test of Calcium Zirconate-Tungsten System Plasma Sprayed on Graphite, 120 Minutes, 1400 to 1500°C

Table 11. Results of Resistance-Oxidation Test of Calcium Zirconate-Tungsten Coatings on Graphite

Temperature	Time*
1400°C 1500°C	> 10 hours
1600°C	90 minutes
1700°C	60 minutes
1800°C	25 minutes
1900°C	20 minutes
2000°C	7 minutes

* Average time when first pinhole or crack appeared in coating, does not represent ultimate failure of coating.

The zirconates of strontium and silicon have yet to be investigated as protective coatings for graphite. However, zirconium silicate (zircon) seems to hold the most promise in that the melting point of this compound is 2420°C and the coefficient of thermal expansion, average from 200 to 1300°C, is 5.45 times 10^{-6}/°C. This value for the CTE lies well within the range of the graphites now available which might be used as substrates for coatings.

3. OXIDATION-PROTECTION COATINGS FOR GRAPHITE VAPOR DEPOSITED BY THE SOURCE-TARGET METHOD

3.1. Introduction

Vapor deposition of coatings by source-target techniques is one of the most promising methods of application. This method has great versatility in that so many different types of coatings may be applied. It is capable of producing smooth, continuous, nonporous coatings of good adherence and bond strength. Where coating-substrate reactions take place, its throwing power is one of the best.[52] These are all desirable characteristics which can be used to good advantage when the oxidation protection of graphite by refractory coatings is contemplated.

Several avenues of approach toward providing this protection were indicated in the literature at the inception of this work. Titanium nitride coatings had been shown to offer significant oxidation protection for graphite even at ultrahigh (about 2200°C) temperatures.[53] It was inferred that zirconium and hafnium nitrides should offer still greater protection. These compounds can easily be applied as coatings on graphite by source-target vapor deposition.[34] Silica and silicate coatings were described in many patents and articles as providing varying degrees of oxidation protection at lower temperatures.[54,55,56,57] Experimental evidence had been presented which showed that beryllium oxide was extremely inert toward graphite.[2] This property would certainly make beryllia coating systems of interest. Thoria is the highest-melting oxide known,[33] and therefore coating systems of this compound naturally were to be considered with great interest.

Protective oxide coatings may be obtained in two ways: first, by direct application of the oxide, and, second, by the application of the desired oxide cation to the substrate in the form of the element or another compound, such as carbide or nitride, and subsequently oxidizing this compound to the oxide form. Although oxide coatings can be, and indeed have been, applied directly by source-target vapor deposition,[34] the problems anticipated in doing this on an easily oxidizable graphite substrate appear quite formidable and unnecessary. Direct deposition by arc-plasma spraying[58] is much better suited for direct application of the oxide coatings. Since an apparatus for plasma spraying was available to this project and was engaged in directly applied oxide coating experiments at the time (See Section 2), it was decided that an attempt to apply oxide coatings directly on graphite by vapor deposition techniques would be unnecessary and a waste of effort.

The second method, that of converting an element or compound to the oxide after deposition, was chosen as the most practical way to achieve vapor-deposited oxide coatings. However, it unfortunately does not always produce physically desirable coatings. Often the oxide coatings obtained by this method are porous and not continuous, primarily due to an incompatibility between the specific volumes of the material under oxidation and the oxide formed.[59] A thermodynamically stable coating sequence is of little value from a protection standpoint if holes or gaps in the coating permit access by oxygen to the vulnerable substrate beneath. On the other hand, materials such as silicon[60] and aluminum[61] do oxidize to produce protective overcoats. In these cases, it is much more efficient to apply the base coating and partially oxidize it during use than it is to apply both coatings in separate operations.

The success of a nonoxide coating system applied by vapor deposition, or other methods for that matter, thus depends profoundly upon the manner in which the coating oxidizes. According to the literature, titanium nitride coatings were found to oxidize favorably.[54] The vapor-deposition program was therefore begun with the application and testing of this coating system.

3.2. Titanium Oxide Coatings

3.2.1. Experimental

All coatings investigated in the titanium oxide system were applied in a high-vacuum furnace. The ambient pressure maintained in the furnace during coating operations was below 10^{-4} mm of Hg for all trials except those during which nitrogen was being flushed through the system to obtain nitride coatings. The coating method used is sometimes referred to as vacuum metallizing,[52] because an evaporator-target setup was employed. The term is a misnomer, however, except for the few times that titanium metal coatings were applied to graphite. In all other cases, chemical reaction with the graphite substrate was intended, thus lending little significance to the term "metallizing". The method entails the raising of the temperature of the evaporator until the vapor pressure of the coating material contained therein becomes high enough for adequate vapor flow to occur. The article to be coated is placed in the path of this vapor flow, and the substrate temperature is regulated so that it will react or not react with the impinging vapor as desired.

Four types of coating operations were employed for the titanium system. Titanium metal coatings were obtained by maintaining titanium metal at 1650°C in the evaporator so as to produce a vapor pressure of 10^{-5} atmospheres.[62] Graphite substrates were adjusted in the vapor

flow so as to attain a temperature of about 1100°C. Coatings from 0.1 to 0.2 mm thick were deposited in one hour at temperature. Titanium carbide coatings were obtained by adjusting the graphite substrate so as to increase its temperature. Temperatures of about 1500°C were sufficient to promote reaction of the titanium vapor with the substrate. Titanium nitride coatings were obtained in two ways. In the first method, titanium nitride powder was placed in the evaporator and vaporized at about 1900°C. The substrate temperature was approximately 1775°C and coatings of about one mm thickness were deposited in three hours of such treatment. In the second method of TiN deposition, titanium metal was vaporized at about 2000°C toward a graphite substrate maintained at 1750°C. The length of time at temperature determined the coating thickness. At the end of the desired coating interval, the vacuum was broken, and maximum purity (99.996 per cent) nitrogen gas was introduced in the coating chamber until a pressure of about one atmosphere had been reached. The nitriding operation required about 10 minutes during which the furnace temperature was found to drop 300°C. The furnace power was shut off, and the system allowed to cool slowly in the nitrogen atmosphere. TiN coatings deposited in this manner were a much brighter yellow than those deposited by the first method, indicating a greater nitrogen saturation.

Temperatures were measured by a disappearing-filament optical pyrometer which had been calibrated using a standard light source. Although black-body conditions did not exist for temperatures read from evaporator surfaces, the error incurred in reading the evaporator temperature was expected to be small. Graphite cylinders, used as evaporators, were heated uniformly and had a height-to-diameter ratio of 2.5. Vapor effused from the cylinders through rectangular apertures in their covers. The ratios of the height of the cylinder to the length and to the width of this aperture are approximately $2\frac{1}{2}$ and 18, respectively. The recommended height-to-diameter ratio for black-body holes drilled into evenly heated objects is 6.[63] Temperatures read through the evaporator aperture should, therefore, be reasonably accurate. Black-body conditions also did not exist for temperatures read from substrate surfaces so these temperatures were subject to emissivity errors and were used only for internal comparisons.

Two sample shapes were used in the titanium oxide coating system. One of these shapes was a 1- by 1- by 4-cm bar. Samples of this shape were coated on all sides by four separate coating operations. The other shape was a $\frac{1}{4}$-inch diameter rod which was coated in the center section during only one firing. The rods were rotated continuously in the vapor path to insure good circumferential coverage. The ends of these rods were uncoated and, therefore, these samples were not totally protected.

A different type of oxidation test was performed on samples of each shape. The bars, which were completely covered by coating, were best tested on an apparatus which continuously recorded the weight change of the specimen as it was heated in a regulated, oxidizing gas stream. The rods, which were not completely covered, were tested by the electric-resistance oxidation apparatus described in Section 2.3.4. Temperatures were measured in the first type of test by a platinum-platinum 10-per cent rhodium thermocouple, and in the second type test by a two-color pyrometer.

Samples tested in the weight-change apparatus were introduced into the furnace at test temperature and allowed to equilibrate for 15 minutes in an inert atmosphere. The oxidizing gas was then passed over the sample at a flow rate of 22.5 standard cubic feet per hour. Oxidation was continued until there was no appreciable weight change during a one-hour period. The sample was removed from the furnace and examined. Samples were tested with the electric-resistance oxidation apparatus in the following manner. First, the ends of the samples were clamped to the power terminals and, in some instances, wrapped with aluminum foil to insure good electrical contact. Second, thermatomic black was packed around the ends of the rods at the regions which were uncoated (see Figure 22, Section 2.3.4) to prevent direct oxidation of the graphite and premature failure. Next, the optical pyrometer was focused on the center of the rod which was expected to be hottest. Finally, the power was turned on and increased slowly and continuously over a 90-second interval until the desired test temperature was attained. Minor adjustments in power were made when necessary to maintain the test temperature during the test, and measurement of voltage and amperage were recorded continuously during the tests. Each sample was oxidized until failure by "burn-through" occurred.

3.2.2. Results and Discussion

The titanium carbide coatings deposited on graphite during the course of this work were continuous, hard, well bonded, and smooth. Each coated sample had mirror-like, metallic finishes on all surfaces. This coating was perhaps the easiest to achieve of all the materials tried. It could be obtained over a wide latitude of temperatures, and it was less sensitive to vapor-flow direction than most of the other coatings. However, even at temperatures as low as 800°C, the TiC coating afforded no measurable oxidation protection for the graphite substrate. In fact, the difference in the oxidation rates of TiC-coated graphite and uncoated graphite could not be discerned.

The results of the oxidation tests performed on titanium nitride-coated graphite are presented in Tables 12 and 13 and in Figures 43 and 44.

Table 12. Results of Weight-Loss Oxidation Test of TiN Coatings on ATJ Graphite

Sample No. *	Coating Thickness, mm	Oxidation Temp., °C	Duration of Complete Protection, hours	Time Required for Complete Oxidation, hours
TiN-1900- O-B	0.25	1000	11.5	45
TiN-1900- II-B	0.95	1000	41.0	69
TiN-1900- O-A	0.25	1200	2.5	10
TiN-1900- II-A	0.95	1200	9.4	21
TiN-1900-III-B	0.34	1400	4.8	7
TiN-1900-III-A	0.34	1600	1.4	5

* 1- by 1- by 4-cm samples

Table 13. Results of Resistance-Oxidation Test of TiN Coatings on ATJ Graphite

Sample No.*	Coating Thickness, mm	Oxidation Temp., °C	Time Required for "Burn-Through", min
TiN-A-18	0.06	1000	372.4
TiN-B-17	0.06	1000	194.7
TiN-B-7	0.05	1000	95.8
TiN-B-18	0.05	1100	102.8
TiN-A-17	0.07	1100	141.8
TiN-A-7	0.05	1100	59.3
TiN-B-2	0.06	1200	53.0
TiN-B-1	0.20	1200	50.5
TiN-A-2	0.05	1200	57.8
TiN-A-1	0.20	1200	85.1
TiN-B-6	0.09	1300	39.9
TiN-B-4	0.07	1300	35.9
TiN-B-13	0.14	1300	243.6
TiN-A-11	0.06	1400	24.5
TiN-A-4	0.06	1400	29.5
TiN-B-11	0.06	1400	31.6
TiN-B-8	0.09	1500	13.5
TiN-B-9	0.28	1500	17.8
TiN-A-12	0.63	1600	10.5
TiN-A-6	0.09	1600	6.4
TiN-A-13	0.13	1600	11.0

*1/4-inch diameter rods

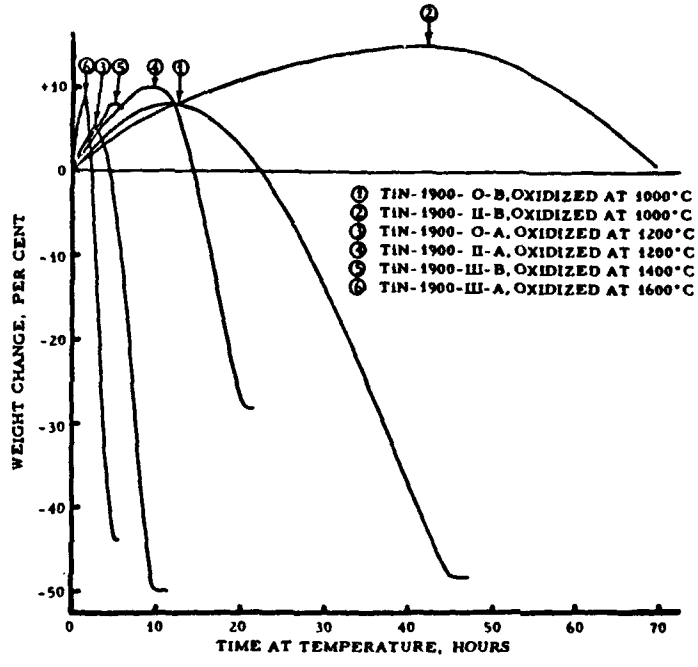

L-396

Figure 43. Results of Weight-Loss Oxidation Test of TiN Coatings on ATJ Graphite

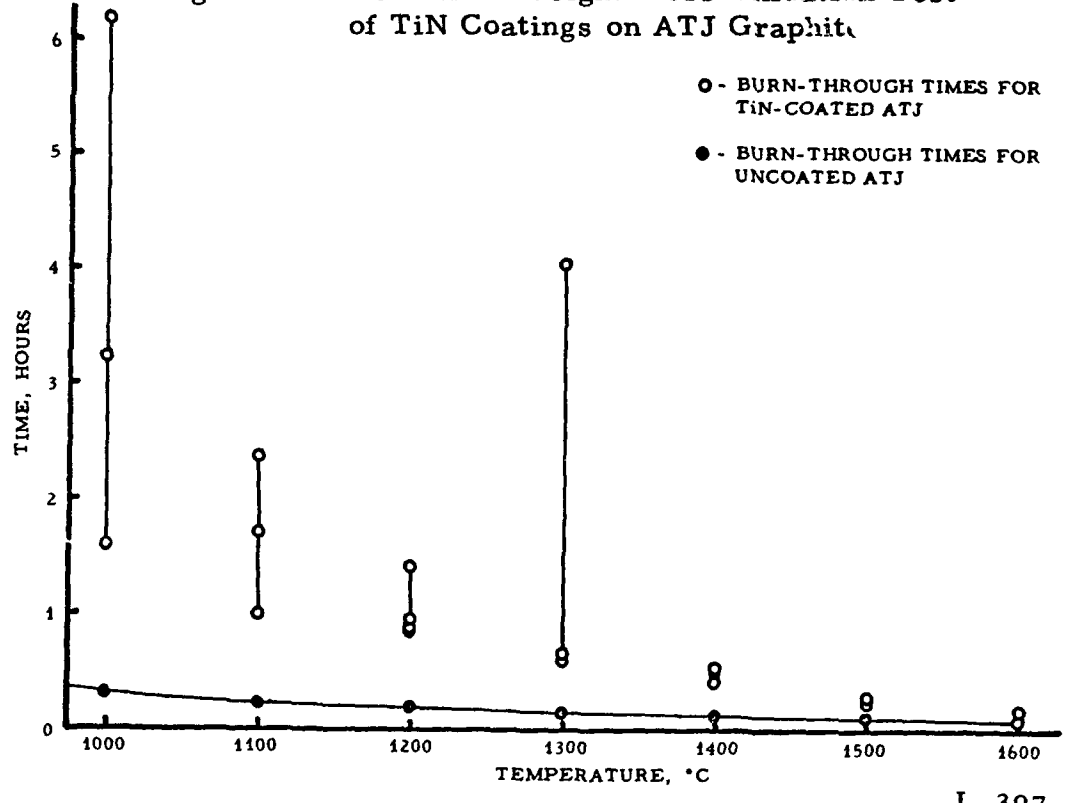

L-397

Figure 44. Results of Resistance-Oxidation Test of TiN Coatings on ATJ Graphite

Table 12 contains the oxidation data for the 1- by 1- by 4-cm samples coated by the sublimation process. The "Duration of Complete Protection" column in Table 12 refers to the time required to reach the peaks in Figure 43. Several oxidation runs were stopped when the weight gains by the samples reached their peaks. Dissection of these samples revealed that there was no attack on the graphite substrates before these peaks were reached. It was concluded, therefore, that the times required to reach the peaks could be used as a measure of the duration of complete protection. The coatings formed by sublimation of titanium nitride powder were yellow in color, though not as rich a yellow as those deposited on the $^1/_4$-inch rods by the nitrogen atmosphere process. The surfaces of both types of coatings had rough, grainy textures, very much unlike the TiC surfaces. Microscopic examination of the coatings revealed an intricate network of cracks, which also were visible to the unaided eye on several of the thicker coatings. It is probable that the cracks were due to CTE mismatches between TiN and ATJ graphite which was used as the substrate. The results of the oxidation test using the weight-loss technique were encouraging and indicate that at least partial healing of the cracks took place upon reheating the sample to oxidation temperature.

The data in Table 13 show that oxidation results for the $^1/_4$-inch diameter rods were not nearly as favorable as those for the bar-shaped samples (Table 12). The rods were tested on the electric resistance-oxidation apparatus which did not yield the meaningful weight-change data obtained using the other oxidation equipment. However, the resistance-oxidation test may be performed at higher temperatures. This test, as mentioned in Section 2.2.2, provides a rather severe measurement of oxidation resistance because of the temperature gradient from the inside of the sample to the coating surface. At high temperatures, the center of the sample can be several hundred degrees hotter than the outside. For TiN-coated graphite samples, this temperature gradient will tend to have an adverse effect on the healing of the crack network incurred during deposition. Since TiN has a higher CTE than ATJ graphite, it can be shown that, for any temperature of TiN below the original deposition temperature (about 1800°C), a higher graphite temperature will serve only to increase the mismatch in dimensional parameters of the two adjacent materials. The situation is reversed for externally heated samples, however, and the temperature of the coating should be equal to, or greater than, that of the graphite substrate. In the later case, a TiN coating on the externally heated sample would tend to elongate and heal its system of cracks at all temperatures below the original deposition temperature. In any event, for the same surface temperature, the expansion stresses and cracks should be less in the samples heated externally than those in samples heated internally. This condition could explain why the coatings listed in Table 12 apparently

are more oxidation resistant than those given in Table 13.

In general, the oxidation resistance afforded graphite by titanium nitride coatings is not encouraging. Greater protection can be achieved by several other coating systems. The hardness and high melting point of TiN could perhaps, in some special cases, suggest its use, but it is not among the most promising materials as an oxidation-resistant coating.

Interest in TiN coatings was originally kindled by an article[53] which indicated that this material would provide substantial temporary oxidation protection for graphite at temperatures as high as 2200°C. This article theorized that protection was achieved by the formation of titanium dioxide films on the TiN coatings. A similarity was inferred between this protection and the protection achieved by the formation of aluminum oxide films on aluminum at lower temperatures. It should be pointed out, however, that thermodynamically the two cases are dissimilar. Aluminum oxide is stable with respect to aluminum at low temperatures, whereas titanium dioxide is not stable with respect to titanium nitride above about 940°C. The formation of the lower oxide, TiO_5, is favorable at temperatures above this point, and the existence of other lower titanium oxides renders the entire system unstable. Thus oxygen may be passed through the coating layers toward the graphite substrate via a sort of thermodynamic "conveyor belt". The slow, methodical weight gain of the coatings as shown in Figure 43 tends to prove the above theory.

It was hoped that, despite the unfavorable thermodynamics of the TiN system, kinetic factors might dominate to the extent that such reactions would be prevented. However, the results of these experiments showed that kinetics allowed only a delaying action which, while substantial at 1000°C, decreased to practically nil at 1600°C. Work on the TiN coating system, therefore, was discontinued.

Because of the unusual success of silicon coatings on graphite (see Section 3.3), it was felt that titanium metal coating might prove satisfactory. Several $^1/_4$-inch graphite rods were coated with titanium metal and oxidized. The oxidation protection of these coatings, however, was significantly less than that of TiN coatings of comparable thickness, and the investigation was not carried further.

3.2.2. Summary

Titanium, titanium carbide, and titanium nitride coatings were vapor deposited onto graphite substrates by source-target methods. Titanium and titanium carbide coatings afforded little or no oxidation protection for the graphite at temperatures above 1000°C. Titanium nitride coatings did offer such limited oxidation protection for the graphite. The degree of protection provided by TiN for the samples used in this work was

largely influenced by the type of oxidation test employed. Externally heated samples exhibited better oxidation resistance than those heated internally by electrical resistance. Using an external heating source, one graphite sample coated with a 0.95-mm layer of TiN was unaffected after 41 hours in an oxidizing atmosphere at 1000°C. Another sample similarly coated and tested withstood 9.4 hours at 1200°C. Oxidation protection by TiN coatings using internal heating at 1600°C was extremely short, a matter of a few minutes at most, while protection lasted in one instance for 1.4 hours at this temperature when the sample was heated externally.

None of the titanium systems investigated is theoretically sound from a thermodynamic standpoint. It was reasoned that the oxidation protection provided by TiN coatings resulted from kinetic factors which served to delay the oxidation process.

3.3. Silicon Oxide Coatings

3.3.1. Experimental

Oxidation-resistant silicon oxide coatings for the protection of graphite were formed by oxidizing silicon metal coatings which had been vapor deposited on graphite samples. Graphite rods, $^1/_4$-inch in diameter, were silicon coated in the high-vacuum furnace previously discussed (Section 3.2.1) for the titanium coatings. Silicon metal, 98.5 per cent pure, was vaporized from a graphite evaporator at temperatures from 1600 to 1650°C. The graphite rods were placed in the vapor path so as to attain a temperature in the range of 1325 to 1375°C, the temperature range at which the best silicon carbide bond between the silicon coating and the graphite substrate was obtained without exceeding the melting point of silicon (1410°C). Uneven coatings which resulted when the substrate temperature exceeded this point were due to the rather poor wettability of graphite by liquid silicon.

The graphite rods were rotated during deposition of the silicon to assure all-around coverage. A coating thickness of approximately 0.1 mm resulted after one hour at the above temperature conditions. The ambient pressure in the furnace was held below 10^{-4} mm of Hg during the deposition process. Temperatures were measured in the same manner as was described in Section 3.2.1.

The silicon-coated rods were tested for oxidation resistance using the electrical-resistance-oxidation apparatus as described in Section 2.2.4.

3.3.2. Results and Discussion

The degree to which silicon coatings can protect graphite may be demonstrated best by comparing the appearance of such coatings after oxidation testing with that of other coatings which have been similarly tested. Figures 45 and 46 are photographs showing, respectively, the appearance of silicon-coated (source-target method) graphite rods and silicon carbide-coated (pack-diffusion process) graphite rods after oxidation for 30 minutes at several temperatures. The superiority of the silicon coatings is evident from these photographs.

The thickness of the silicon coating had little effect on its oxidation protection. Coatings which differed in thickness by a factor of 10 were oxidized at several temperatures. In all cases below 1700°C, the coatings were protective for the duration of the tests regardless of their thickness. The minimum coating thickness tested was 0.027 mm; the thickest coating was 0.355 mm.

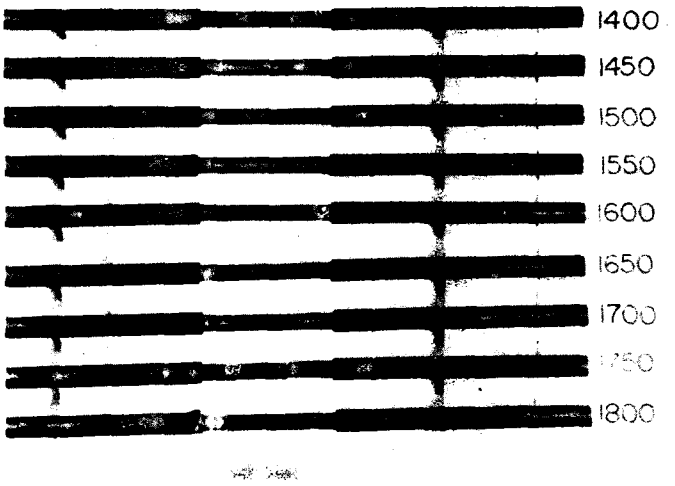

Figure 45. Resistance-Oxidation Test of Silicon Coating on Graphite Applied by Source-Target Method, 30 Minutes, 1400 to 1800°C

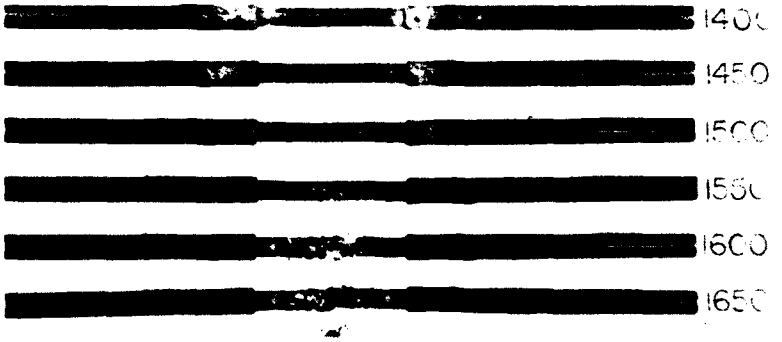

Figure 46. Resistance-Oxidation Test of Silicon Carbide Coating on Graphite Applied by Pack-Diffusion Method, 30 Minutes, 1400 to 1650°C

An accurate determination of the oxidation resistance provided by silicon coatings was not possible on the electrical-resistance-oxidation apparatus. Long oxidation tests always resulted in failure of the specimens near the ends, where they were not coated. Packing thermatomic black around the unprotected areas delayed the oxidation of the uncoated graphite, but it was not possible to obtain tests of more than five hours duration.

Five-hour oxidation tests of silicon-coated graphite rods were performed at temperature intervals of 50°C from 1400 to 1750°C. In most cases, the appearance of the rods after these tests was virtually identical to that shown in Figure 45 for the 30-minute tests. In several instances it was found, however, that at 1700°C and above, a tendency toward rapid oxidation, bordering on combustion, developed. The silicon-coated samples oxidized at 1750 and 1800°C (Figure 45) show the effect of this type of oxidation. Other samples oxidized at these temperatures behaved normally.

It was discovered that, by preoxidizing the silicon-coated samples at temperatures between 1400 and 1600°C for several minutes, the oxidation resistance at higher temperatures could be improved. One such

sample was preoxidized at 1600°C for 30 minutes before being subjected to oxidation at 1750°C for a similar period. After the sample had cooled to room temperature, it was observed that the coating was still smooth, continuous, and protective. The sample was then oxidized at 1775°C for 30 minutes. After cooling to room temperature, the coating was observed to be unchanged and still protective. The sample was then heated to 1800°C. At this temperature the sample was unaffected for 25 minutes, at which time a few small bubbles were noted in the hottest zone. The sample was held at 1800°C for a total of 30 minutes and then cooled to room temperature. Although the bubbles somewhat marred the appearance of the coating, the graphite beneath was relatively unaffected, and looked much the same as that of the 1800°C specimen shown in Figure 45.

The explanation for the above behavior probably lies in the basic mechanism of oxidation protection afforded by the silicon coating. It is postulated that protection is achieved by oxidation of the surface silicon to a layer of silicon dioxide which in turn limits further oxidation of the underlying materials. It would appear from the results of this work that it is advantageous, and in some cases necessary, to develop this protective oxide layer at moderate temperatures before subjecting the coating to high temperatures. The silicon dioxide layers formed by oxidizing silicon coatings at the higher temperatures do not offer the same protection as those formed by oxidizing at lower temperatures. In the temperature range of 1700 to 1800°C, where many of the nonpreoxidized samples failed, silicon dioxide is the most favorable oxidation product of silicon in strongly oxidizing atmospheres. It is true that in a strongly convective situation, such as would be inherent with the oxidation apparatus used, some quantity of silicon monoxide gas would be formed and swept away by the gas flow. The samples, however, did not reach these temperatures instantaneously; in most cases they were raised from room temperature to test temperature over a period of 90 seconds. Thus, it is thought that there is ample time for at least some minute thickness of the dioxide to form at the lower temperatures where the formation of the monoxide gas is not nearly so favorable. Silicon dioxide, not silicon, surfaces should be presented to the oxidizing atmosphere at test temperature and, therefore, the formation of nonequilibrium silicon monoxide at the surface is unlikely. Should oxygen penetrate the surface coating, however thin, by diffusion, reaction with silicon will tend to form the thermodynamically favored species, the dioxide. By this reasoning, the only effect which should be noted, as the oxidation test proceeds, is a buildup of the protective dioxide layer. Failure of the coating should occur only when the diffusion of oxygen has reached the point where silicon carbide or graphite are affected. The production of carbon monoxide from these reactions must then become sufficiently large to rupture the coating.

The above theory of diffusion mechanism does not explain how preoxidation of the silicon coating can apparently prevent failure at the higher temperatures. Diffusion of oxygen certainly is taking place. If it were not, the thickness of the dioxide coating would not increase beyond a few atomic layers. X-ray-diffraction analysis has indicated a much greater quantity of cristobalite than would be anticipated from this small thickness. However, the diffusion rate of oxygen through silicon dioxide at 1700 to 1800°C should be the same for equal coating thicknesses regardless of whether the coating had been preoxidized or not. The true explanation of coating failure and the preventing of it in this temperature range appears not to be in consideration of oxygen-silicon or oxygen-silicon dioxide equilibria, but rather in consideration of silicon-silicon dioxide.

Silicon in contact with silicon dioxide can give rise to the following reaction:

$$^1/_2Si_{(c,l)} + {}^1/_2SiO_{2(c,l)} \rightarrow SiO_{(g)}. \qquad (20)$$

The free energy of this reaction becomes zero, and hence the vapor pressure of silicon monoxide becomes one atmosphere, when the temperature of the system reaches 1820°C. Assuming the ambient pressure about the coating to be one atmosphere, temperatures in excess of 1820°C will cause the silicon monoxide pressure to rise above this point and apply outward forces on the protective coating in excess of those striving to maintain coating-substrate contact. Rupture of the coating will result if it is not strong enough to accommodate these excess forces.

It is reasonable to assume that a thicker coating should be stronger than a thin coating. By preoxidizing a coating at temperatures where the silicon monoxide pressure is low, a relatively thick layer of silicon dioxide will form and this layer should become thicker when the sample is raised to test temperature. This means, then, that the preoxidized coating should have a much thicker dioxide layer at testing temperature than does the unoxidized coating. If the test temperature is such that the silicon monoxide pressure is greater than the ambient pressure about the coating, the thicker and stronger dioxide coating should be able to withstand higher pressure differentials. Since the pressure of silicon monoxide is a function of temperature, the thicker coating should provide protection to higher temperatures.

Although the formation of silicon monoxide gas from silicon and silicon dioxide provides an explanation for the failure of silicon coatings, the temperatures at which many failures have been observed are below

that required to achieve sufficient silicon monoxide pressure. The reason for this could be inaccurate thermodynamic data used for equilibrium temperature calculation or it could be incorrect test temperature measurements. In Figure 45, the sample shown as being tested at 1400°C was apparently tested at a temperature above 1400°C. The dark center section can be attributed to the melting of silicon which occurs at 1410°C. This center section can be followed in the photograph as it becomes progressively wider with increasing temperature and the edges of this section should represent the point at which the sample surface was at 1410°C. The very center of the 1400°C sample, at which point the temperature was measured, undoubtedly w[illegible]nsiderably above 1410°C. The 1700°C sample exhibits a still darke[illegible]a within the 1410°C limit and, in all probability, this section resulted [illegible]om the melting of silicon dioxide which occurs at 1723°C. The center of this section, therefore, was also higher than the measured temperature.

More important than the apparent errors in measuring surface temperatures is the fact that, because of the manner in which the samples were heated by the oxidation apparatus, the temperature beneath the surface, where the Si-SiO_2 reaction should occur, is certain to be higher than that observed on the surface. (The considerations surrounding this phenomenon are discussed in Section 2.3.4 of this report.) It is the Si-SiO_2 interface temperature which determines the SiO pressure to be developed, not the surface temperature.

The above, then, are several reasons why failure of a coating could occur at temperatures where the SiO pressure mechanism should apparently be inoperative.

The question now arises as to why silicon carbide coatings do not appear to provide the same degree of protection for graphite as do silicon coatings. Both coatings oxidize to form protective silicon dioxide layers. However, in the former coating, oxidation results in SiC-SiO_2 contact, while in the latter a Si-SiO_2 contact is achieved. A Si-SiO_2 reaction (equation (20)) has been calculated to take place above 1820°C. The reaction

$$SiC_{(c)} + SiO_{2(c,l)} \rightarrow Si_{(c,l)} + SiO_{(g)} + CO_{(g)} \qquad (21)$$

reaches a total gas pressure of one atmosphere at 1715°C. Thus, under the same conditions, silicon coatings should be protective for slightly more than 100°C higher than silicon carbide coatings. As shown in Figure 45 this is approximately what happens experimentally. Silicon carbide coatings have been shown to fail by rupture at an apparent surface temperature of 1550°C. Although most of the silicon coatings tested at 1700°C were extremely protective, two coatings which were not preoxidized

failed at this temperature. The 150°C difference (1550°C for SiC coatings and 1700°C for Si coatings) agrees well with the theoretical considerations which were advanced.

Preoxidation of silicon carbide coatings should not have the beneficial effect that it does for silicon coatings. In SiC coatings, oxygen must diffuse through the surface layer where it meets silicon carbide. The reaction at this point forms silicon dioxide, to be sure, but carbon monoxide also is produced by this reaction. The formation of CO is detrimental because, should the oxygen diffusion rate be high enough, rupture of the coating could be caused by the buildup of CO pressure at the lower, preoxidation temperature. This carbon monoxide problem is not present to any large extent with the oxidation of silicon coatings.

As far as is known, the oxidation protection provided graphite by silicon coatings is greater than that of any other coating thus far developed. By preoxidation treatments, silicon coatings have been shown to protect their substrates for significant periods of time to temperatures as high as 1800°C. The coating is certainly a liquid at this temperature but it appears to withstand at least moderate gas-impingement rates such as those encountered in the strongly convective atmosphere of the electrical-resistance-oxidation apparatus. Below 1723°C, the melting point of silicon dioxide, the coating should be much stronger and more resistant to erosion.

At the time of this writing, work is being conducted toward applying silicon coatings to larger graphite articles by source-target vapor deposition. Coatings have thus far been successfully deposited on cones as large as 8 inches in diameter but oxidation results have not as yet been obtained.

3.3.3. Summary

Coatings consisting of SiC-Si sequences were shown to provide oxidation protection for graphite to higher temperatures than any coatings heretofore reported. Although the mechanism of protection, the formation of an SiO_2 surface, is identical to that offered by silicon carbide coatings, the oxidation protection is much greater. Oxidation tests by electrical-resistance heating showed that graphite articles coated with SiC-Si coatings were unattacked at 1700°C during the standard 5-hour exposures. Several specimens exhibited similar protection at 1750 and 1800°C. Above 1700°C, however, a few samples showed a tendency toward rapid coating oxidation bordering on combustion. It was found that, by preoxidizing these samples at lower temperatures before proceeding to

the higher test temperatures, these failures could be prevented to a large extent. In any event, this coating sequence should provide excellent oxidation protection up to 1723°C, the melting point of SiO_2.

4. VAPOR DEPOSITION OF PROTECTIVE COATINGS FOR GRAPHITE BY PACK-DIFFUSION PROCESS

4.1. Introduction

Coating of both ferrous and nonferrous metals, for many years, has been accomplished by vapor deposition through the use of the pack-diffusion process. At present, this type of coating process is being employed as a means for applying oxidation-resistant coatings to such refractory metals as tungsten, tantalum, molybdenum, and niobium.

The purpose of this section is to describe the development work under the contract with regard to pack diffusion as a technique for applying protective coatings to graphite substrates. Results are also reported on the oxidation resistance afforded graphite substrates by the coatings achieved by the pack-diffusion process.

The pack-diffusion process takes place basically in three steps. First, coating material is supplied to the substrate by vapor transport. Second, as the vapor concentration increases in close proximity to the substrate material, a surface reaction takes place between the coating metal and the substrate. Finally, atoms from the substrate are transferred by diffusion through the newly formed surface to sustain the coating vapor-substrate reaction. These processes will continue either until the coating becomes too thick to allow sufficient substrate diffusion or until the coating material is exhausted.

A fundamental requirement, which must be satisfied for this type of coating process, is to have sufficient amounts of the coating metal in the vapor phase. There are several ways in which this may be accomplished. The most obvious method is to simply heat the metal to a temperature high enough to provide substantial amounts of vaporized metal for coating. Adequate amounts of metal vapor, in some cases, are supplied only at high temperatures where the substrate and/or substrate-vapor reaction products are no longer thermally stable. In these instances volatile compounds of the coating metal, which decompose and react on the substrate, are substituted for the free metal as the source of coating vapor. Halides and carbonyls of the coating metal are the most common volatile compounds used for these substitutes. Another source of coating vapor is obtained through the use of a carrier gas to react with the metal, forming a volatile intermediate compound which in turn decomposes on the substrate and forms the desired coating.

Graphite substrates to be coated by the pack-diffusion process are placed in a mixture of elemental silicon and an inert filler inside a graphite susceptor. The coating reaction is promoted by inductively heating the susceptor and pack to a temperature of 1800 to 2000°C for 4 to 8 hours, after which the pack is cooled, disassembled, and the coated parts removed.

The major advantage of the pack-diffusion process is that the pack completely surrounds the article to be coated, thereby eliminating the necessity for an apparatus to support or suspend the substrate during the coating operation. All other coating techniques require such an apparatus for suspending the substrate in the stream of coating vapor. If the substrate requires coating on all sides, coating by the source-target method or the plasma-spraying method must be done in at least two separate coating operations in order to cover those portions of the substrate which were marked by the suspension apparatus. The pack-diffusion process, by surrounding the substrate with the source of coating vapor, permits complete coating of complicated shapes in a single operation.

The pack-diffusion method of coating graphite poses certain differences from coating metals or low-temperature ceramics. In the case of a metal substrate, the temperature range for the coating reaction is 900 to 1200°C, whereas for graphite substrates the reaction temperature range is much higher as indicated above. Only a limited number of materials are available which can be used as filler in the pack and which are thermodynamically stable at the increased temperature. In addition, since only the metal carbides can be formed by this coating process, the number of metal carbides which provide protective coatings on graphite in an oxidizing atmosphere is another limiting factor. As discussed in Section 1 of this report, silicon carbide is one of the very few single-layer coatings that will furnish this oxidation protection to graphite.

The pack-diffusion process has been used for a number of years to apply silicon carbide coatings on graphite with titanium carbide serving as the inert filler in the pack. The development work on the pack-diffusion process conducted under this contract was concerned with different filler materials to improve the coatings as well as the coating process.

4.2. Experimental Procedures

4.2.1. Substrate Specimens

Grade ATJ graphite rods, $^1/_4$ of an inch in diameter by $4^1/_2$ inches in length, were machined for use as substrate specimens to be coated by the pack-diffusion process. The center portion of each rod was reduced to $^3/_{16}$ of an inch in diameter over a $1^1/_2$-inch length to provide more uniform heat concentration during testing of the coated rod on the resistance-oxidation apparatus (see Section 2.3.4). Rods approximately the same size were used for coating by the source-target method; therefore, it was possible to make comparisons between the pack-diffusion coatings and coatings applied by the source-target method.

4.2.2. Coating Method

Silicon metal and an inert filler material were weighed, placed in a twin-shell blender, and blended for two hours. The ratio by weight of these mixtures generally was maintained at 20 per cent silicon to 80 per cent filler. It was necessary in several instances, however, to increase the per cent of silicon to counteract high impurity levels present in a few of the filler materials that were investigated.

Rods to be coated were first wrapped with paper and placed vertically in a graphite susceptor. The purpose of this paper was to reduce sintering and sticking of the pack materials to the coated substrate. Upon firing, the paper was carbonized and formed a quasi barrier which reduced transport of filler particles to the substrate. Uncoated surfaces on each end of the rods were required to provide good electrical contact so that the coated specimens could be tested by the resistance-oxidation method. The uncoated portions were obtained by packing each end of the rod in a layer of thermatomic black with the silicon filler material covering the center portion of the rod between the layers of black. Figure 47 is a cross-sectional sketch of a single rod packed in this manner. Graph-

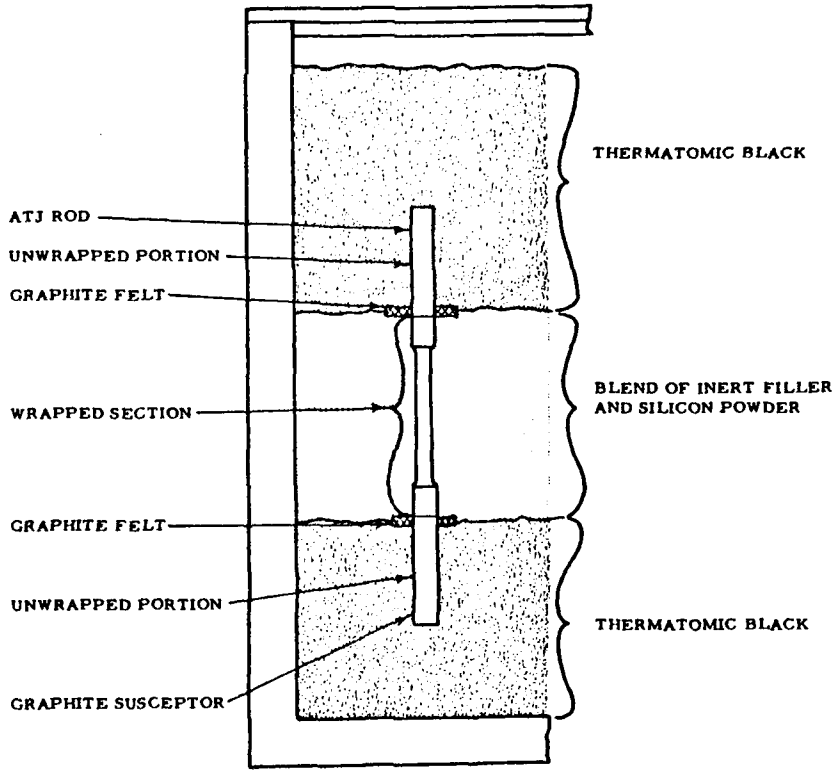

Figure 47. Sketch Showing Method of Packing Graphite Rods for Coating by the Pack-Diffusion Process

ite-felt washers were inserted on each rod to reduce the reaction at the interface between the pack and thermatomic black, thereby facilitating removal of the rods after firing.

Carbon vent tubes were placed throughout the pack to permit the easy escape of volatiles formed during coating. The gases were vented to the air gap between the cover plate and the top layer of thermatomic black and were then expelled from this to the atmosphere through an exhaust stack mounted in the center of the cover plate. Argon was introduced to the air gap to prevent oxygen from reaching the pack through the exhaust port.

The complete assembly was packed in thermatomic black inside a ceramic sagger and inductively heated by use of a 50-kw, 3000-cps induction unit. A cross-sectional view of the furnace assembly and induction coil are shown in Figure 48.

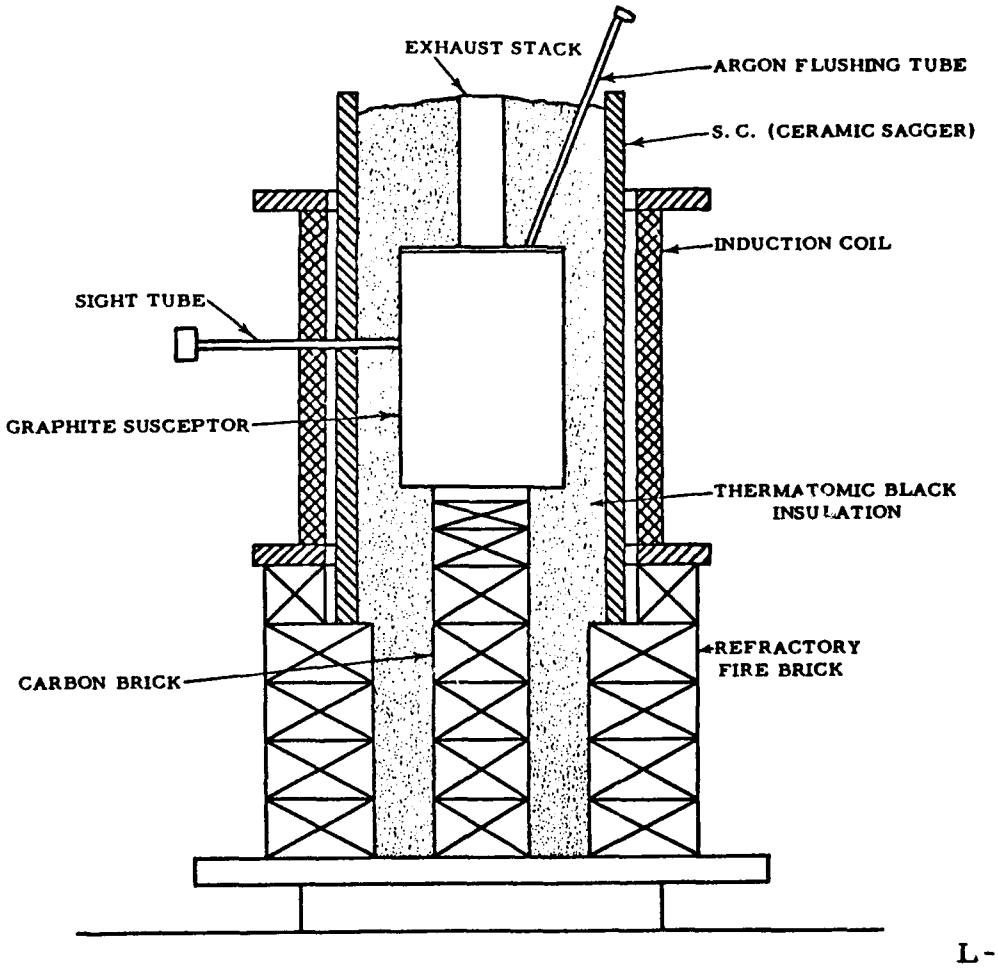

Figure 48. Cross-Sectional View of Furnace Assembly for Producing Coatings by the Pack-Diffusion Process

4.2.3. Testing Method

Oxidation resistance of the coating from each type of pack was used as an indirect method of comparing various filler materials. These tests were performed on the resistance-oxidation apparatus which was described in Section 2.3.4 and illustrated in Figures 21 and 22.

Grade ATJ rods, of the size specified in Section 4.2.1, were coated in packs containing each of the filler materials under investigation.

The oxidation testing program for evaluation of the filler materials was conducted in two phases. In the first or screening phase, two coated rods from each type of pack were oxidized for 30 minutes using the resistance-oxidation apparatus, one each at 1550 and at 1600°C. The coatings exhibiting the best oxidation resistance were chosen for the final testing phase. Eight coated rods from each type pack selected as described above, were subjected to the resistance-oxidation test over the temperature range from 1400 to 1750°C in 50°C increments. The duration of the test was 30 minutes and one rod was tested at each temperature. All oxidations were performed in natural-convection air with the surface temperature of the hot zone kept constant. Time to reach the test temperature was 80 seconds, in every case, and this time was not considered as a part of the oxidation time.

4.3. Discussion and Results

As mentioned above, in the conventional pack-diffusion process for the application of silicon carbide on graphite, titanium carbide is used as the inert filler in the pack. In order that other filler materials could be compared to titanium carbide, rods coated in a TiC pack were oxidized at 50°C intervals from 1400°C until burn-through of the rod at 1650°C. The oxidation-exposure time for each rod was 30 minutes at temperature. Figure 49 shows the appearance of these rods after oxidation. The failure threshold for the coatings produced with the TiC-Si pack was 1550°C. The compounds tested as filler materials were Al_2O_3, B_4C, CrB_2, Cr_3C_2, NbB_2, SiC, TiB_2 and ZrC.

4.3.1. Screen Test Phase

The results obtained from the screening phase of the testing program for each filler investigated were as follows:

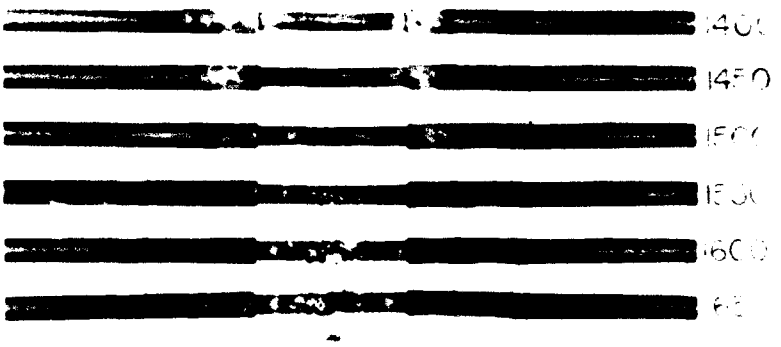

Figure 49. Resistance-Oxidation Test of Silicon Carbide Coating on ATJ Graphite Applied by TiC-Si Pack-Diffusion Method, 30 Minutes, 1400 to 1650°C

1) Al_2O_3 Filler

This pack was highly sintered, making it extremely difficult to remove the test rods. Severe bubbling of the coating on the sample, which was oxidized at 1550°C, caused failure of the rod after only 23 minutes of oxidation.

2) B_4C Filler

Examination of the test rods coated in the pack using this filler revealed no evidence of a coating of any type on the rods. The presence of boron silicides in the fired pack was determined by X-ray analysis indicating that a reaction took place proving interaction between the filler material and the coating metal.

3) CrB_2 Filler

This pack was not sintered and removal of the coated rods was much easier than with the TiC pack. The oxidation resistance of the coating produced from the CrB_2-Si pack compared favorably with

that of the coatings from the TiC-Si pack.

4) Cr_3C_2 Filler

The pack using this filler was highly sintered, making it impossible to extract the test rods from the fired pack.

5) NbB_2 Filler

The coatings produced in the NbB_2-Si pack bubbled upon oxidation at 1550°C with the evolution of a noticeable amount of smoke. At 1600°C, the coating appeared to boil and the smoke evolution became much more vigorous.

6) SiC Filler

Sintering in this pack was at a minimum and the coated rods were easily removed. Oxidation of the coatings produced with the SiC-Si pack showed no bubbling at 1550°C and only very slight bubbling at 1600 °C.

7) TiB_2 Filler

Appearance of the oxidized coatings from this pack was very similar to that of the oxidized coatings from the TiC-Si pack at 1550 and 1600°C. However, sintering was much less in the TiB_2 pack than in the TiC packs.

8) ZrC Filler

The coating produced from this pack showed little, if any, bubbling upon oxidation at 1550 and 1600°C. In each case, however, the rods burned through before the 30-minute test was completed. Examination of the substrate revealed very extensive oxidation which indicated a porous or discontinuous coating. Additional rods were coated and oxidized but the substrate was oxidized in each case which confirmed the initial results.

Summarizing the results obtained in the first phase of testing: (a) Al_2O_3, B_4C and Cr_3C_2 fillers were rejected because of interaction occurring between the coating metal and the filler material; (b) coatings produced from packs containing NbB_2 and ZrC fillers failed at temperatures below 1550°C and, consequently, these materials were rejected as fillers; (c) the remaining compounds (CrB_2, SiC and TiB_2) investigated in the screening phase were the only materials to equal or surpass TiC as an inert filler.

4.3.2. Final Test Phase

The results obtained on CrB_2, TiB_2, and SiC in the final phase of the investigation were as follows:

1) CrB_2 Filler

The full-scale oxidation test of the coatings from the CrB_2 pack filler indicated a molten phase existing as low as 1400°C. Bubbling of the coating, as shown in Figure 50, started at 1400°C and increased rapidly with each 50°C rise in the temperature. Although the coating appeared to provide protection for the substrate up to 1700°C, this protection would be lost if the bubbles were ruptured or removed by erosion as might happen in a rapidly moving gas stream.

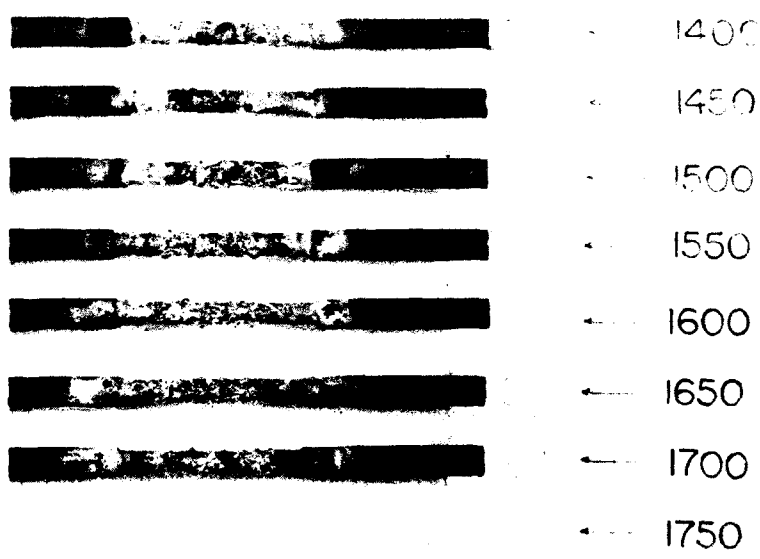

Figure 50. Resistance-Oxidation Test of Silicon Carbide Coating on ATJ Graphite Applied by CrB_2-Si Pack-Diffusion Method, 30 Minutes, 1400 to 1700°C

2) TiB_2 Filler

Coatings prepared using the TiB_2 filler (Figure 51) were quite similar in oxidation resistance to those prepared using TiC filler (Figure 49). The failure threshold for the coatings from the TiB_2-Si pack appeared to be at 1550°C or slightly above. Sintering in the TiB_2-

Si pack was not nearly as severe as that in the TiC-Si pack. The advantages of the TiB_2 filler, however, did not offset the disadvantage of its higher cost, since TiB_2 costs about 10 times as much as TiC.

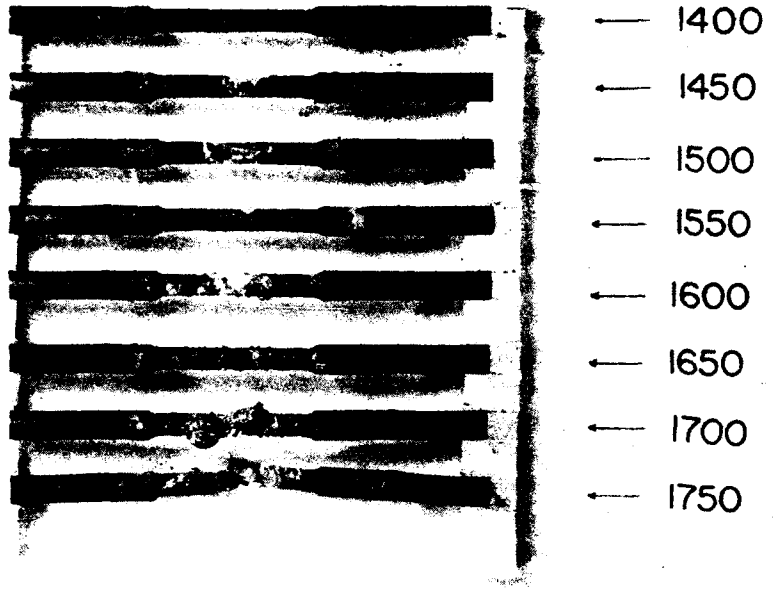

Figure 51. Resistance-Oxidation Test of Silicon Carbide Coating on ATJ Graphite Applied by TiB_2-Si Pack-Diffusion Method, 30 Minutes, 1400 to 1750°C

3) SiC Filler

Silicon carbide was the only filler tested that produced coatings with improved resistance to oxidation as compared to TiC fillers. As shown in Figure 52, 1600°C was the first temperature at which a noticeable bubble formation occurred on the coatings from the SiC-Si pack. The sintering of this pack was very slight and the samples were removed with comparative ease. The cost of SiC is 50 to 70 per cent lower than the cost of TiC.

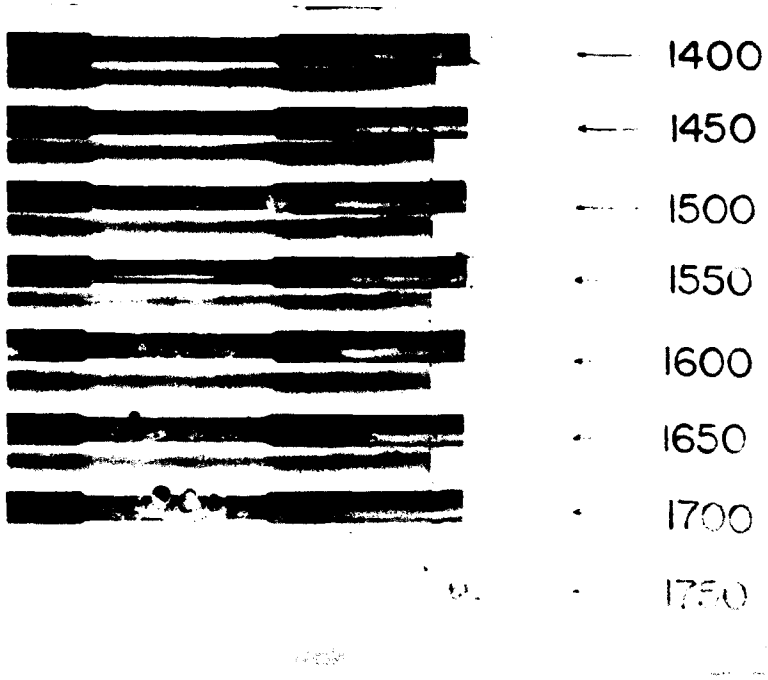

Figure 52. Resistance-Oxidation Test of Silicon Carbide Coating on ATJ Graphite Applied by SiC-Si Pack-Diffusion Method, 30 Minutes, 1400 to 1700°C

4.4. Conclusions and Recommendations

4.4.1 Conclusions

1) Al_2O_3, B_4C, Cr_3C_2, NbB_2, ZrC and CrB_2 are not satisfactory filler materials to blend with silicon for use in the vapor deposition of coatings on graphite by the pack-diffusion process.

2) TiB_2 compares very favorably with TiC as filler material in the pack-diffusion process. However, the present cost of the TiB_2 cannot justify use as a replacement for TiC.

3) The SiC-Si pack provides a coating on graphite with a slightly improved oxidation resistance over the coating produced in the TiC-Si pack. The cost of SiC is 50 to 70 per cent less than that of TiC.

4.4.2. Recommendations

1) A study should be initiated to determine the feasibility of re-using fired pack filler. If TiB_2 could be reused, the cost

factor might no longer present a disadvantage.

2) Investigation of the use of SiC filler should be extended to larger and more irregularly shaped substrates.

5. LIST OF REFERENCES

(1) See, for example, M. W. Riley, Materials in Design Engineering, 56 (3) M/DE Manual No. 199, p. 113 (1962).

(2) Johnson, P. D., J. Am. Ceram. Soc., 33 (5) 168 (1950).

(3) Howard, R. A. and E. L. Piper, Development of a Fine-Grain Isotropic Graphite for Structural and Substrate Applications, WADD TR 61-72, Vol. XIII (1962).

(4) See Section 3, this report.

(5) Runck, R. J., Oxides, High-Temperature Technology, I. E. Campbell, Ed. (John Wiley & Sons, Inc., New York, 1956), p. 31.

(6) Reference (5), p. 32.

(7) Dergazarian, T. E., et al., JANAF Interim Thermochemical Tables I and II (The Dow Chemical Company, Midland, Michigan 1960-1962).

(8) Glassner, A., The Thermochemical Properties of the Oxides, Fluorides, and Chlorides to 2500°K, ANL-5750 (1957).

(9) Litz, L. M., Graphite, Carbide, Nitride and Sulfide Refractories, Natl. Carbon Res. Lab. TM-428 (1959).

(10) Driesner, A. R., Et al., Inst. Radio Eng. Trans. on Nuclear Sci., NS-9, 247 (Jan. 1962).

(11) Reference (5), p. 33.

(12) Klinger, N., et al., Study of the Reaction Rates Between Refractory Oxides and Graphite, Aeronautical Res. Lab. Rept. No. 62-325 (1962).

(13) Sheipline, V. M. and R. J. Runck, Carbides, High-Temperature Technology, I. E. Campbell, Ed. (John Wiley & Sons, Inc., New York, 1956), p. 117.

(14) Sax, N. I., Dangerous Properties of Industrial Materials (Reinhold Publishing Corp., New York, 1960), p. 359.

5. LIST OF REFERENCES (CONT'D)

(15) Mah, A. D., Heats and Free Energies of Formation of Gallium Sesquioxide and Scandium Sesquioxide, USBM RPI-5965 (1962).

(16) Montgomery, R., Thermodynamics of Rare-Earth Compounds, USBM RPI-5468 (1959).

(17) Reference (13), p. 121.

(18) Reference (5), p. 75.

(19) Reference (5), p. 77.

(20) Thomas, D. E. and E. T. Hayes, The Metallurgy of Hafnium, USAEC (U. S. Government Printing Office, Washington, 1960).

(21) Zhelankin, V. I., et al., Russian Journal of Physical Chemistry, (Eng. Trans.) 35, 1288 (1961).

(22) Norton, J. T., Substances with High Melting Temperatures, Proc. Symp. High Temperature - A Tool for the Future (Stanford Res. Inst., Menlo Park, Calif., 1956), p. 81.

(23) Kirk, R. E. and D. F. Othmer, Ed., Encyclopedia of Chemical Technology, 10 (The Interscience Encyclopedia, Inc., New York, 1953), p 843.

(24) Schwartz, M. M., The Iron Age, 74 (Oct. 4, 1962).

(25) Reference (6), p. 42.

(26) Reference (6), p. 67.

(27) Gibson, J. A., et al., The Properties of the Rare-Earth Metals and Compounds (Battelle Memorial Inst., Columbus, Ohio, 1959).

(28) Reference (13), p. 120.

(29) Reference (5), p. 66.

(30) Kirk, R. E., and D. F. Othmer, Ed., Encyclopedia of Chemical Technology, 11 (The Interscience Encyclopedia, Inc., New York 1953), p. 504.

5. LIST OF REFERENCES (CONT'D)

(31) Austerman, S. B., Decrepitation of Beryllium Oxide at High Temperatures, USAEC NAA-SR-6428 (1961).

(32) Ackermann, R. J. and R. J. Thorn, Vaporization of Oxides, Progress in Ceramic Science, Vol. I, J. E. Burke, Ed. (Pergammon Press, New York, 1961), p. 70.

(33) Reference (5), p. 74.

(34) Campbell, I. E., Vapor Deposition of High-Temperature Coatings, Proc. Symp. High Temperature - A Tool for the Future (Stanford Res. Inst., Menlo Park, Calif., 1956), p. 177.

(35) Cacciotti, J. J. (To General Electric Co.), Rhenium-Bonded Composite Material and Method, U. S. 3,024,522 (1962).

(36) Portnoy, K. I., et al., Izvest. akad. nauk SSSR, met. i toplivo/ Tehkn/ p.p. 147-9 (No. 2, 1961).

(37) Hansen, M., Constitution of Binary Alloys (McGraw-Hill Book Co., Inc., New York, 1958), p. 370.

(38) Reference (37), p. 382.

(39) Reference (37), p. 382.

(40) Dollof, R. T., U. S. Dept. of Commerce, Office of Tech. Serv. P. B. Rept. No. 171, 365.

(41) Reference (37), p. 386.

(42) "A more recent determination of the ZrC-C eutectic temperature places it at 2850°C;" R. T. Dollor, Aeronautical Systems Division Contract No. AF 33(616)-6286, Prog. Rept. No. 3 (Dec. 10, 1962).

(43) Blocker, J. M., Jr., Sulfides, High-Temperature Technology, I. E. Campbell, Ed. (John Wiley & Sons, Inc., New York, 1956), p. 190.

(44) Wehrmann, R., Silicides, High-Temperature Technology, I. E. Campbell, Ed. (John Wiley & Sons, Inc., New York, 1956).

5. LIST OF REFERENCES (CONT'D)

(45) Brewer, L., et al., The Chemistry and Metallurgy of Miscellaneous Materials, L. L. Quill, Ed. (McGraw-Hill Book Co., Inc., 1950).

(46) Powell, C. F., Borides, High-Temperature Technology, I. E. Campbell, Ed. (John Wiley & Sons, Inc., New York, 1956), p. 148.

(47) Brewer, L. and H. Haraldsen, Electrochem. Soc. J., 102, 399 (1955).

(48) Zeitsch, K. J., and J. Criscione, Oxidation-Resistant Graphite-Base Composites, WADD TR 61-72, Vol. XXX (1963).

(49) Manofsky, M. B., and J. G. Kemp, Coating and Testing of Graphite for Protection Against Oxidation and Erosion, Natl. Carbon Co. TM-C4 (1957).

(50) Kummer, D. L., et al., Hypersonic Glide Re-Entry Vehicle Nose Tip Applications and Oxidation Protection of Graphite at 4000°F, paper presented at 64th Am. Ceram. Soc. Convention (1962).

(51) Goodman, E., et al., Electrodeposition of Erosion and Oxidation-Resistant Coatings for Graphite, Final Summary Rept., Bureau of Naval Weapons, Contract No. 61-0670-C (1962).

(52) Blocher, J. M., Jr., Chemical Vapor Deposition, The Promise and Problems of Chemical Vapor Deposition (Battelle Memorial Inst., Columbus, Ohio, 1962), DMIC 170.

(53) Wakelyn, N. T., NASA Rept. No. TND-722 (Feb. 1961).

(54) Montgomery, H. R., and J. W. Szymaszek (to Norton Co.), U.S. 2,677,627 (1954).

(55) Wheildon, W. M., Jr. (to Norton Co.), U.S. 2,707, 691 (1955).

(56) Mole, Norton, SPA, Ital. 494,463 (1954).

(57) Kozhen, C. W. (to Union Carbide Corp.), U.S. 2,925,357 (1960).

5. LIST OF REFERENCES (CONT'D)

(58) See Section 2.3, this report.

(59) Cubicciotti, D. D. Jr., Reaction of Metals with Their Environs at High Temperature, Proc. Symp. High Temperature - A Tool for the Future (Stanford Res. Inst., Menlo Park, Calif., 1956) p. 121.

(60) Atalla, M. M., Properties of Elemental and Compound Semiconductors (New York, 1960), p. 163.

(61) Kirk, R. E. and D. F. Othmer, Ed., Encyclopedia of Chemical Technology, 1 (The Interscience Encyclopedia, Inc., New York, 1953) p. 592.

(62) Stull, D. R. and G. C. Sinke, Thermodynamic Properties of the Elements (Am. Chem. Soc., Washington, 1956).

(63) Dike, P. H., Temperature and Stress Measurement, High-Temperature Technology, I. E. Campbell, Ed. (John Wiley & Sons, Inc., New York, 1956), p. 342.